Title
MIGRATION IN SUPPORTED ELECTROLYTE SOLUTIONS WITH FREE CONVECTION

Authors
Selraan, Jan Robert
John
Newman

Publication Date
1971

UCRL-20322
UC-25 Metals,
Ceramics and Materials
TID-4500 (57th Ed.)

c.2

MIGRATION IN SUPPORTED ELECTROLYTE SOLUTIONS WITH FREE CONVECTION

Jan Robert Selman and John Newman

January 1971

AEC Contract No. W-7405-eng-48

LAWRENCE RADIATION LABORATORY
UNIVERSITY of CALIFORNIA BERKELEY

UCRL-20322

c.2

DISCLAIMER

UNIVERSITY OF CALIFORNIA
Lawrence Radiation Laboratory
Berkeley, California 94720

June 1, 1971

ERRATUM

TO: All recipients of UCRL-20322

FROM: Technical Information Division

SUBJECT: UCRL-20322: Migration in Supported Electrolyte Solutions with Free Convection, Jan Robert Selman and John Newman, January 1971

Please make the following category change on the cover (second line): UC-25 Metals, Ceramics and Materials should read UC-4 Chemistry.

MIGRATION IN SUPPORTED ELECTROLYTE SOLUTIONS WITH FREE CONVECTION

Contents

Abstract

The migration contribution to the current in free convection is evaluated by numerical solution of the appropriate partial differential equations, with the assumption that the Schmidt number is very high. Results are presented for the systems $CuSO_4$ - H_2SO_4 - H_2O and $K_3Fe(CN)_6$ - $K_4Fe(CN)_6$ - KOH(NaOH) - H_2O.

The migration contribution in $CuSO_4$ - H_2SO_4 - H_2O is not very different from that in forced convection. In all cases, except in the unsupported systems, there occurs apparently a density maximum as well as a minimum, which leads to a velocity maximum within the diffusion layer. In a well-supported ferri-/ferrocyanide system this density inversion is strong enough to cause physically implausible results.

The composition at the electrode and the shear stress were also obtained in the course of the computation.

UCRL-20322

MIGRATION IN SUPPORTED ELECTROLYTE SOLUTIONS WITH FREE CONVECTION

Jan Robert Selman and John Newman

Inorganic Materials Research Division,
Lawrence Radiation Laboratory, and
Department of Chemical Engineering,
University of California, Berkeley

January 1971

1. INTRODUCTION

This investigation concerns the contribution which migration, in the electric field imposed on an electrolytic solution, makes to the current density in free convection, i.e., when stirring of the solution takes place exclusively due to density changes in the solution near the electrodes. The question is of practical interest when one wants to measure diffusional mass transfer of a reacting ion by free convection. In that case the electric field contribution should be eliminated as much as possible. Usually this is done by adding excess inert (or supporting) electrolyte to the solution, thereby lowering the electric field. However it remains to be determined how effective this is in suppressing migration. For the case of forced convection in various flow geometries the migration contribution has been evaluated numerically.[13-15,17,21] In free convection there is the additional complication that migration of non-reacting ions changes the composition and density of the solution near the electrodes and thus interacts with the free convection. It is even conceivable that it may prevent a stable, laminar velocity profile from being attained.

In this study free convection is considered at a vertical plane electrode. The results, however, are also valid with only small

modifications to other geometries (except horizontal plates), provided the Schmidt number of the solution is large.[8] After a brief review of migration in electrolytic solutions (section 2), pertinent information about free convection at a vertical plate by heat or mass transfer will be summarized in section 3. The next sections present the formal treatment of the problem in terms of partial differential equations and a numerical method of solution. Current density, shear stress, and composition of the solution near the electrode are solved for in a few ternary systems: $CuSO_4$ - H_2SO_4 - H_2O (cathodic), $K_3Fe(CN)_6$ - $K_4Fe(CN)_6$ - H_2O (cathodic and anodic); and in the systems $K_3Fe(CN)_6$ - $K_4Fe(CN)_6$ - KOH - H_2O and $K_3Fe(CN)_6$ - $K_4Fe(CN)_6$ - NaOH - H_2O (cathodic and anodic).

2. MIGRATION IN ELECTROLYTIC SOLUTIONS

When a potential is applied between conducting plates in an electrolytic solution, the resultant change in electrochemical potential of the metal ions and electrons in each electrode will lead to a surface reaction at the electrode. This reaction may be a deposition or dissolution reaction, or a redox reaction involving only species in solution. A general expression for the electrode reaction is:

$$\sum_i s_i M_i^{z_i} \rightarrow n e^- \quad . \tag{2.1}$$

If the rate of the reaction is not restricted by its kinetic characteristics, the electrode reaction is "reversible" and its rate is transport-controlled.

The current density by stoichiometry is proportional to the reacting ion flux (or fluxes in the case of a redox reaction):

$$s_i \underline{i} = - nF\underline{N}_i \qquad (2.2)$$

Therefore, if the driving force of the mass transfer process can be expressed in a practical form, e.g., as a concentration gradient of the reacting species near the electrode, or as a concentration difference electrode/bulk, one may be able to relate the mass transfer rate in a general way to the concentration driving force. This can take the form of an effective diffusivity (if the concentration gradient is known):

$$\underline{N}_i = -D_i^{eff} \nabla c_i \quad , \qquad (2.3)$$

or of a mass-transfer coefficient (if the concentration difference is known):

$$\underline{N}_i = k_i (c_i^e - c_i^b) \quad . \qquad (2.4)$$

However if current measurements are to serve for evaluation, by analogy, of non-ionic mass transfer or heat transfer, it is desirable that the electric field make either a negligible contribution to the current or, otherwise, that its contribution be known so that it can be accounted for. Furthermore, limiting current curves obtained in complete absence of supporting electrolyte frequently will not show a clearly defined plateau. In dilute solutions it is convenient to distinguish

various contributions to the flux of ionic species i:

$$\underline{N}_i = - D_i \nabla c_i - c_i z_i u_i F \nabla \Phi + \underline{v} c_i \qquad (2.5)$$

The second term represents the migration in a field of strength $\underline{E} = - \nabla \Phi$. The mobility u_i is defined as the average velocity due to a unit force per mole (units, e.g., cm^2 - mole/joule-sec) and is related to the ionic diffusion coefficient D_i by the Nernst-Einstein equation:

$$D_i = RTu_i \quad . \qquad (2.6)$$

In the limiting current method of measuring mass transfer coefficients, the reacting ion concentration at the electrode is made vanishingly small by applying a large potential. Likewise in the present study of free convection with migration we shall be concerned with the case where the reacting ion concentration at the electrode is zero, there will be, according to (5), no direct contribution of the electric field to the reacting ion flux <u>at the electrode</u>, except for a binary electrolyte. But the electric field does affect the concentration profiles of reacting and non-reacting ions and thereby contributes indirectly to the current.

The evaluation of this contribution implies solving material balances for all ionic species:

$$\frac{\partial c_i}{\partial t} = - \nabla \cdot \underline{N}_i \quad , \qquad (2.7)$$

taking into account that the concentrations everywhere are related by the electroneutrality condition:

$$\sum_i z_i c_i = 0 \quad . \tag{2.8}$$

The boundary conditions at the electrode are given by (2); s_i is zero for non-reacting species. Equation (7) differs from the non-ionic convective diffusion equation only in that the flux $\underline{N}_i$ contains a migration contribution, $-z_i u_i F c_i \nabla\Phi$.

There are two cases in which the set of equations (7) and (8) can be proven equivalent to a single non-ionic convective diffusion equation:

$$\frac{\partial c}{\partial t} + \underline{v}\cdot\nabla c = D\nabla^2 c \quad . \tag{2.9}$$

These cases are that of a <u>binary electrolyte</u> and that of a minor reacting species in excess inert electrolyte.[10]

In the case of a binary electrolyte c signifies the salt concentration; the salt diffusion coefficient D_s accounts for the migration effect and is defined by

$$D_s = \frac{z_+ u_+ D_- - z_- u_- D_+}{z_+ u_+ - z_- u_-} \tag{2.10}$$

or, if (6) is valid,

$$D_s = \frac{D_+ D_- (z_+ - z_-)}{z_+ D_+ - z_- D_-} \quad , \tag{2.11}$$

The physical meaning of this formulation is that in the absence of current the salt will diffuse as a single species, due to a balance of separating forces (different diffusivities) and mutual attraction in the field created by charge separation. When a current is passed, the current expression[4]

$$\frac{i}{z_+ \nu_+ F} = -(D_+ - D_-)\nabla C - (z_+ u_+ - z_- u_-)Fc\nabla\Phi = -nF\nu_+ D_s \nabla c_s \qquad (2.12)$$

shows that approach of the limiting current causes the field strength in the solution near the cathode to become theoretically infinite, corresponding to a forced charge separation.

In "well-supported" solutions, i.e., solutions with an excess of inert electrolyte, the reacting ion is a minor species and the electric field strength is low due to the supporting electrolyte concentration. Thus not only is the migration flux of the reacting ion zero at the electrode, but also away from the electrode it is a small quantity of second order. The reacting ion concentration obeys the equation of convective diffusion (9), with D representing the ionic diffusion coefficient. The concentrations of the non-reacting ions and the electric field strength near the electrode are determined by the concentration profile of the reacting ion.[10] This approximation is valid in the limit of vanishingly small reactant concentrations. It is frequently used since one likes to measure the limiting current in excess inert electrolyte, in spite of the uncertainty about the ionic diffusion coefficient in such concentrated electrolyte mixtures. "Supported solutions" have the

advantage of high conductivity and of relatively uniform density, viscosity, diffusivities and activity coefficients.

When the composition of the solution is intermediate between a binary salt and a well-supported solution, the equations (7) have to include the migration contribution:

$$\frac{\partial c_i}{\partial t} + \underline{v}\cdot\nabla c_i = D_i\nabla^2 c_i + z_i u_i F\nabla\cdot(c_i\nabla\Phi) \qquad (2.13)$$

and their solution by analytic means is hardly tractable,[18-20] even if the velocity $\underline{v}$ corresponds to a simple hydrodynamic situation. Newman[13] solved (13) numerically for a variety of electrolytic systems in the following cases: steady mass transfer to a rotating disk; unsteady mass transfer to a growing drop; unsteady mass transfer into a stagnant semi-infinite fluid; and steady mass transfer in a Nernst (stagnant) diffusion layer of finite thickness. The migration effect was expressed as the ratio of limiting current I_L to the limiting "diffusion current" I_D, corresponding to absence of migration, i.e., an excess of supporting electrolyte. Values of I_L/I_D were obtained for a range of compositions characterized by the ratio of supporting electrolyte to total electrolyte. Only in those cases where the diffusivity of the reacting ion differs very much from that of the counter-ion, is there an appreciable difference between I_L/I_D values for the different hydrodynamic situations. This is particularly so with H^+ as a reacting ion in deposition reactions. Redox reactions show only a small migration effect, no more than ten percent, and somewhat higher when no supporting electrolyte is present and the product ion is also absent in the bulk.

The effect of migration on the current to a growing mercury drop was also solved numerically by Okada, Yoshizawa, Hine and Asada.[14] Newman[15] showed that the case of migration through laminar diffusion layers generally, at high Schmidt numbers, is mathematically identical to that of migration to the rotating disk, solved earlier.[1]

In the case of a Nernst diffusion layer the diffusivities of the different species drop out of equation (13), if the Nernst-Einstein equation (6) is valid. The effect of migration in a stagnant diffusion layer containing 3 univalent ionic species was first treated by Eucken.[11] The I_L/I_D value for a certain composition depends only on the valence of the ions in solution; so does the composition of the solution at the electrode. Table 1 lists the maximum I_L/I_D value and the composition of the solution at the electrode for a number of ion combinations which occur in deposition reactions. Also shown are the values for the ferricyanide/ferrocyanide redox reaction. These involve besides the valences of the ions the ratio of diffusivities of product and reacting ion. The calculations leading to these results are given in Appendix E.

The concept of a stagnant layer, although it is obviously in error, has been used frequently to estimate the concentration of supporting electrolyte at the electrode. This quantity, which is of secondary interest in forced convection, is very important if one wants to calculate the density difference which is the driving force for free convection. Recently Ravoo[28,52] has applied the stagnant layer model to free convection with a centrifugal acceleration as driving force. In this case, as in free convection over a horizontal electrode, the

convective velocity cannot be expressed in a simple mathematical form and the use of a simplified model is necessary. However, it is clear that the stagnant layer model is of limited value since it does not distinguish between different patterns of convective velocity and moreover does not take into account that the diffusion layer thickness ought to be a different one for every ion in view of the unequal diffusivities.

Another simplified model which has been applied to free convection in order to estimate interfacial electrolyte composition in free convection is that of Wilke, Eisenberg and Tobias.[24] This model is based on the assumption that the migration contribution to the current for any composition can be excluded from the total current by using for the reactant flux the expression*

$$N_R = \frac{i(1-t_R)}{z_R} = -D_R \nabla c_R \quad . \tag{2.14}$$

Likewise it is assumed that the flux of the supporting ion, which is zero at the electrode, can be written:

---

*This expression was apparently first given by Heyrovský[12] who rejected Eucken's analysis,[11] in which a stagnant layer was assumed, because it did not agree with polarographic experiments for the discharge of hydrogen ions from HCl-KCl solutions. Newman's analysis[13] for the growing mercury drop showed good agreement with these same data (see also reference 16), thereby removing Heyrovský's objections to the methods of analysis based on the equations of electrolytic mass transfer.

$$N_i = \frac{it_i}{z_i F} - D_i \nabla c_i = 0 \quad . \tag{2.15}$$

Next the diffusion fluxes (14) and $-D_i \nabla c_i$ in (15) are related to the mass transfer rates resulting from concentration differences across the diffusion layer. Convection is taken into account by the use of overall mass transfer coefficients k for free convection of non-ionic components:

$$\frac{i(1-t_R)}{z_R} = - D_R \nabla c_R = k_R \Delta c_R \quad , \tag{2.16}$$

$$\frac{it_i}{z_i} = D_i \nabla c_i = k_i \Delta c_i \quad . \tag{2.17}$$

since the mass transfer coefficients k in (16) and (17) are related to the concentration driving force by, e.g.,

$$\frac{k_i L}{D_i} = C \left(\frac{\Delta \rho g L^3}{\rho \nu D_i} \right)^{1/4} \tag{2.18}$$

where C is supposedly independent of the species, one has from (16), (17) and (18):

$$\frac{\Delta c_i}{\Delta c_R} = - \frac{z_R t_i}{z_i (1-t_R)} \left(\frac{D_R}{D_i} \right)^{3/4} \quad . \tag{2.19}$$

since t_i and t_R depend on the composition of the solution by the definition

$$t_i = \frac{z_i^2 u_i c_i}{\sum_i z_i^2 u_i c_i} \qquad (2.20)$$

and D_i is also concentration-dependent, it is necessary to solve for Δc_i in (19) by iteration.

It is clear that this estimation method is quite general and can be applied to forced convection as well as different kinds of free convection. The only difference this will cause in (19) is that the exponent of D_R/D_i will be the same as the power to which the mass transfer coefficient k depends on D in that particular kind of situation.[50]

It is also clear that the expression (17) is equally valid for the counter-ion and that the resulting counter-ion concentration at the electrode may not satisfy electroneutrality. This difficulty is avoided by not using ionic diffusivities D_i, which are anyway certain only at infinite dilution, according to (6).

Binary electrolyte diffusivities are used, e.g., D_{CuSO_4} and $D_{H_2SO_4}$, instead of ionic diffusivities. The inherent assumption of binary salts diffusing without mutual interaction is of course not plausible.

However, a more immediate objection to this migration model is the use of transference numbers in (14) and (15) to distinguish the fraction of the current contributed by migration of a certain ion. This use is contradicted by the fact that concentration gradients occur near the electrode, so that diffusion and migration contributions to the current coexist there. In such a situation the use of transference numbers to assign migration contributions is meaningless.[10] The use of expression

(14) can be traced back to its validity in the case of a binary electrolyte.[12] With excess supporting electrolyte the error made by using (14) is inconspicuous since the transference number of the reacting ion is very small, as is the migration contribution to the current. In intermediate cases, however, there are no firm grounds for the use of this approximation.

For comparison with results of this work, electrolyte compositions at the electrode calculated according to the method of Wilke, Tobias and Eisenberg are shown in Table 2 for a range of bulk electrolyte compositions. Ionic diffusivities at infinite dilution have been used. The formulas leading to these results are collected in Appendix F.

More elaborate attempts to obtain an approximate solution to the problem of migration are also necessarily more restricted. Gordon, Newman and Tobias[17] treated the rotating disk electrode (for the systems $K_3Fe(CN)_6$ - $K_4Fe(CN)_6$ - KOH or NaOH) by assuming a constant potential gradient in the diffusion layer.

A special class of approximate solutions are those using the integral method of von Karman and Pohlhausen applied to the diffusion and velocity boundary layer. Wagner[25] was the first to apply this method to free convection in electrolytic solutions, specifically to the case of $CuSO_4$ with H_2SO_4 as a supporting electrolyte in large excess. His procedure takes into account that the H^+-ion diffusion layer extends farther into the solution than the Cu^{++}-ion layer. The concentration excess of H_2SO_4 at the electrode is therefore, at the limiting current, not 1/3 of the $CuSO_4$ bulk concentration (see Table 1), but:

$$\Delta c_{H_2SO_4}/\Delta c_{CUSO_4} = \frac{1}{3}\,\Delta = \frac{\delta_{H^+}}{3\delta_{Cu^{++}}} \qquad (2.21)$$

The value of Δ depends on the assumed concentration and velocity profiles. Wagner approximated the profiles, schematically shown in figure 1, by quadratic expressions:

$$\frac{u}{u_{max}} = 1 - (1 - \frac{y}{\delta_v})^2 \quad \text{for } 0 < y < \delta_v \quad ; \qquad (2.22)$$

$$\frac{c_i - c_{i\infty}}{c_{io} - c_{i\infty}} = (1 - \frac{y}{\delta_i})^2 \quad \text{for } y < \delta_v \quad . \qquad (2.23)$$

It was assumed that δ_v (location of the velocity maximum) coincides with $\delta_{Cu^{++}}$. Ultimately Δ depends only on the transference number of H^+ in the bulk solution and is found to be 1.41, so that $\Delta c_{H_2SO_4}/\Delta c_{CuSO_4} = 0.47$.

Ibl and Braun[26] applied the integral method to free convection at a vertical electrode with the boundary condition of uniform current density. They used the same concentration profiles as Wagner,[4] but replaced the velocity profile by:

$$\frac{u}{u_{max}} = \frac{27}{4}\,\frac{y}{\delta_v}\,(1 - \frac{y}{\delta_v})^2 \quad \text{for } 0 < y < \delta_v \quad , \qquad (2.24)$$

which has a maximum at $y = \delta_v/3$. Again δ_v was assumed equal to $\delta_{Cu^{++}}$. For a solution of $CuSO_4$ with large excess of H_2SO_4 ε was 1.50. The calculation was also made for a solution of 1 M $CuSO_4$ + 1 M H_2SO_4, which

is the composition used in Brenner's experiment,[29] where the diffusion layer was frozen instantaneously and analyzed after slic ng. Here the transference number of the reacting ion cannot be neglected and (2.21) has to be modified. $\Delta c_{H_2SO_4}/\Delta c_{CuSO_4}$ was found to be 0.385.* Asada, Hine, Yoshizawa and Okada[27] applied the integral method to the complex problem of finding the current distribution at parallel vertical electrodes in a situation intermediate between limiting current (uniform concentration at the electrodes) and uniform current density (predominance of ohmic drop and kinetic overpotential). They employed cubic polynomials for concentration and velocity profiles, and obtained $\Delta c_{H_2SO_4}/\Delta c_{CuSO_4} = \frac{2}{3}$, i.e., $\Delta = 2$, for a solution of 0.1 M $CuSO_4$ + 1.5 M H_2SO_4.

The last two cases[26,27] are not directly comparable to the present work, since they use the constant current boundary condition. The integral method, however, does not distinguish between various boundary conditions as far as the calculation of $\Delta c_{supp.}/\Delta c_{react.}$ is concerned.

3. FREE CONVECTION

Flow along a vertical wall as the result of a density gradient shows a boundary-layer structure. The pressure in horizontal planes is uniform and constant, equal to the hydrostatic pressure. The convection is caused by the difference in density along horizonal planes. The equation of motion is then, since

---

*This is in good agreement with Brenner's result as quoted by Ibl and Braun[26]: 0.405; not, however, with the value calculated directly from Brenner's figures[29] 3 and 4, namely: 0.72.

$$\frac{\partial p}{\partial x} = -\rho_\infty g_x \quad , \tag{3.1}$$

$$u \frac{\partial u}{\partial x} + v \frac{\partial u}{\partial y} = \nu \frac{\partial^2 u}{\partial y^2} - g_x \frac{\rho - \rho_\infty}{\rho_\infty} \tag{3.2}$$

where the coordinates are as in figure 1 and the density is supposed to be the only variable physical property.

If the density gradient is caused by the concentration variation of dissolved material, the equation of motion is coupled to the equation of convective diffusion for species i:

$$u \frac{\partial c_i}{\partial x} + v \frac{\partial c_i}{\partial y} = D \frac{\partial^2 c_i}{\partial y^2} \quad . \tag{3.3}$$

The densification can be represented by a linear expression in terms of concentration differences:

$$\rho - \rho_\infty = \sum_i \alpha_i (c_i - c_{i\infty}) \rho_\infty \tag{3.4}$$

If temperature variations are causing the density gradient, equation (3) is replaced by the convective conduction equation and (4) by a thermal densification expression. This case is completely analogous to that of free convection due to concentration variations in a binary solution of a nonelectrolyte.

Finally the motion must satisfy continuity:

$$\frac{\partial u}{\partial x} + \frac{\partial v}{\partial y} = 0 \quad , \tag{3.5}$$

which is a reason for introducing the stream-function ψ defined by

$$u = \frac{\partial \psi}{\partial y} \quad , \quad v = - \frac{\partial \psi}{\partial x} \qquad . \tag{3.6}$$

In the classical solution to the thermal free convection problem, due to Pohlhausen,[2] here transcribed in terms of concentration variation of a single solute, a similarity transformation is introduced:

$$\zeta = \frac{y}{E} \left(\frac{4}{3x}\right)^{1/4} \quad ; \quad f = \left(\frac{3}{4x}\right)^{1/4} \frac{\psi E}{\nu} \quad ; \quad \theta = \frac{c - c_\infty}{c_o - c_\infty} \tag{3.7}$$

where $E = \left[\frac{\nu^2}{g\alpha(c_o - c_\infty)}\right]^{1/4}$.

The equation of motion is reduced to

$$f''' + ff'' - \frac{2}{3}(f')^2 + \theta = 0 \tag{3.8}$$

and the convective diffusion equation to

$$\theta'' + Scf\theta' = 0 \tag{3.9}$$

where primes denote differentiation with respect to ζ and Sc is the Schmidt number, ν/D . The boundary conditions:

$$u = v = 0, \; c = c_o \text{ at } x > 0, \; y = 0; \tag{3.10a}$$

$$u = 0 \quad , \; c = c_\infty \text{ at } x > 0, \; y \to \infty; \tag{3.10b}$$

$$u = 0 \quad , \; c = c_\infty \text{ at } x = 0, \; y > 0; \tag{3.10c}$$

are transformed into:

$$f = f' = 0, \ \theta = 1 \quad \text{at } \eta = 0; \tag{3.11a}$$

$$f' = 0 \quad , \ \theta = 0 \quad \text{at } \eta = \infty. \tag{3.11b}$$

The concentration and velocity distribution in the boundary-layer follow from the solution to (8) and (9), and are shown in figure 2 for various values of the Schmidt number. The thickness of the diffusion layer and of the velocity boundary-layer are proportional to $x^{1/4}$.

The quantities of practical interest following from the solution of (8) and (9), are the mass transfer to the wall and the shear stress at the wall:

$$N_{loc} = -D \left.\frac{\partial c}{\partial y}\right|_o = -D(c_o - c_\infty) \left\{ \frac{3g\alpha(c_o - c_\infty)}{4\nu^2 x} \right\}^{1/4} \left.\theta'\right|_o ; \tag{3.12}$$

$$\tau_{o,loc} = \left.\mu \frac{\partial u}{\partial y}\right|_o = -\mu \left(\frac{4x}{3\nu^2}\right)^{1/4} (g\alpha(c_o - c_\infty))^{3/4} \left.f''\right|_o \tag{3.13}$$

Integrating to average flux and shear stress over a length L, one can write the result in the form:

$$Nu = C_1 \, Gr^{1/4} \quad ; \tag{3.14}$$

$$\frac{\tau_o}{\rho L g\alpha(c_o - c_\infty)} = B_1 \, Gr^{-1/4} \quad . \tag{3.15}$$

Here the Nusselt number Nu is defined by

$$Nu = \frac{N_{avg} L}{D(c_o - c_\infty)} \quad ; \tag{3.16}$$

the Grashof number Gr by:

$$Gr = \left| \frac{g\alpha(c_o - c_\infty)L^3}{\nu^2} \right| \tag{3.17}$$

and C_1 and B_1 are constants which depend only on the value of the Schmidt (or Prandtl) number since it appears as a parameter in equation (9). Table 3 lists some values of C_1 and B_1 from the literature.

It is important to realize in which manner the convection profile changes when the viscosity of the solution increases and/or the diffusivity of the solute decreases, or vice versa, i.e., when the Schmidt number increases or decreases. As long as the kinematic viscosity ν and the diffusivity D are of the same order of magnitude, the hydrodynamic boundary layer will extend approximately the same distance as the concentration boundary layer. This is seen in figure 2 where velocity and concentration profiles in terms of the classical dimensionless variables (7) are plotted for a wide range of Schmidt numbers.

Now let first the diffusivity become very large compared to the viscosity. This applies in practice only to the thermal diffusivity in the case of liquid metals, i.e., liquids with very low Prandtl number ν/a. Then the thermal boundary layer extends much farther into the solution than that part of the hydrodynamic boundary layer in which the velocity increases; i.e., the part of the boundary-layer in which the

friction at the wall propagates itself is very small compared to the complete boundary layer. The larger part of the boundary layer is characterized by a balance of buoyancy and inertial terms in the equation of motion (2). Figure 2 shows that the classical variables become inappropriate in this situation.

A dimensional analysis based on equal importance of all terms in the equation of motion (2) would lead to a hydrodynamic boundary-layer thickness δ_v in accordance with the classical analysis, of the order:

$$\delta_v/L \sim Gr^{-1/4} \tag{3.18}$$

where L characterizes the geometry of the problem. Instead one finds from the balance of buoyancy and inertial terms in (2) and of convective and diffusive terms in (3) that the concentration boundary layer thickness δ_c is stretched by $Sc^{-1/2}$ compared to δ_v:

$$\delta_c/L \sim Gr^{-1/4}Sc^{-1/2} \tag{3.19}$$

The appropriate replacement of the mass transfer relation (13) is then

$$Nu = C_2(Gr\ Sc^2)^{1/4} \quad ; \tag{3.20}$$

values of C_2 are also given in Table 3.

It can be shown[9] that in the limit of $Sc \to 0$ one should have, from matching perturbation expansions:

$$\frac{Nu}{(GrSc^2)^{1/4}} = 0.80051 - 0.43179\ Sc^{1/2} + O(Sc) \qquad (3.21)$$

The first term was first given by Le Fevre[4] as 0.800544.

The shear stress at the electrode is determined by the inner viscous part of the boundary layer and, therefore, is not affected by stretching the coordinate. In the limit of $Sc \to 0$ one has[9]

$$-\frac{\tau_o}{\rho L g \alpha \Delta c} = Gr^{-1/4}[1.21051 - 1.13253\ Sc^{1/2} + O(Sc^{2/3})] \qquad (3.22)$$

The opposite case, of very small D and large Sc, is the one dealt with in this investigation since electrolyte solutions are invariably characterized by Schmidt numbers above 1000. Here the physical situation is that of a very thin diffusion layer, vanishingly small in the limit $Sc \to \infty$, and a much larger hydrodynamic boundary layer in which the liquid is dragged by the buoyancy created near the wall. Figure 2 shows how again, the classical variables become inappropriate due to the disparity between diffusion layer thickness and extended velocity layer thickness. In the extended velocity layer buoyancy plays no role, so that it has the character of a forced convection boundary layer with a spatially varying slip velocity at the wall. In the wall layer, where the density varies, the velocity is determined by a balance of buoyancy and viscous stresses, the inertial terms in the equation of motion (2) being negligible.

Morgan and Warner[5] have first shown that the appropriate distance variable to express the thickness of the wall layer, where the concentration

varies, is

$$\delta_c/L \sim Gr^{-1/4}Sc^{-1/4} \quad , \tag{3.23}$$

i.e., the classical variable ζ is stretched by a factor $Sc^{1/4}$. As a result the mass transfer expression (14) is replaced, in the case of high Schmidt number, by:

$$Nu = C(GrSc)^{1/4} \quad . \tag{3.24}$$

The shear stress at the electrode is of course involved in the stretching, and the relation (15) is replaced by:

$$-\frac{\tau_o}{\rho L g \alpha \Delta c} = B(GrSc)^{-1/4} \tag{3.25}$$

Values of C and B from the literature are included in Table 3.

Kuiken[6] has treated free convection at large Schmidt number by matching perturbation expansions. In the limit of $Sc \to \infty$ he obtained

$$\frac{Nu}{(GrSc)^{1/4}} = 0.67033 - 0.1757\ Sc^{-1/2} + 0.0633\ Sc^{-1} + O(Sc^{-3/2}) \quad ; \tag{3.26}$$

The first term was first given by Le Fevre[4] as 0.670327 .

For the shear stress he found:

$$-\frac{\tau_o}{\rho L g \alpha \Delta c} = 0.932833 - 0.346989\ Sc^{-1/2} + 0.253707 Sc^{-1}$$

$$+ O(Sc^{-3/2}) \qquad (3.27)$$

Another result of importance is the value of the constant parallel velocity at the outer edge of the inner layer. The parallel velocity, in terms of the dimensionless streamfunction, is

$$u = \left(\frac{4 g \alpha \Delta C}{3 \nu D x}\right)^{1/2} D x \frac{\partial \bar{f}}{\partial \eta} \qquad (3.28)$$

where

$$\eta = \zeta\ Sc^{-1/4},\ \bar{f} = f Sc^{3/4}$$

i.e., the stretched variables of the inner layer. For $\bar{f}'_\infty$ Kuiken[6] found:

$$\bar{f}'_\infty = 0.884522 + 0.58688\ Sc^{-1/2} + 0.827052\ Sc^{-1} + O(Sc)^{-3/2} \qquad (3.29)$$

A similar perturbation treatment was given by Roy.[7]

The present analysis of migration in electrolytic solutions under free convection conditions employs the assumption $Sc \to \infty$ and therefore uses the stretched variable η introduced by Morgan and Warner.[5] In terms of η the equations without migration are, instead of (3.8), (3.9):

$$\bar{f}''' + \bar{\theta} = 0 \quad ; \qquad (3.30)$$

$$\bar{\theta}'' + \bar{f}\,\bar{\theta}' = 0 \quad , \qquad (3.31)$$

with the boundary conditions (3.11) except that

$$\bar{f}'' = 0 \text{ as } \eta = \infty \quad . \tag{3.32}$$

This is identical to the zero approximation of the inner problem, leading to the main term in the inner expansion of $\bar{f}$ and θ, in a perturbation treatment along the lines of Kuiken.[6]

In the outer problem the main term of θ, as well as all perturbations of θ, are zero. Consequently the equation of motion, in terms of the outer variables

$$\tilde{f}(\xi) = f(\eta)\ Sc^{-1/2} \quad ; \tilde{\eta} = \eta\ Sc^{-1/2} \quad , \tag{3.33}$$

is

$$\tilde{f}''' + 3\tilde{f}\tilde{f}'' - 2\tilde{f}'\tilde{f}' = 0 \quad , \tag{3.34}$$

with the boundary conditions

$$\tilde{f}'(\infty) = 0 \quad , \quad \tilde{f}'(0) = f'(\infty) \tag{3.35}$$

In fact the outer problem is completely determined by the inner problem, which makes it unnecessary to solve for the outer problem in order to get the main terms of the inner expansion for f and θ (taking migration into account). It can be shown that not only is $\tilde{\theta}_n(\xi) = 0$, but also that the matching condition

$$\lim_{\eta\to\infty} Sc^{-1/4}\,\bar{f}(\eta) = \lim_{\hat{\eta}\to 0} \tilde{f}(\eta Sc^{-1/4}) \tag{3.36}$$

implies that

$$\bar{f}_o''(\infty) = 0 \tag{3.37}$$

which makes the zero-order inner problem self-sufficient as far as the boundary conditions are concerned.

The analysis given above, as well as the one following which takes migration into account, is valid for other geometries besides the vertical plate. If in equation (2) the body force is modified as follows (see figure 3)

$$-g\,\frac{\rho-\rho_\infty}{\rho_\infty}\sin\varepsilon \tag{3.38}$$

then similarity transformations of the same kind as that used by Morgan and Warner[5] may be applied, provided:

$$\sin\varepsilon = ax^m \tag{3.39}$$

where a and m are arbitrary constants such that $a > 0$, $m \geq 0$. Acrivos[8] showed that the transformation for two-dimensional geometries is:

$$\eta = \frac{y\left(\frac{3g\alpha\Delta c}{4\nu D}\right)^{1/4}}{[(\sin\varepsilon)^{-4/3}\int_o^x(\sin\varepsilon)^{1/3}dx]^{1/4}} \tag{3.39a}$$

$$\psi = \frac{4}{3}\left(\frac{3g\alpha\Delta c}{4\nu D}\right)^{1/4} D\sin\varepsilon[(\sin\varepsilon)^{-4/3}\int_o^x(\sin\varepsilon)^{1/3}dx]^{3/4}\bar{f}(\eta) \tag{3.35b}$$

In the limit of high Schmidt numbers this gives again equations (3.30,3.31). The constant C in (3.24) is now:

$$C[\frac{1}{L}\int_o^L (\sin\varepsilon)^{1/3}dx]^{3/4} \qquad (3.35c)$$

For the axisymmetric case, see reference 8 or 23.

The addition of supporting electrolyte to a solution does not make the free-convection problem directly comparable to that of heat transfer and nonelectrolytic mass transfer in a binary fluid because, while it does reduce the effect of ionic migration, the concentration variation of the supporting electrolyte affects the density variation to roughly the same extent as the reactant and thus influences the velocity profile. Nevertheless, it has frequently been assumed that the mass-transfer rate is adequately expressed by equation 24. Ibl[22,51] has reviewed the experimental work on electrolytic free convection and the applicability of equation 24 (see also reference 23).

Not all experiments in free convection have involved a supporting electrolyte and a vertical electrode. Ibl and Muller[30] have used aqueous solutions of $CuSO_4$. Schütz[31] investigated experimentally free-convection mass transfer to spheres and horizontal cylinders (see also reference 23).

4. ANALYSIS

The set of equations which determine free convection as a result of concentration variations in electrolytic solutions near a vertical electrode are the following:

$$\frac{\partial u}{\partial x} + \frac{\partial v}{\partial y} = 0 \quad ; \tag{4.1}$$

$$u\frac{\partial u}{\partial x} + v\frac{\partial u}{\partial y} = \nu\frac{\partial^2 u}{\partial y^2} - g_x \sum_i \alpha_i (c_i - c_{i\infty}) \quad ; \tag{4.2}$$

$$u\frac{\partial c_i}{\partial x} + v\frac{\partial c_i}{\partial y} = D_i \frac{\partial^2 c_i}{\partial y^2} + z_i u_i F \frac{\partial}{\partial y}\left(c_i \frac{\partial \Phi}{\partial y}\right) \quad ; \tag{4.3}$$

$$\sum_i z_i c_i = 0 \quad . \tag{4.4}$$

There is one equation (3) for every solute species in the solution.

Denoting the reacting species with subscript R, we have for boundary conditions:

$$x > 0,\ y = 0\ , \quad u = v = 0,\ c_R = c_{RO} \tag{4.5}$$

$$D_i \frac{\partial c_i}{\partial y} + z_i u_i F c_i \frac{\partial \Phi}{\partial y} = \frac{s_i}{s_R}\left(D_R \frac{\partial c_R}{\partial y} + z_R u_R F c_R \frac{\partial \Phi}{\partial y}\right) \quad ;$$

$$\left.\begin{aligned} x = 0\ , \quad y \geq 0 \\ x > 0\ , \quad y \to \infty \end{aligned}\right\} \quad u = 0\ , \quad c_i = c_{i\infty} \quad . \tag{4.6, 4.7}$$

Here the electrode reaction is represented by the relation (2.1).

At high Schmidt numbers the inertial terms in (2) are negligible within the diffusion layer, so that it reduces to:

$$\nu \frac{\partial^2 u}{\partial y^2} = g_x \sum_i \alpha_i (c_i - c_{i\infty}) \quad , \tag{4.8}$$

while the boundary condition (7)

$$x > 0 \ , \quad y \to \infty \ , \quad u = 0 \quad ,$$

is replaced by:

$$x > 0 \ , \quad y \to \infty \ , \quad \frac{\partial u}{\partial y} = 0 \quad . \tag{4.9}$$

We now introduce the similarity transformation:

$$\eta = y\left[\frac{3g\alpha_R(c_{R\infty}-c_{Ro})}{4\nu D_R x}\right]^{1/4} \quad , \tag{4.10}$$

$$\psi = \frac{4}{3} D_R \, x \left[\frac{3g\alpha_R(c_{R\infty}-c_{Ro})}{4\nu D_R x}\right]^{1/4} f(\eta)^* \tag{4.11}$$

and the dimensionless variables:

$$\phi = \frac{\Phi}{RT} \quad : \tag{4.12}$$

$$\theta_i = \frac{c_i}{c_{R\infty}-c_{Ro}} \quad . \tag{4.13}$$

Then the equations become

$$f''' = \sum_i \frac{\alpha_i}{\alpha_R} (\theta_i - \theta_{i\infty}) \quad ; \tag{4.14}$$

$$\frac{D_i}{D_R}\theta_i'' + \frac{z_i u_i RT}{D_R} (\theta_i \phi')' + f\theta_i' = 0 \quad ; \tag{4.15}$$

$$\sum_i z_i \theta_i = 0 \quad . \tag{4.16}$$

---

*The bar on $\bar{f}$ will be omitted henceforth.

Here primes denote derivatives with respect to η.

The boundary conditions become:

$$\eta = 0 \,, f = f' = 0 \quad , \quad \theta_R = \theta_{Ro} \quad , \tag{4.17}$$

$$\frac{D_i}{D_R}\,\theta'_i + \frac{z_i u_i RT}{D_R}\,\theta_i\phi' = \frac{s_i}{s_R}\left(\theta'_R + \frac{z_R u_R RT}{D_R}\,\theta_R\phi'\right)$$

$$\eta \to \infty \quad , \; f'' = 0 \; , \; \theta_i = \theta_{i\infty} \tag{4.18}$$

The result of primary interest is the current:

$$i_{local} = \frac{nFD_R(c_{R\infty}-c_{Ro})^{5/4}}{s_R}\left(\frac{3g\alpha_R}{4\nu D_R x}\right)^{1/4}\left(\theta'_R + \frac{z_R u_R RT}{D_R}\,\theta_R\phi'\right)_o \quad , \tag{4.19}$$

Averaged and brought in the form of a Nusselt number, this is:

$$\frac{i_{avg}\, s_R L}{nFD_R(c_{R\infty}-c_{Ro})} = Nu_R = \left(\frac{4}{3}\right)^{3/4}\left(\theta'_R + \frac{z_R u_R RT}{D_R}\,\theta_R\phi'\right)_o (Gr_R Sc)^{1/4} \quad . \tag{4.20}$$

where $Gr_R = \dfrac{g\alpha_R(c_{R\infty}-c_{Ro})L^3}{\nu^2}$

i.e., the Grashof number referred to the reacting ion densification (a partial densification).

Of interest is also the shear stress at the electrode:

$$\tau_{o,local} = -\rho g\alpha_R(c_{R\infty}-c_{Ro})\left[\frac{4\nu D_R x}{3g\alpha_R(c_{R\infty}-c_{Ro})}\right]^{1/4} f''_o \tag{4.21}$$

Averaged over a length L, this gives

$$\frac{\tau_o}{\rho L g \alpha_R (c_{R\infty} - c_{Ro})} = \frac{4}{5} \left(\frac{4}{3}\right)^{1/4} f_o'' \, (Gr_R Sc)^{-1/4} \tag{4.22}$$

Further significant information is obtained in the form of the parallel velocity far from the electrode:

$$u_\infty = \left(\frac{4}{3} \frac{g \alpha_R (c_{R\infty} - c_{Ro}) D_R x}{\nu} \right)^{1/2} f_\infty' \quad . \tag{4.23}$$

Finally the concentrations of the nonreacting ions at the electrode, θ_{io}, are objectives of this calculation.

5. NUMERICAL PROCEDURE

The equations (41) through (43) form a set of coupled, non-linear differential equations with boundary conditions at zero and infinity. These equations can be linearized about a trial solution producing a series of coupled, linear differential equations. In finite difference form these give coupled, tridiagonal matrices which can be solved readily on a high-speed digital computer.[32] The non-linear problem is then solved by iteration. Usually 150 meshpoints were used.

It is convenient to have in the finite difference formulation two velocity variables instead of f, namely:

$$f_1 \equiv f' \quad ; \tag{5.1}$$

$$f_2 \equiv \int_o^\eta f d\eta \quad . \tag{5.2}$$

This adds another equation to the set (41-43):

$$f_1 = f_2'' \quad . \tag{5.3}$$

In the equation of motion f''' is replaced by f_1'' and in the diffusion equation f is replaced by f_2'.

The total number of equations is now N + 3, if N is the number of species in the solution. The unknown variables are the N species concentrations, f_1, f_2, and ϕ.

The problem parameters are all in the form of ratios with respect to a reacting ion concentration or property (except for the valences):

$$\theta_{i\infty} = c_i/(c_{R\infty}-c_{Ro})$$

$$T_i \equiv \alpha_i/\alpha_R$$

$$R_i \equiv D_i/D_R$$

$$\frac{z_i u_i RT}{D_R} = z_i \frac{D_i}{D_R} = z_i R_i \text{ (using eq. (6))}$$

Because of electroneutrality one of the densification coefficients of ionic species can be set equal to zero. The total number of parameters is therefore 4(N-1).

It can be expected that the computation will not converge to a solution when the conductivity of the solution is very small near the electrode, for example, when cupric ions are discharged from a solution with very little supporting electrolyte.

Appendix B contains a reproduction of the actual Fortran program used in the computations.

The physical property parameters used for the various electrolyte systems are given in Table 4, and the data on which they are based in Appendix D.

6. RESULTS FOR THE SYSTEM $CuSO_4$ - H_2O.

As a preliminary check on the accuracy of the numerical method, the equations (41) through (43) were solved for the case of discharge of an ion from an unsupported electrolyte. This problem is completely analogous to that of heat or mass transfer by natural convection at high Prandtl or Schmidt number, if the diffusion coefficient (2.10) is used. One has then:

$$N_R = \frac{i}{z_R F} \tag{6.1}$$

$$N_s = - D_s \nabla c_s = \frac{i(1-t_R)}{z_R \nu_R F} \tag{6.2}$$

and, consequently:

$$Nu_s = \frac{N_s L}{c_s D_s} = \frac{N_R (1-t_R) L}{c_s D_s \nu_R} = Nu_R \frac{(1-t_R) D_R}{D_s} \quad . \tag{6.3}$$

In the mass transfer expression

$$Nu_s = C_s (Gr_s Sc_s)^{1/4} \quad , \tag{6.4}$$

with all dimensionless numbers based on physical properties of the binary salt, the constant C_s is

$$C_s = C_R(1-t_R)\left(\frac{D_R}{D_s}\right)^{3/4}\left(\frac{\alpha_R}{\alpha_s}\right)^{1/4} \quad , \tag{6.5}$$

where C_R is the dimensionless flux given in (4.20):

$$C_R = \left(\theta_R' + \frac{z_R u_R RT}{D_R}\theta_R\phi'\right)_o\left(\frac{4}{3}\right)^{3/4} \quad . \tag{6.6}$$

Similarly for the shear stress:

$$\frac{\tau_o}{Lg\Delta\rho_s} = -B_s(Gr_s Sc_s)^{-1/4} \quad , \tag{6.7}$$

we have:

$$B_s = B_R\left(\frac{D_R}{D_s}\right)^{1/4}\left(\frac{\alpha_R}{\alpha_s}\right)^{3/4} \quad , \tag{6.8}$$

where according to (4.22):

$$B_R = \left(\frac{4}{5}\right)\left(\frac{4}{3}\right)^{1/4} f_o'' \quad . \tag{6.9}$$

In the case of the binary salt it is necessary to take the concentration at the electrode nonzero since otherwise the field strength near the electrode will increase without bounds and the solution will not converge. Furthermore it is immaterial what values are chosen for the physical properties, since C_s and B_s do not depend on them. The actual values used can be found in Table 4.

Values of C_s and B_s were determined for various meshwidths, using 100 meshpoints, and are collected in Table 5. To obtain an independent estimate

of C_s and B_s the equations (3.8) and (3.9), for free convection involving the inertial terms in the equation of motion, were solved for several Schmidt numbers, using various meshwidths and field lengths. The values estimated by extrapolation are collected in Table 6 and compared with the results of Ostrach[1] and the perturbation series developed by Kuiken.[6]

The agreement between the asymptotic values indicates that the results of the numerical procedure are accurate to five significant sigures. On the basis of these results a mesh width of approximately 0.06 for 150 meshpoints was adopted for the calculations on the systems $CuSO_4$ - H_2O and $CuSO_4$ - H_2SO_4 - H_2O.

Figure 3 shows the normalized density and velocity profiles. The velocity profile is normalized with respect to

$$\bar{f}'_\infty = 0.8845 \qquad \text{(see 3.29)}$$

7. RESULTS FOR $CuSO_4$ - H_2SO_4 - H_2O.

When H_2SO_4 is present in the $CuSO_4$ solution, the effect of migration is to make the H_2SO_4 concentration at the electrode different from the bulk concentration, thereby changing the driving force for the free convection. It is then desirable to use a Grashof number based on total density difference

$$Gr_\rho \equiv \frac{g\Sigma\alpha_i(c_{i\infty}-c_{io})L^3}{\nu^2} \qquad (7.1)$$

instead of the one based on densification due to the reacting ion, Gr_R (see 4.20). This permits a comparison of C in

$$Nu = \frac{i_{avg} s_R L}{nFD_R(c_{R\infty}-c_{Ro})} = C(Gr_\rho Sc)^{1/4} \quad , \tag{7.2}$$

with the constant C_s found for the binary salt (6.4), where only the reacting ion is responsible for densification, and with the general mass-and heat transfer expression for free convection:

$$Nu = C(Gr_\rho Sc)^{1/4} \quad . \tag{3.24}$$

It is also desirable to refer the shear stress at the electrode to the total density difference

$$\frac{\bar{\tau}_o}{Lg\rho \sum_i \alpha_i \Delta c_i} = -B\ (Gr\ Sc)^{-1/4} \quad , \tag{7.3}$$

The relationship between C and C_R, B and B_R is then

$$C = C_R \left[\frac{\Sigma \alpha_i \Delta c_i}{\alpha_R \Delta c_R}\right]^{-1/4} \tag{7.4}$$

$$B = B_R \left[\frac{\Sigma \alpha_i \Delta c_i}{\alpha_R \Delta c_R}\right]^{-3/4} \tag{7.5}$$

The result of interest is now the behavior of current density (C), shear stress (B), maximum velocity (f'_∞) and composition of the solution ($\Delta C_{H_2SO_4}/C_{CuSO_4}$), with an increase of supporting electrolyte concentration. This concentration is expressed in r, the ratio of H_2SO_4 to total H_2SO_4 + $CuSO_4$. As $r \to 1$ one would expect C and B to approach the values 0.670327

and 0.93283, respectively, corresponding to completely diffusive mass transfer by free convection. These values are identical to the constants C_s and B_s, respectively, of the previous section. In figure 4 C and B are plotted normalized with respect to C_s and B_s. Also plotted are f' as well as the maximum velocity f'_{max} (to be discussed below), and the acid accumulation at the electrode $\Delta C_{H_2SO_4}/C_{CuSO_4}$.

The results in figure 4 are based on the assumption that H_2SO_4 is completely dissociated into H^+ and $SO_4^=$ ions. The abscissa is not r but $r^{2/3}$, to check whether the stagnant film model does predict the asymptotic behavior correctly (see Appendix E). This is not of particular interest for the extreme $r \to 1$ since C, B and f'_∞ will be linear in r or $r^{1/n}$. (Note, however, that the asymptotic values at r = 1 are not $C/C_s = B/B_s = 1$ but appreciably less than 1. This anomalous behavior will be discussed below.) The more significant limit is $r \to 0$, but here the linearity is not verifiable since not enough points are available at low r. The numerical solution does not converge below r = 0.09. An arbitrary extrapolation to r = 0 has been made, which necessarily contains an inflection point (dashed lines).

The stagnant diffusion model predicts $C/C_s = 2$ at r = 0, and $\Delta C_{H_2SO_4}/C_{CuSO_4} = 0.333$ at r = 1. These values are not correct. The convection accumulates more H_2SO_4 at the electrode than the stagnant layer model (with equal thickness for all ions) would predict. On the other hand $C_{r=0}/C_{r=1}$ is very close to 2, as predicted. This points to the importance of the high diffusivity of H^+, which causes the diffusion layer thickness of H^+ to be greater than that of the other ions. This

effect is more important when the H_2SO_4 concentration is appreciable, but apparently leads only to a higher concentration difference of H^+ ions between bulk and electrode, not to a change in gradient which, in turn, would influence the reactant flux by electroneutrality.

Figure 4 shows also the shear stress, which varies remarkably little with composition. This again indicates that whatever changes occur in the velocity profile as a result of H^+-accumulation near the electrode, take place away from the electrode. That the changes are quite marked, can be seen again in figure 4 where the asymptotic velocity with excess supporting electrolyte is only 2/3 of that in a binary solution. Moreover a velocity maximum starts appearing when the supporting electrolyte concentration is increased. The maximum velocity, plotted as f'_{max}, is only slightly higher than the asymptotic velocity.

The reason for the velocity maximum is again that the H^+ profile, because of the higher diffusivity, extends farther into the solution, and is less steep than, the Cu^{++} profile. Profiles of the concentration differences with respect to the bulk are shown in figure 5. The differences are normalized with respect to the reacting ion bulk concentration. The electrolyte is 99.998 mol% H_2SO_4, i.e., the velocity maximum is most pronounced.

The velocity maximum (figure 6) is caused by a density minimum due to overcompensation of Cu^{++} deficit by H^+ excess over a short range. The densification with respect to the bulk is a linear combination of Cu^{++} and H^+ excess, with the latter having only 0.21 times the weight of

the former; $SO_4^=$ has been arbitrarily assigned zero densification coefficient. The density profile which results is qualitatively similar to the $SO_4^=$ profile in figure 5, which is likewise a linear combination of H^+ excess and Cu^{++} deficit. Figure 7 presents the refractive index profile, which has a much less pronounced maximum.

Since the present treatment of the free convection boundary-layer is limited to the inner layer, we should be surprised to see that the velocity maximum is located inside the inner layer, instead of being identifical with the outer limit of the inner layer. The velocity profile also shows an inflection, as a result of the boundary condition:

$$\eta \to \infty \quad , \qquad f'' = 0 \quad .$$

Some questions connected with this type of velocity profile will be discussed in section 9 (supported ferri/ferrocyanide solutions), where the same profile is encountered with a much more pronounced maximum.

The assumption that HSO_4^- is completely dissociated is contradicted by the rather low value of the dissociation constant $K_{HSO_4^-} = 0.01$ at 25°C.

Figure 8 combines the values of C/C_s for dissociated and undissociated HSO_4^- in one graph, which also shows the migration current at a rotating disk and at a growing mercury drop.[13] The abscissa here is $\sqrt{r}$.

It can be seen that again C/C_s does not extrapolate to 1 as $r \to 1$, but to a slightly lower value. Compare this with the values for the rotating disk and growing mercury drop, which to extrapolate to 1. The values of B/B_s are not shown since they are in the same range as those for full dissociation and vary just as little with composition. They also do not extrapolate to 1 as $r \to 1$, but to 0.8343.

The asymptotic behavior of C/C_s in free convection migration can be understood by comparing the shape of the velocity profiles for the binary salt and for the well-supported solution. This comparison is made in figure 9. Whereas in forced convection the velocity profile is independent of migration effect, it is here strongly influenced. In particular the formation of a maximum is due to it. The influence of densification by itself has been eliminated by introducing the distance variable $\eta_{\Delta\rho}$ based on total densification at the electrode, $\Delta\rho_o$:

$$\eta_{\Delta\rho} = \eta \left[\frac{\Sigma\alpha_i (c_{i\infty}-c_{io})}{\alpha_R (c_{R\infty}-c_{Ro})} \right]^{1/4} , \tag{7.6}$$

and the streamfunction $f_{\Delta\rho}$ based on $\Delta\rho_o$:

$$f_{\Delta\rho} = f \left[\frac{\Sigma\alpha_i (c_{i\infty}-c_{io})}{\alpha_R (c_{R\infty}-c_{Ro})} \right]^{-1/4} \tag{7.7}$$

The velocity profiles in figure 9 show that the migration influence has its effect far from the electrode and not very much on the velocity derivative at the electrode, i.e., on the shear stress. An attempt to correct for dissimilar velocity profiles, by using the shear stress and its known correlation with Gr_ρ and Sc in a Lévèque type approach, will therefore fail. This approach would be based on the assumption that the streamfunction f can be approximated by a quadratic expression

$$f = 3b\eta^2 \tag{7.8}$$

over the range of η where concentration varies. The equation of convective

diffusion (4.15) without migration reduces then to:

$$\theta' + f\,\theta' = 0 \tag{7.9}$$

where θ refers to the reactant. Using (7.8) the equation becomes:

$$\theta'' + 3b\eta^2\theta' = 0 \quad , \tag{7.10}$$

The solution then would be:

$$\theta'(0) = -\frac{b^{1/3}}{\Gamma(\frac{4}{3})} \quad , \tag{7.11}$$

$$Nu_{avg} = (\tfrac{4}{3})^{3/4}\,\frac{b^{1/3}}{\Gamma(\frac{4}{3})}\,(Gr\ Sc)^{1/4} \quad , \tag{7.12}$$

or

$$C = (\tfrac{4}{3})^{3/4}\,\frac{b^{1/3}}{\Gamma(4/3)} \quad , \tag{7.13}$$

where b can be related to the average shear stress by

$$b = (\tfrac{5}{4})\,\frac{\tau_o}{8\mu DL}\left(\frac{4\nu DL}{3g\alpha\Delta c}\right)^{3/4} = \frac{5}{32}(\tfrac{4}{3})^{3/4}\,B \tag{7.14}$$

The value derived for C in this way is 0.78586, ie.., 17% too high.

On the other hand, when the complete velocity profile is known as a result of the numerical computation, one can solve (7.9) numerically by two integrations:

$$\theta'(0) = \frac{+1}{\int_o^\infty \left[\exp -\int_o^\eta f\,d\eta\right] d\eta} \quad , \tag{7.15}$$

hence:

$$C^* = (\tfrac{4}{3})^{3/4} \Big/ \int_0^\infty \exp\Big(- \int_0^\eta f d\eta \Big)\, d\eta \qquad (7.16)$$

C^* is now the coefficient of diffusive mass transfer corresponding to the particular f profile. If we then normalize the values C_R by the value C^* corresponding to each, we do obtain the expected asymptotic behavior:

$$\frac{C_R}{C^*} \to 1 \quad \text{as} \quad r \to 1 \quad .$$

This can be seen in Table 7, where the most important results of the computation are collected.

Important differences exist between the results obtained on the assumption of complete dissociation of HSO_4^- and those for a system containing HSO_4^- only. The difference as far as the current is concerned, was already evident in figure 8. For the solution composition at the electrode the bisulfate model predicts a <u>decrease</u> in H_2SO_4 concentration at the electrode instead of an increase. This is illustrated in figure 10a, where the results[13] for migration at a rotating disk electrode and at a growing mercury drop have been sketched in for comparison. Also shown are the results of assuming a stagnant ("Nernst") diffusion layer, and some values obtained by the method of Wilke, Eisenberg and Tobias (see Table 2 and Appendix F).*

---

*The latter are different from actual excess concentrations reported by Wilke, Eisenberg and Tobias[24] and by Fenech and Tobias[50] (see figure 10b).

Since the two models predict very different acid concentrations at the electrode, the most direct test of their correctness would be to determine the solution composition at the electrode. Brenner[29] long ago succeeded in instantaneously freezing the solution surrounding a hollow cathode and cutting slices off the frozen mass in order to analyze them. His result (0.72) is not shown in figure 10 but appears to vindicate the assumption of complete dissociation. The freezing method is subject to criticism since the freezing, however fast it may occur, could change the composition in the very thin diffusion layer. Moreover, only one point has been obtained. However, interferometric measurements, which would not disturb the composition, have not been reported for free convection, so far. Measurements made in stagnant diffusion situations indicate that there is certainly an excess of H_2SO_4 at the cathode.[21,36] One of the difficulties is that the refractive index change depends on both $CuSO_4$ and H_2SO_4 concentration. For optical reasons interference patterns are hard to interpret at currents close to the limiting current; when working below the limiting current an independent measurement relating $CuSO_4$ and H_2SO_4 concentration is necessary.

That the sulfate model is correct, appears to contradict the limited dissociation which would follow from the constant:

$$K_{HSO_4^-} = \frac{a_{H^+}\, a_{SO_4^=}}{a_{HSO_4^-}} = 0.01 \text{(at 25°C)} \quad ,$$

reported in the literature. In fact, if this constant is taken into account in a computation of migration effects, the results are always very close to those for bisulfate only. This can be verified in Table 8, which lists the ratio C (partial dissociation)/C(bisulfate only) as a function of composition, for the rotating disk electrode.

However, the constant reported in the literature is a thermodynamic dissociation constant and is related to the true stoichiometric dissociation constant:

$$K'_{HSO_4^-} = \frac{c_{H^+} c_{SO_4^=}}{c_{HSO_4^-}}$$

by

$$K' = K f_{HSO_4^-} / f_{H^+} f_{SO_4^=} \qquad (7.17)$$

where f_i is the molar activity coefficient of the indicated ionic species. Therefore K' can be considered a function of the true ionic strength of the solution:

$$I_r = \frac{1}{2} \Sigma_i c_i z_i^2 \quad ,$$

where c_i is based on the dissociation equilibrium of HSO_4^-. Newman[21] recently correlated K' data from Raman spectral analysis of H_2SO_4 solutions by the expression:

$$\ln \left(\frac{K'}{K}\right) = \frac{5.29\sqrt{I_r}}{1+0.56\sqrt{I_r}} \qquad (7.18)$$

where K = 0.0104 mole/l and I_r is in mole/l. Figure 11 shows that K' varies by 3 orders of magnitude over a range of H_2SO_4 concentrations extending from 0 to 3 M. This would adequately explain the location of Brenner's datum, since his solution was 1 M $CuSO_4$ + 1 M H_2SO_4.

8. RESULTS FOR $K_3Fe(CN)_6$ - $K_4Fe(CN)_6$ - H_2O.

Although natural convection has been studied more frequently on vertical copper electrodes in acidified $CuSO_4$, there has also been made use of supported solutions of ferri- and ferrocyanide. The redox reaction:

$$Fe(CN)_6^{3-} + e \rightleftarrows Fe(CN)6^{4-} \qquad (8.1)$$

has the advantage of not changing the electrode surface, while copper deposition at or near the limiting current leads to an increase in area due to dendrite formation, apart from the obvious qualitative change which this causes in the structure of the electrode surface. On the other hand, the ferri/ferrocyanide system when supported is at least a four-component system, with the additional complications this entails in determining physical properties, changes in composition, etc. Also the densification in the system is much weaker than in $CuSO_4$, since the excess product ion compensates largely for the reactant deficit. Finally, the solubility of potassium ferri- and -ferrocyanide is much smaller than that of copper sulfate, which means that depletion of the electrolyte may be important if catholyte and anolyte are separated by a diaphragm.

As a preliminary to the supported ferri-/ferrocyanide system, the simple redox reaction (8.1) at a vertical cathode, and at a vertical anode, was studied.

In this system we cannot expect the migration current to be important, since the presence of a product ion will always lead to a reduced field strength near the electrode. This was already observed in migration calculations for ferri-/ferrocyanide reaction at the rotating disk.[13]

Figure 12 shows C/C_s values as a function of the ratio ferri-/ferrocyanide in the bulk. The variation is at most 20%. The solid lines are the main results, i.e., those for the physical properties listed in Table 4. Two points for the rotating disk are shown also. The dashed lines represent various alternatives where the physical properties have been given various arbitrary values. Figure 13 shows the surface concentrations of the product ion for these same situations. Here there is even less variation with bulk composition.

From these fictitious models one can try to make some inferences about the relative importance of diffusivity effects, compared to densification effects. The stagnant layer model and the rotating disk show practically the same values for maximum migration current and for surface product concentration. Migration in itself depresses the cathodic current and increases the anodic current. The ratio of importance for both current and surface concentration changes due to migration is:

$$\frac{z_1 D_1}{z_3 D_3}$$

where 1 is the supporting ion, 3 the reacting ion. If the diffusivities are equal, the excess surface concentrations assume values depending on the ratio z_1/z_3 (see Table 1), corresponding to electroneutrality with K^+ concentration uniform. There is no reason for any variation since in the stagnant model the layer thickness is the same for all ions and the identical diffusivities preclude changes in the shape of the profiles within the layer. The actual values of the diffusivity (D ferricyanide

is 21 % greater than D ferrocyanide) compensate partially for the difference in valence, so that the excess ferricyanide and the deficit ferrocyanide concentrations are smaller. Table 1 shows that the maximum migration contribution to the current (positive or negative) corresponds quantitatively to the fraction change in the excess surface concentration.

The solid lines in figures 12 and 13 indicate that the free convection generated by the concentration changes at the electrode, leads to a small increase in the limiting current, near $r_a = 1$ and $r_c = 1$, i.e., the concentration profiles close to the electrode are steepened, while the excess product concentrations change slightly in opposite directions. These effects, however, are all second-order compared to the migration effect itself. The relative unimportance of free convection interacting with migration is evidenced by the fact that it makes very small difference in C/C_s or the product concentrations, if we assign equal densification coefficients to reacting and product ions, although the sign of the driving density difference is then reversed! (see Table 9)

It appears that the only significant change occurring in the concentration profiles when the bulk composition is varied, is a change in their tails, i.e., the distance to which they extend into the solution, and a small change in the gradient at the electrode. Figure 14 shows the concentration profiles for cathodic and anodic cases in an equimolar solution, with actual diffusivities and densification coefficients.

From figure 12 it can be seen that only the assumption that diffusivities of reactant and product ion are equal, leads to a more pronounced change in migration current. This must be due to the fact that the difference in diffusivity no longer counteracts the difference

in valence, as illustrated earlier in the case of the stagnant layer model. However, setting all diffusivities equal, i.e., setting D of K^+ equal to that of the others and, in effect, lowering it thereby, steepens the K^+ profiles at the cathode and anode considerably and spreads the reactant and product profiles, thereby lowering their gradients at the electrode.

An important conclusion of this study of various physical property assumptions is that density differences driving the convection in the ferri-/ferrocyanide system are very small, and that a change in their sign can reverse the convection velocity without greatly affecting the concentration profiles. This is in part illustrated in Table 9, where the velocity far from the electrode is practically the same for the cases $\alpha_1 = \alpha_3$ and $\alpha_1 \neq \alpha_3$; so is the shear stress. The only change of significance when $\alpha_1 = \alpha_3$ is assumed and the driving density difference changes sign, is the appearance of a very inconspicuous maximum in the velocity, corresponding to a minimum in the driving density difference. Such a minimum was already encountered in the system $CuSO_4$ - H_2SO_4 - H_2O, where it was attributed to the very much greater diffusivity of H^+ ions which therefore extend the H^+ concentration excess far enough into the solution to compensate, at a certain point, the density deficit due to Cu^{++} ions.

Here we can expect the same to happen when OH^- ions are added to the solution. However, the distortion of the velocity profile will be more drastic since the driving force, $\Delta\rho/\Delta\rho_R$, is relatively smaller and the concentration profiles, when no OH^- is present, are more crowded toward the electrode than in the case of $CuSO_4$ (figure 14).

Table 10 summarizes the most important results of the computations for $K_3Fe(CN)_6$ - $K_4Fe(CN)_6$ - H_2O.

9. RESULTS FOR SUPPORTED FERRI-/FERROCYANIDE

Two supporting electrolytes were considered: KOH and NaOH. The latter, although leading to a five-ion system with consequent complications in physical property estimation, has been used as frequently as the former in reported investigations.[37,38]

Figure 15 shows the values of the migration current for equimolar ferri-/ferrocyanide solutions with various amounts of KOH added. Conspicuous is the deviation of these results from those for the rotating disk, indicating a strong dissimilarity of the density profile in the supported solution compared to that in a binary solution. This dissimilarity appears to grow stronger as the amount of KOH is increased. Beyond $c_{OH^-}/c_{K^+} = 0.85$ the cathodic case does not converge. The reason for this behavior is plain from figure 16 and, more directly, from figure 17, which shows the velocity profiles. There is a velocity maximum which at weak concentrations of OH^- occurs at a fair distance from the electrode, approximately comparable to the distance at which the maximum occurs in $CuSO_4$ with excess H_2SO_4 (see figure 9). However, at higher OH^- concentrations the maximum occurs much closer to the electrode and at the same time decreases in amplitude. The reason for this is suggested by the profile for $c_{OH^-}/c_{K^+} = 0.95$, which yields a converged, but physically inconsistent solution: the velocity far from the electrode has reversed sign.

Apparently there is with increasing OH^- concentration such a strong reversal of the density difference at some distance from the

electrode, that eventually the velocity has a tendency toward inversion. The resulting velocity profile is physically inconsistent since the boundary layer model clearly breaks down when reversed flow occurs.

This situation is only different in degree from the one encountered in the case of supported $CuSO_4$. The two cases are compared in figure 18, where the normalized density profiles are plotted against the dimensionless distance (based on characteristic density difference at the electrode).

It can be shown that for $f'(\infty)$ to be zero or negative the first moment of the density distribution has to be zero or negative:

$$f''' = \Delta\rho \quad \rightarrow$$

$$f'' = \int_{\infty}^{\eta} \Delta\rho \, d\eta \quad \rightarrow$$

$$f' = \int_{0}^{\eta} \int_{\infty}^{\eta} \Delta\rho \, d\eta \, d\eta =$$

$$\eta \int_{\infty}^{\eta} \Delta\rho \, d\eta + \int_{0}^{\eta} \eta\Delta\rho d\eta =$$

$$\eta \left[\int_{\infty}^{0} \Delta\rho \, d\eta - \int_{\eta}^{0} \Delta\rho \, d\eta \right] + \int_{0}^{\eta} \eta\Delta\rho \, d\eta =$$

$$\eta f''(0) + \int_{0}^{\eta} \Delta\rho(\eta + \xi) \, d\xi \quad \rightarrow$$

$$f'(\infty) = \int_{0}^{\infty} \Delta\rho\eta d\eta$$

Therefore, the closer to the electrode a reversal of density difference occurs, the greater the chance that the asymptotic velocity is negative. But even before this happens, the velocity profile may have become unstable. It is known from the theory of hydrodynamic

instability[39,40] that boundary layers with an inflected velocity profile are inherently less stable with respect to certain low perturbation frequencies. It follows that if transition to turbulence takes place in supported solutions, being induced by ionic mobility differences, it may take place at lower Grashof numbers than for regular free convection in binary solutions or due to heat transfer. This conclusion should be open to experimental verification.

Unfortunately the experimental evidence on transition in free convection is rather confusing. Only in heat transfer experiments with air (Pr = 0.7) has a transition region been defined by measuring velocity and temperature fluctuations. In air the lower limit of the transition region is, by agreement of several experimenters[41,42]:

$$Gr > 2.10^9 \quad ,$$

below which the laminar relation is valid:

$$Nu = 0.472\ Gr^{1/4}$$

An upper limit of transition is:

$$Gr < 10^{10}$$

above which turbulent heat transfer takes place. In air, if $8.10^9 < Gr < 2.10^{10}$, it appears that:

$$Nu = 0.1\ (GrPr)^{1/3}$$

represents the experimental data[41,45] well, but in full turbulence, $Gr > 2.10^{10}$, there is a better fit with the expression

$$Nu = 0.021\ (Gr\ Pr)^{0.4}$$

In heat transfer experiments[45] with water and with liquids of $Pr \approx 100$, the exponent 1/3 seems to be more satisfactory on Gr, but Pr has a different exponent, 0.43. This points to a dependence on Pr which apparently also exists in the transition criterion, since the separation between regimes was put at $Gr\ Pr = 4.10^{10}$.

Wilke, Tobias and Eisenberg[46] report experiments on dissolution of organic acids in water, where laminar mass transfer relations still hold at $Gr\ Sc = 2 \times 10^{10}$. Wagner,[43] in salt dissolution experiments, observed that the flow was still laminar at $Gr\ Sc = 5 \times 10^{11}$.

Fouad and Ibl[38] place the transition in acidified $CuSO_4$ solutions, observed optically, between $2 \times 10^{11} < Gr\ Sc < 4 \times 10^{13}$. They suggest that there is a separate dependence on Sc. Wilke, Eisenberg and Tobias[24] correlate laminar free convection in acidified $CuSO_4$ solutions up to $Gr\ Sc = 5 \times 10^{11}$. Fouad and Gouda[44] report transition in ferricyanide reduction with excess NaOH at $Gr\ Sc = 4.6 \times 10^{11}$.

One can hardly infer that destabilization had taken place in the supported solutions. However, in such solutions the density difference has to be estimated (usually by the method of Wilke, Eisenberg and Tobias[24]), which can lead to appreciable errors.

Since the inertial terms in the equation of motion were neglected in this analysis it follows that a theoretical treatment of instability in electrolytic free convection could also simplify the unsteady equation of motion, retaining only viscous and buoyancy terms. The result would be analogous in form to the so-called viscous solutions in forced flow instability,[40] except for the unknown effect of coupling to the diffusion equation. No solutions are available for high Pr free convection instability. Gebhart[47] reports the absence, in low Pr free convection instability, of a critical layer (corresponding in forced flow to the velocity profile inflection) where the disturbance velocity equals the steady velocity. One might conclude therefore, that the velocity profile inflection obtained in this work does not necessarily indicate instability.

The appearance of velocity profiles which exhibit velocity maxima also has implications for the concept of similarity as applied to supported solutions in free convection. The analyses in the past have utilized the assumption that similarity variables based on the total density difference between electrode and bulk solution will characterize the velocity and density profiles for each composition. Clearly this single parameter is not sufficient if one would want to design a similarity transformation that should also encompass the profiles in solutions of different composition. Figure 18 shows that there is not only a minimum density at the electrode, but also a maximum at some distance into the solution. A complete similarity over the range of r would imply that the maximum always occur at the same distance from the electrode (in terms of the new variable). This is already contradicted by the absence of a density maximum when OH^- is absent.

Figure 19 shows the surface concentrations with excess KOH. It is remarkable how close the values are to those for the rotating disk, and how little this similarity is disturbed by the anomaly of the velocity profile as the OH^- concentration increases. This is another confirmation of the earlier statement that what happens close to the electrode is very little influenced by the densification, i.e., the specific shape of the velocity profile, and more by the relative mobility of the ions, as in a stagnant layer model.

Table 11 gives the main results for the system

$K_3Fe(CN)_6$ - $K_4Fe(CN)_6$ - KOH - H_2O.

The current and surface concentrations for the system $K_3Fe(CN)_6$ - $K_4Fe(CN)_6$ - NaOH - H_2O are very similar to those obtained with KOH. The values are summarized in Table 12. Figures 20, 21 and 22 illustrate the results in complete analogy to figures 15, 16 and 19. The velocity f'_∞ in figure 21 shows negative, anomalous, values beyond $c_{OH^-}/(c_{K^+} + c_{Na^+}) = 0.75$, in the cathodic case. The anodic reaction shows a smooth, converged behavior all the way to $c_{OH^-}/(c_{K^+} + c_{Na^+}) = 1$, but the curve of f'_∞, though positive throughout, has an incongrous tail as c_{OH^-} excess is reached. Figure 22 shows how close the surface concentrations are to those reported with KOH as supporting electrolyte, and, by implication, to those for the rotating disk.

Finally, figure 23 shows typical concentration profiles in the system $K_3Fe(CN)_6$ - $K_4Fe(CN)_6$ - NaOH - H_2O.

10. ALTERNATIVE PROCEDURE FOR NUMERICAL SOLUTION

In the computations above, the equation of motion, the equations of convective diffusion and the electroneutrality equation were solved simultaneously after linearization. This procedure is simple and, if it converges, does so fast since convergence is quadratic. On the other hand there is no guarantee that convergence will occur, in particular when density differences change sign from one iteration to the next, as is bound to happen, e.g., in the case of supported ferri-/ferrocyanide. In some of these cases use was made of an alternative procedure which is slower to converge but offers more probability of convergence since it uncouples the equation of motion from the equations of convective diffusion.

First the equations of convective diffusion and the electroneutrality equation are solved with an assumed velocity profile of the general form:

$$f = 3b\eta^2 \quad . \tag{7.8}$$

Upon convergence an improved streamfunction profile is computed from the density profile by a triple integration:

$$f'''(\eta) = \Delta\rho(\eta) \quad ; \tag{10.1}$$

$$f''(\eta) = \int_{\infty}^{\eta} \Delta\rho \, d\eta \; ; \tag{10.2}$$

$$f'(\eta) = \int_{0}^{\eta} \int_{\infty}^{\eta} \Delta\rho \, d\eta \, d\eta \; ; \tag{10.3}$$

$$f(\eta) = \int_{0}^{\eta} \int_{0}^{\eta} \int_{\infty}^{\eta} \Delta\rho \, d\eta \, d\eta \, d\eta \quad . \tag{10.4}$$

The new f is inserted in the equations of convective diffusion:

$$\frac{D_i}{D_R}\theta_i'' + \frac{z_i u_i RT}{D_R}(\theta_i\phi')' + f\theta_i' = 0 \qquad (4.15)$$

and the system of equations is solved again, producing a new density profile which yields a new velocity profile, etc. Convergence with a fixed velocity profile is usually faster than in the completely uncoupled procedure, but convergence to a final velocity profile can be very slow.

Convergence of the velocity profile can be helped by adjusting the variables f and η so that they are based on the densification at the electrode after every iteration. One assumes then a new streamfunction proportional to f:

$$f_1 = A_1 f \qquad (10.5)$$

and a new distance variable

$$\xi = A_2\eta \quad , \qquad (10.6)$$

The factors A_1 and A_2 are adjusted so that the current at the electrode is numerically the same as in the (f,η) profile:

$$C = \frac{(\frac{4}{3})^{3/4}\ \Theta'_{R,o}}{\left[\sum_i A_i(\Theta_{i,o}-\theta_{i,\infty})\right]^{1/4}} = \frac{(\frac{4}{3})^{3/4}\ \Theta'_{R,o}}{(f'''_o)^{1/4}} = \frac{(\frac{4}{3})^{3/4}}{(f'''_o)^{1/4}\int_o^\infty \exp\left[-\int_o^\eta f d\eta\right]d\eta}$$

$$= \frac{(\frac{4}{3})^{3/4}\ (A_1A_2)^{1/4}}{\left(\frac{d^3f_1}{d\xi^3}\right)_o \int_o^\infty \exp\left[-A_1A_2\int_o^\xi f_1 d\xi\right]d\xi} \qquad (10.7)$$

so, $A_1A_2 = 1$, and

$$\left(\frac{d^3f_1}{d\xi^3}\right)_o = 1 \rightarrow \frac{A_1}{A_2^3}\ f'''_o = 1 \rightarrow$$

$$A_2 = \left(\frac{\Delta\rho}{\alpha_R \Delta c_R}\right)^{1/4}$$

It is easy to see that f_1 and ξ are identical, respectively, to $f_{\Delta\rho}$ and $\eta_{\Delta\rho}$ as defined in (7.6) and (7.7).

The actual program used is reproduced in Appendix C.

11. FREE CONVECTION WITH UNIFORM FLUX

The work reported so far concerns free convection under conditions of uniform concentration at the electrode. Another boundary condition, of considerable importance in electrochemical systems, is that of uniform current density at the electrode. Wagner[49] has shown that at current densities below approximately 1/3 of the limiting current density, there is a substantially uniform distribution of the

current over vertical plate electrodes facing each other, as a result of kinetic limitations and ohmic drop.

The equation of convective diffusion and the equation of motion were solved for a binary electrolyte, with the condition of uniform flux at the electrode. It appears from the literature that this has not been done earlier for the case of $Sc \to \infty$.

The appropriate equations in this case are:

$$\nu \frac{\partial^3 \psi}{\partial y^3} + \frac{\rho - \rho_\infty}{\rho_\infty} g_x = 0 \quad , \tag{11.1}$$

$$\frac{\partial \psi}{\partial y} \frac{\partial c_s}{\partial x} - \frac{\partial \psi}{\partial x} \frac{\partial c_s}{\partial y} = D_s \frac{\partial^2 c_s}{\partial y^2} \quad , \tag{11.2}$$

$$\frac{\rho - \rho_\infty}{\rho_\infty} = \alpha_s (c_s - c_{s,\infty}) \quad , \tag{11.3}$$

and the boundary conditions:

$$\frac{\partial \psi}{\partial y} = - \frac{\partial \psi}{\partial x} = 0 \quad , \quad N_s = - D_s \frac{\partial c_s}{\partial y} \text{ at } y = 0 \quad , \tag{11.4}$$

$$\frac{\partial^2 \psi}{\partial y^2} = 0 \quad , \quad c_s = c_{s,\infty} \text{ at } y = \infty \quad , \tag{11.5}$$

$$\frac{\partial \psi}{\partial y} = 0 \quad , \; c_s = c_{s,\infty} \text{ at } x = 0 \quad . \tag{11.6}$$

The appropriate transformation is now:

$$\eta_s = \frac{y (Gr_s^*)^{1/5}}{(5xL^4)^{1/5}} \quad , \tag{11.7}$$

$$\psi = D_s \left(\frac{5x}{L}\right)^{4/5} (Gr_s^*)^{1/5} f_s(\eta_s) \quad , \tag{11.8}$$

$$c_s - c_{s,\infty} = \frac{N_s L}{D_s} \left(\frac{5x}{LGr_s^*}\right)^{1/5} \theta_s(\eta_s) \quad , \tag{11.9}$$

where $$Gr_s^* = \frac{g_x \alpha_s N_s L^4}{\nu D_s^2} \quad . \tag{11.10}$$

The equations become:

$$\frac{d^3 f_s}{d\eta_s^3} + \theta_s = 0 \quad , \tag{11.11}$$

$$\frac{d^2\theta_s}{d\eta_s^2} + 4f_s \frac{d\theta_s}{d\eta_s} - \theta_s \frac{df_s}{d\eta_s} = 0 \quad , \tag{11.12}$$

and the boundary conditions:

$$\text{at } \eta_s = 0 \quad , \quad f_s = \frac{df_s}{d\eta_s} = 0 \quad , \quad d\theta_s/d\eta_s = -1 \quad , \tag{11.13}$$

$$\text{at } \eta_s = \infty \quad , \quad \theta_s = 0 \quad , \quad \frac{d^2 f_s}{d\eta_s^2} = 0 \quad . \tag{11.14}$$

These equations were solved by the method discussed in section 5. Only (11.12) and one boundary condition in (11.13) are different from the set of equations solved in section 6.

The results of interest are:

$$c_{s,0} - c_{s,\infty} = \frac{N_s L}{D_s} \left(\frac{5x}{LGr_s^*}\right)^{1/5} \theta_s(0) \tag{11.15}$$

$$\tau_o = - \frac{\mu D_s}{L^2} \left(\frac{5x}{L}\right)^{2/5} (Gr_s^*)^{3/5} f''(0) \qquad (11.16)$$

Table 13 shows these results in comparison with values computed by Sparrow and Gregg[48] for finite Schmidt numbers. They agree very well with the trend of Sparrow and Gregg's results.

An attempt can be made to extend this work to supported electrolyte solutions under uniform flux conditions. Equation (11.2) is then replaced by one equation each for all species:

$$\frac{\partial \psi}{\partial y} \frac{\partial c_i}{\partial x} - \frac{\partial \psi}{\partial x} \frac{\partial c_i}{\partial y} = D_i \frac{\partial^2 c_i}{\partial y^2} - z_i u_i F \frac{\partial}{\partial y} (c_i E_y) \qquad (11.17)$$

where E_y is the y-component of the electric field in the solution. Further one has the electroneutrality condition:

$$\sum_i z_i c_i = 0 \quad . \qquad (11.18)$$

The densification is:

$$\frac{\rho - \rho_\infty}{\rho_\infty} = \sum_i \alpha_i (c_i - c_{i\infty}) \quad . \qquad (11.19)$$

The boundary conditions for the species concentrations are:

$$s_i i_y = - nFN_{iy} = nF\left(D_i \frac{\partial c_i}{\partial y} - z_i u_i F c_i E_y\right) \qquad (11.20)$$

$$\text{at } y = 0 \quad ,$$

$$c_i = c_{i\infty} \quad \text{at} \quad y = \infty \quad , \tag{11.21}$$

$$c_i = c_{i\infty} \quad \text{at} \quad x = 0 \quad . \tag{11.22}$$

Assume similarity variables as follows:

$$\eta = \frac{y}{(5xL^4)^{1/5}} (Gr_R^*)^{1/5} \quad , \tag{11.23}$$

$$E_y = \frac{RT}{FL} Qx^q \varepsilon(\eta) \quad , \tag{11.24}$$

$$c_i - c_{i\infty} = \frac{s_R i_y L}{nFD_R} \left(\frac{5x}{LGr_R^*}\right)^{1/5} \theta_i(\eta) \quad , \tag{11.25}$$

$$\psi = D_R \left(\frac{5x}{L}\right)^{4/5} (Gr_R^*)^{1/5} f(\eta) \quad , \tag{11.26}$$

where

$$Gr_R^* = - \frac{s_R i_y \alpha_R q_x L^4}{nFD_R^2 \nu} \quad . \tag{11.27}$$

Then the equations become:

$$f''' - \sum_i \frac{\alpha_i}{\alpha_R} \theta_i = 0 \tag{11.28}$$

$$\sum_i z_i \theta_i = 0 \tag{11.29}$$

$$4f\theta_i' - f'\theta_i + \frac{D_i}{D_R} \left\{ \theta_i'' - \frac{z_i Q}{AL} x^{q+\frac{1}{5}} \left[(\theta_i \varepsilon)' + \frac{c_i^\infty \varepsilon'}{Bx^{1/5}} \right] \right\} = 0 \tag{11.30}$$

and the boundary conditions:

$$\eta = 0 \quad , \quad f = f' = 0 \tag{11.31}$$

$$\eta = 0 \quad , \quad \frac{D_R s_i}{D_i s_R} = \left\{ \theta_i' - \frac{z_i Q}{AL} x^{q+\frac{1}{5}} \left[\theta_i \varepsilon + \frac{c_i^{\infty} \varepsilon}{B x^{1/5}} \right] \right\} \quad , \qquad (11.32)$$

$$\eta = \infty \quad , \quad \theta_i = 0 \quad , \quad f'' = 0 \qquad (11.33)$$

where

$$AL = \left(\frac{1}{5} LGr_R^*\right)^{1/5} \text{ and } B = \frac{s_R i_y L}{nFD_R} \left(\frac{5}{LGr_R^*}\right)^{1/5} .$$

There are 3 tractable cases:

1. $c_i << Bx^{1/5}$ or $BL^{1/5}$, i.e., long electrodes, dilute solutions, high currents, since:

$$\frac{1}{5} Gr_R^{*\,1/5} << \frac{s_R i_y L}{nFD_R \sum_i c_{i\infty}} \quad . \qquad (11.34)$$

If one sets $q = -1/5$, $Q = AL$, then:

$$E_y = \frac{RT}{FL} \left(\frac{LGr_R^*}{5x}\right)^{1/5} \varepsilon(\eta) \qquad (11.35)$$

The mass transfer equation becomes:

$$4f\theta_i' - f'\theta_i + \frac{D_i}{D_R} \left\{ \theta_i'' - z_i (\theta_i \varepsilon)' \right\} = 0 \quad , \qquad (11.36)$$

and the flux condition:

$$\frac{D_R s_i}{D_i s_R} = \theta_i' - z_i \theta_i \varepsilon \quad \text{at} \quad \eta = 0 \quad . \qquad (11.37)$$

Since $c_{Ro} = c_{R\infty} + Bx^{1/5}\theta_R(0)$, and $\theta_i(0)$ is of order unity, the condition

$$Bx^{1/5} >> c_{R\infty}$$

implies that c_{Ro} is negative, i.e., a physically impossible situation.

2. $c_i^\infty >> Bx^{1/5}$ or $BL^{1/5}$, i.e., short electrodes, concentrated solutions, low currents, since:

$$(\frac{1}{5} Gr_R^*)^{1/5} >> \frac{s_R i_y L}{nFD_R \Sigma c_{i\infty}} \tag{11.38}$$

If one sets $q = 0$, $\frac{Q}{LAB} \Sigma z_i^2 c_{i\infty} = 1$, then:

$$E_y = \frac{RT}{FL} \frac{s_R i_y L}{nFD_R \Sigma z_i^2 c_{i\infty}} \varepsilon(\eta) \quad . \tag{11.39}$$

The mass transfer equation becomes:

$$4f\theta_i' - f'\Theta_i + \frac{D_i}{D_R}\left[\Theta_i'' - z_i \frac{c_{i\infty}\varepsilon'}{\Sigma z_i^2 c_{i\infty}}\right] = 0 \quad , \tag{11.40}$$

and the flux condition becomes:

$$\frac{D_R s_i}{D_i s_R} = \theta_i' - \frac{z_i c_{i\infty} \varepsilon}{\Sigma z_i^2 c_{i\infty}} \quad \text{at} \quad \eta = 0 \tag{11.41}$$

This case is valid only under a very restrictive assumption, implying that the current level is far below the limiting current, and that the effect of migration is small to start with (low field strength).

3. ε can be eliminated in the case of a binary solution. This was done at the beginning of this section, where equations (11.1-11.6) were written as for an undissociated solute. The relation with the species equations (11.17) is obtained via the definitions:

$$\theta_e = \theta_+/\nu_+ = \theta_-/\nu_- \quad , \tag{11.42}$$

$$\alpha_s = \nu_+\alpha_+ + \nu_-\alpha_- \quad , \tag{11.43}$$

$$D_s = \frac{\nu_+ D_+ + \nu_- D_-}{\nu_+ + \nu_-} \quad . \tag{11.44}$$

Elimination of E_y leads to the equations:

$$f''' - \frac{\alpha_s}{\alpha_R}\theta_e = 0 \quad , \tag{11.45}$$

$$4f\theta_e' - f'\theta_e + \frac{D_s}{D_R}\theta_e'' = 0 \quad , \tag{11.46}$$

with boundary conditions:

$$\eta = 0 \quad , \quad f = f' = 0 \quad , \tag{11.47}$$

$$\eta = 0 \quad , \quad \theta_e' = \frac{D_R}{s_R(\nu_+ + \nu_-)}\left(\frac{s_+}{D_+} + \frac{s_-}{D_-}\right) \quad , \tag{11.48}$$

$$\eta = \infty \quad , \quad \theta_e = 0 \quad , \; f'' = 0 \quad . \tag{11.49}$$

The similarity variables η, f, θ_e above are still those defined in (11.23, 11.25-11.27).

To obtain the equations (11.1-11.6) these variables are redefined, or "stretched", as follows:

$$\eta_s = A\eta \quad , \tag{11.50}$$

$$\theta_s = B\theta_e \quad , \tag{11.51}$$

$$f = Cf_s \quad , \tag{11.52}$$

where, e.g., for the case $s_- = 0$, $s_+ = s_R$, $D_+ = D_R$:

$$A = \left(\frac{\alpha_s D_R}{(\nu_+ + \nu_-)\alpha_+ D_s}\right)^{1/5} \tag{11.53}$$

$$B = -(\nu_+ + \nu_-)\left(\frac{\alpha_s D_R}{(\nu_+ + \nu_-)\alpha_+ D_s}\right)^{1/5} \tag{11.54}$$

$$C = \frac{D_s}{D_R}\left(\frac{\alpha_s D_R}{(\nu_+ + \nu_-)\alpha_+ D_s}\right)^{1/5} \quad . \tag{11.55}$$

Table 1. Ratio of maximum limiting current to limiting diffusion current (I_L/I_D) and electrolyte composition at the electrode for limiting diffusion current ($\Delta c_{supp.,prod.}/\Delta c_{react.}$) according to the Nernst (stagnant) layer model.

reacting ion	counter ion	supporting ion	I_L/I_D (r=0)	$\Delta c_{supp.}/\Delta c_{react.}$ (r=1)
Cu^{++}	$SO_4^{=}$	H^+	2	$\Delta c_{H_2SO_4}/\Delta c_{CuSO_4} = 0.333$
Cu^{++}	HSO_4^-	H^+	3	$\Delta c_{H_2SO_4}/\Delta c_{CuSO_4} = 0$
H^+	Cl^-	K^+	2	$\Delta c_{KCl}/\Delta c_{HCl} = 0.5$
		product ion	I_L/I_D***	$\Delta c_{prod.}/\Delta c_{react.}$
*$Fe(CN)_6^{3-}$	K^+	$Fe(CN)_6^{4-}$	0.8389	$\Delta c_{ferroc.}/\Delta c_{ferric.} = 0.843$
*$Fe(CN)_6^{4-}$	K^+	$Fe(CN)_6^{4-}$	1.2178	$\Delta c_{ferric.}/\Delta c_{ferroc.} = 1.207$
**$Fe(CN)_6^{3-}$	K^+	$Fe(CN)_6^{4-}$	0.90215	$\Delta c_{ferroc.}/\Delta c_{ferric.} = 0.80$
**$Fe(CN)_6^{4-}$	K^+	$Fe(CN)_6^{3-}$	1.1277	$\Delta c_{ferric.}/\Delta c_{ferroc.} = 1.25$

*$D_{ferric.}/D_{ferroc.} = 1.2132$

**$D_{ferric.}/D_{ferroc.} = 1$

***Product ion absent in bulk

Table 2. Supporting electrolyte concentrations in various electrolytic solutions according to the method of Wilke, Eisenberg and Tobias.[24] *

$CuSO_4$-H_2SO_4-H_2O	$\sqrt{r}$	$\frac{\Delta C_{H_2SO_4}}{\Delta C_{CuSO_4}}$ at cathode	
$r = \frac{c_{H_2SO_4}}{c_{CuSO_4}+c_{H_2SO_4}}$	0.1	0.0182	
	0.25	0.0932	
	0.50	0.2267	
	0.75	0.3086	
	0.9	0.3385	
	1	0.3533	
$K_3Fe(CN)_6$-$K_4Fe(CN)_6$-H_2O	r	$\frac{\Delta c_{ferro}}{\Delta c_{ferri}}$	$\frac{\Delta c_{ferri}}{\Delta c_{ferro}}$ **
$r = \frac{c_{ferro}}{c_{ferro}+c_{ferri}}$	0	2.4203	0.4132
	0.5	0.8696	1.1499
	1.0	0.4062	2.4617
$K_3Fe(CN)_6$-$K_4Fe(CN)_6$ -KOH-H_2O	r_{OH}	$\frac{\Delta c_{OH}}{\Delta c_{ferri}}$	$\frac{\Delta c_{OH}}{\Delta c_{ferro}}$
$r = 0.5$ $r_{OH} = \frac{c_{OH^-}}{c_{K^+}}$	0.25	-0.1798	0.1935
	0.5	-0.3005	0.3101
	0.75	-0.3871	0.3879
	1.0	-0.4523	0.4523

(Table 2. Continued)

---

*Salt diffusivities and ionic transference numbers are based on infinite silution mobilities (see Table 4).

**$$\frac{\Delta c_{ferri}}{\Delta c_{ferro}}_{anodic} = \left(\frac{\Delta c_{ferro}}{\Delta c_{ferri}}\right)^{-1}_{cath}$$.

***$\frac{\Delta c_{OH}}{\Delta c_{ferri}}$ $\frac{\Delta c_{OH}}{\Delta c_{ferro}}$ does not agree with the value of

$\frac{\Delta c_{ferro}}{\Delta c_{ferri}}$ for r = 0.5

Table 3. Coefficients of mass-transfer and shear stress relations for free convection, according to Ostrach,[1] Sparrow and Gregg,[3] Le Fevre[4] and Kuiken.[9]

Sc(Pr)	Source (Ref.)	C_1	C_2	C	B_1	B
0	4,9		0.800544		1.21051	
0.003	3	0.0425	0.776	0.1816	1.1566	0.2707
0.01	11	0.07656	0.7656	0.2421	1.1158	0.3528
0.03	3	0.1269	0.7327	0.3049	1.0617	0.4418
0.72	1	0.4757	0.5607	0.5165	0.7648	0.7045
0.733	1	0.4789	0.5594	0.5176	0.7627	0.7057
1	1	0.5347	0.5347	0.5347	0.7265	0.7265
10	1	1.1025	0.3486	0.6200	0.4743	0.8434
100	1	2.066	0.2066	0.6532	0.2848	0.9005
1000	1	3.739	0.1182	0.6649	0.1641	0.9225
∞	4			0.670327		0.932835

$$Nu = C_1\, Gr^{1/4} = C_2(GrSc^2)^{1/4} = C(GrSc)^{1/4}$$

$$\frac{\tau_o}{\rho Lg\alpha\Delta c} = B_1 Gr^{-1/4} = B(GrSc)^{-1/4}$$

Table 4. Physical property parameters used for various electrolytic systems, at 25°C.

	R_i	T_i	s_i	z_i
H^+	13.0522	0.2139	0	1
$SO_4^=$	1.4925	0	0	-2
Cu^{++}	1	1	1	2
H^+	13.0522	0.2996	0	1
HSO_4^-	1.8657	0	0	-1
Cu^{++}	1	1	1	2
OH^-	5.8692	0.2708	0	-1
Na^+	1.4885	-0.0402	0	1
$Fe(CN)_6^{4-}$	0.8243	1.3506	1	-4
K^+	2.1837	0	0	1
$Fe(CN)_6^{3-}$ (reacts)	1	1	-1	-3
OH^-	7.1206	0.2005	0	-1
Na^+	1.8059	-0.0298	0	1
$Fe(CN)_6^{3-}$	1.2132	0.7404	-1	-3
K^+	2.6492	0	0	1
$Fe(CN)_6^{4-}$ (reacts)	1	1	1	-4

Table 5. Values of C_s and B_s in equations (6.4) and (6.5) depending on meshwidth H (100 meshpoints).

H	C_s	B_s
0.02	1.0788	0.49981
0.025	0.89344	0.61202
0.035	0.72723	0.78763
0.045	0.68055	0.88267
0.050	0.67388	0.90603
0.075	0.67019	0.93245
0.100	0.67016	0.93296
0.120*	0.67008	0.93294
0.140*	0.67001	0.93308

*70 meshpoints.

Table 6. Values of C_s and B_s in equations (6.4) and (6.5) obtained with the complete equation of motion, compared to literature values.

Sc	C This work	C Kuiken[6]	C Ostrach[1]	B This work	B Kuiken[6]	B Ostrach[1]
10	0.6200	0.46582	0.61999		0.84848	0.8434
100	0.6533	0.65339	0.65323		0.90067	0.9005
1000	0.6653	0.66484	0.66494		0.92211	0.9225
			Le Fevre[4]			Le Fevre[4]
$^*_\infty$	0.670327	0.67033	0.670327	0.93283	0.93283	0.932835

Table 7. Principal results for the system $CuSO_4$-H_2SO_4-H_2O.

A. System Cu^{++}-$SO_4^{=}$-H^+-H_2O. (H=0.0611, NJ=150)

r	C	C_R/C^*	B	f'_∞	f'_{max}	$\Delta C_{H_2SO_4}/C_{CuSO_4}$
0.	1.28106	1.86489	0.97569	0.9675		0
0.0909	0.98728	1.48050	0.91609	0.8823	0.8852	0.1739
0.16667	0.90573	1.36961	0.90386	0.8867	0.8538	0.2412
0.33333	0.80727	1.23374	0.89064	0.7926	0.8103	0.3234
0.55556	0.73037	1.12763	0.87964	0.7352	0.7682	0.3879
0.83333	0.66651	1.04043	0.86882	0.6738	0.7263	0.4406
0.98039	0.64005	1.00471	0.86364	0.6443	0.7070	0.4619
0.99800	0.63712	1.00077	0.86304	0.6409	0.7048	0.4642
0.99980	0.63683	1.00037	0.86298	0.6405	0.7046	0.4644
0.99998	0.63680	1.00033	0.86297	0.6405	0.7046	0.4644

B. System Cu^{++}-HSO_4^--H^+-H_2O. (H=0.0611, NJ=150)

r	C	C_R/C^*	B	f'_∞	f'_{max}	$\Delta C_{H_2SO_4}/C_{CuSO_4}$
0.56250	1.07659	1.61485	0.91307	0.8734	0.8847	-0.3095
0.64000	0.89753	1.37271	0.88724	0.7782	0.8081	-0.0994
0.72250	0.79716	1.23642	0.87092	0.7072	0.7563	0.0186
0.81000	0.72556	1.13955	0.85762	0.6458	0.7143	0.1014
0.90250	0.66897	1.06348	0.84567	0.5897	0.6784	0.1653
0.98010	0.63043	1.01211	0.83657	0.5467	0.6506	0.2079
0.99800	0.62176	1.00144	0.83357	0.5291	0.6424	0.2175
0.99980	0.62157	1.00039	0.83435	0.5363	0.6441	0.2175
0.99998	0.62149	1.00028	0.83433	0.5362	0.6441	0.2176

Table 8. C(partial dissociation)/C(bisulfate only) for the rotating disk electrode (K=0.01).

r	$c_{H_2SO_4}$		
	1.5M	1.0M	0.5M
0.95	0.9994	0.9991	0.5M
0.90	0.9987	0.9980	0.9960
0.85	0.9976	0.9964	0.9927
0.80	0.9954	0.9929	0.9852
0.75	0.9818	0.9729	0.9505

$$r = c_{H_2SO_4} / (c_{H_2SO_4} + c_{CuSO_4})$$

Table 9. Specific density difference electrode/bulk, dimensionless velocity far from the electrode, and shear stress in various systems.

System	$\frac{\Delta C}{\Delta C_R}$	f'_∞	f''_o
$CuSO_4$-H_2O	1	0.9675	0.97569
$CuSO_4$-H_2SO_4-H_2O			
excess H_2SO_4	0.8952	0.6405	0.86297
$K_3Fe(CN)_6$-$K_4Fe(CN)_6$-H_2O			
equimolar			
cathodic $\alpha\neq\alpha$, $D\neq D$	-0.1368	0.335	0.94988
$\alpha=\alpha$, $D\neq D$	0.1583	0.345	0.93640
$\alpha\neq\alpha$, $D_1=D_3$	-0.0974	0.360	1.06851
$\alpha=\alpha$, $D_1=D_2=D_3$	-0.0805	0.258	0.94904
anodic $\alpha\neq\alpha$, $D\neq D$	0.1140	0.320	0.95507
$\alpha=\alpha$, $D\neq D$	-0.1966	0.375	0.90116
$\alpha\neq\alpha$, $D_1=D_3$	0.0910	0.348	1.05478
$\alpha=\alpha$, $D_1=D_2=D_3$	0.0745	0.232	0.90991
$K_3Fe(CN)_6$-$K_4Fe(CN)_6$-KOH-H_2O			
equimolar, $c_{OH^-}/c_{K^+}=0.5$			
cathodic	-0.4298	0.6365	0.85743
anodic	0.3812	0.6713	0.86447
$K_3Fe(CN)_6$-$K_4Fe(CN)_6$-NaOH-H_2O			
equimolar, $c_{OH}/(c_{K^+}+c_{Na^+})=0.5$			
cathodic	-0.4230	0.6035	0.84164
anodic	0.3680	0.6478	0.85216

Table 10. Principal results for the system $K_3Fe(CN)_6$-$K_4Fe(CN)_6$-H_2O

A. Cathodic reaction. (H=0.08, NJ=150)

r_c	C	C_R/C^*	B	f'_∞	$\Delta c_{ferroc}/\Delta c_{ferric}$
0.000286	0.58726	0.86816	0.95211	0.9043	0.8379
0.1	0.59753	0.88338	0.95154	0.9061	0.8387
0.25	0.61236	0.90531	0.95081	0.9087	0.8399
0.5	0.63551	0.93947	0.94988	0.9128	0.8417
0.75	0.65694	0.97102	0.94923	0.9164	0.8434
0.9	0.66907	0.98883	0.94894	0.9185	0.8444
0.9996	0.67683	1.00023	0.94878	0.9198	0.8450

B. Anodic reaction. (H=0.08, NJ=150)

r_a	C	C_R/C^*	B	f'_∞	$\Delta c_{ferric}/\Delta c_{ferroc}$
0.0004	0.79340	1.16384	0.95634	0.9643	1.1922
0.10	0.78352	1.14976	0.95607	0.9620	1.1930
0.25	0.76809	1.12774	0.95567	0.9583	1.1943
0.50	0.74080	1.08870	0.95507	0.9517	1.1966
0.75	0.71129	1.04637	0.95459	0.9442	1.1992
0.90	0.69238	1.01919	0.95438	0.9392	1.2008
0.999714	0.67927	1.00030	0.95427	0.9357	1.2019

$r_c = c_{ferricyanide}/(c_{ferricyanide}+c_{ferrocyanide})$

$r_a = c_{ferrocyanide}/(c_{ferricyanide}+c_{ferrocyanide})$

Table 11. Principal results for the system $K_3Fe(CN)_6$-$K_4Fe(CN)_6$-KOH-H_2O.

A. Cathodic reaction. (H=0.08, NJ=150)

$\frac{c_{OH^-}}{c_{K^+}}$	r_c	C	C_R/C^*	B	f'_∞	$\frac{\Delta c_{ferroc}}{\Delta c_{ferric}}$	$\frac{\Delta c_{OH^-}}{\Delta c_{ferric}}$
0	0.5	0.63553	0.93947	0.94992	0.9130	0.8417	0
0.1	0.5	0.63167	0.94401	0.93321	0.8587	0.8573	-0.0495
0.25	0.5	0.62540	0.95118	0.90735	0.7815	0.8831	-0.1302
0.50	0.5	0.61111	0.96447	0.85743	0.6365	0.9352	-0.2889
0.75	0.5	0.58990	0.98030	0.79692	0.4709	1.0060	-0.4988
0.80	0.5	0.58390	0.98390	0.78243	0.4295	1.0237	-0.5506
0.85	0.5	0.57705	0.98768	0.76694	0.3849	1.0431	-0.6070
0.90	0.5	not converged					
0.95	0.5	0.51268	0.99624	0.69068	-0.0944	1.0767	-0.7295
0.5	0.9	0.62915	0.99363	0.85461	0.6457	0.9419	-0.3033
0.5	0.75	0.62247	0.98321	0.85520	0.6390	0.9394	-0.2981
0.5	0.25	0.59868	0.94375	0.86015	0.6361	0.9307	-0.2792
0.5	0.10	0.59050	0.93023	0.86184	0.6354	0.9278	-0.2731

B. Anodic reaction. (H=0.08, NJ-150)

$\frac{c_{OH^-}}{c_{K^+}}$	r_a	C	C_R/C^*	B	f'_∞	$\frac{\Delta c_{ferric}}{\Delta c_{ferroc}}$	$\frac{\Delta c_{OH^-}}{\Delta c_{ferroc}}$
0	0.5	0.74080	1.08870	0.95507	0.9517	1.1966	0
0.1	0.5	0.72769	1.08104	0.93805	0.8985	1.1733	0.0591
0.25	0.5	0.70714	1.06925	0.91149	0.8161	1.1363	0.1514
0.50	0.5	0.66997	1.04846	0.86447	0.6713	1.0682	0.3183
0.75	0.5	0.62754	1.02565	0.81322	0.5103	0.9892	0.5080

Table 11. (Continued)

$\frac{c_{OH^-}}{c_{K^+}}$	r_a	C	C_R/C^*	B	f'_∞	$\frac{\Delta c_{ferric}}{\Delta c_{ferroc}}$	$\frac{\Delta c_{OH^-}}{\Delta c_{ferroc}}$
0.80	0.5	0.61810	1.02078	0.80223	0.4743	0.9719	0.5494
0.85	0.5	0.60818	1.01580	0.79089	0.4360	0.9539	0.5921
0.90	0.5	0.59767	1.01071	0.77907	0.3945	0.9355	0.6361
0.95	0.5	0.58633	1.00550	0.76658	0.3482	0.9165	0.6815
0.9998	0.5	0.57376	1.00023	0.75308	0.2938	0.8972	0.7280
0.5	0.0004	0.69455	1.08742	0.86179	0.6764	1.0583	0.3353
0.5	0.1	0.69004	1.08026	0.86230	0.6756	1.0601	0.3321
0.5	0.25	0.68290	1.06893	0.86309	0.6741	1.0630	0.3271
0.5	0.75	0.65553	1.02571	0.86591	0.6678	1.0737	0.3089
0.5	0.9	0.64603	1.01078	0.86682	0.6653	1.0773	0.3030
0.5	0.9997	0.63933	1.00027	0.86743	0.6634	1.0797	0.2989

$r_c = c_{ferrocyanide}/(c_{ferrocyanide} + c_{ferricyanide})$

$r_a = c_{ferricyanide}/(c_{ferrocyanide} + c_{ferricyanide})$

Table 12. Principal results for the system $K_3Fe(CN)_6$-$K_4Fe(CN)_6$-NaOH-H_2O.

A. Cathodic reaction (H=0.08, NJ=150).

$\frac{c_{OH^-}}{c_{K^+}+c_{Na^+}}$	r_c	C	C_R/C^*	B	f'_∞	$\frac{\Delta c_{ferroc}}{\Delta c_{ferric}}$	$\frac{\Delta c_{OH^-}}{\Delta c_{ferric}}$	$\frac{\Delta c_{Na^+}}{\Delta c_{ferric}}$
0	0.5	0.63551	0.93947	0.94988	0.9128	0.8417	0	0
0.10	0.5	0.63024	0.94373	0.92991	0.8547	0.8567	-0.0498	0.0337
0.25	0.5	0.62143	0.95058	0.89864	0.7649	0.8817	-0.1319	0.0902
0.50	0.5	0.60323	0.96363	0.84164	0.6035	0.9330	-0.2962	0.2057
0.75	0.5	0.57577	0.97969	0.77313	0.4034	1.0036	-0.5170	0.3631
0.80	0.5	not converged						
0.85	0.5	0.51072	0.98850	0.69562	-0.0956	1.0329	-0.6364	0.4128
0.90	0.5	note converged						
0.95	0.5	0.42693	0.99666	0.65457	-0.3634	1.0497	-0.7402	0.4310
0.5	0.9996	0.62482	1.00023	0.83682	0.6054	0.9412	-0.3144	0.2132
0.5	0.90	0.62086	0.99347	0.83773	0.6051	0.9397	-0.3109	0.2118
0.5	0.75	0.61458	0.98281	0.83915	0.6046	0.9373	-0.3056	0.2096
0.5	0.25	0.59061	0.94243	0.84429	0.6018	0.9284	-0.2863	0.2016
0.5	0.10	0.58233	0.92859	0.84598	0.6005	0.9255	-0.2801	0.1989
0.5	0.000286	0.57649	0.91886	0.84715	0.5995	0.9235	-0.2758	0.1970

Table 12. (Continued)

B. Anodic reaction (H=0.08, NJ=150)

$\frac{c_{OH^-}}{c_{K^+}+c_{Na^+}}$	r_a	C	C_R/C^*	B	f'	$\frac{\Delta c_{ferroc}}{\Delta c_{ferric}}$	$\frac{\Delta c_{OH^-}}{\Delta c_{ferric}}$	$\frac{\Delta c_{Na^+}}{\Delta c_{ferric}}$
0	0.5	0.74080	1.08870	0.95507	0.9517	1.1966	0	0
0.10	0.5	0.72659	1.08143	0.93494	0.8927	1.1741	0.0594	-0.0380
0.25	0.5	0.70447	1.07005	0.90443	0.8031	1.1380	0.1533	-0.1000
0.50	0.5	0.66463	1.04953	0.85216	0.6478	1.0706	0.3260	-0.2197
0.75	0.5	0.61847	1.02642	0.79611	0.4709	0.9914	0.5258	-0.3658
0.80	0.5	0.60786	1.02142	0.78392	0.4289	0.9739	0.5698	-0.3987
0.85	0.5	0.59642	1.01628	0.77108	0.3821	0.9559	0.6153	-0.4328
0.90	0.5	0.58368	1.01101	0.75717	0.3269	0.9375	0.6625	-0.4678
0.95	0.5	0.56837	1.00561	0.74104	0.2536	0.9190	0.7112	-0.5027
0.9998	0.5	0.53574	1.00018	0.71002	0.0475	0.9044	0.7608	-0.5259
0.5	0.9997	0.63366	1.000253	0.8554	0.6398	1.0822	0.3061	-0.2121
0.5	0.90	0.64044	1.01101	0.8547	0.6417	1.0797	0.3103	-0.2137
0.5	0.75	0.65004	1.02627	0.8537	0.6442	1.0762	0.3164	-0.2161
0.5	0.25	0.67770	1.07045	0.8507	0.6507	1.0654	0.3350	-0.2230
0.5	0.10	0.68491	1.08204	0.8498	0.6521	1.0625	0.3400	-0.2249
0.5	0.0004	0.68946	1.08936	0.8493	0.6529	1.0606	0.3433	-0.2261

$$r_c = c_{ferrocyanide}/(c_{ferrocyanide}+c_{ferricyanide})$$

$$r_a = c_{ferricyanide}/(c_{ferrocyanide}+c_{ferricyanide})$$

Table 13. Dimensionless concentration and shear stress at the electrode in free convection with uniform flux condition.

Sc		0.1	1	10	100	∞
$\theta_{s,0}$	This work					1.14747
	Ref. 48	1.7356	1.3574	1.2163	1.1697	
$\phi_{s,0}$	This work					0.83789
	Ref. 48	0.65425	0.72196	0.76962	0.79628	

Note: The values tabulated as $\theta(0)$ and $f''(0)$ in Appendix B of reference 48 are, in the notation of this report:

$$\theta(0) = \theta_{s,0} \; Sc^{-1/5}$$

$$f''(0) = \phi_{s,0} \; Sc^{3/5}$$

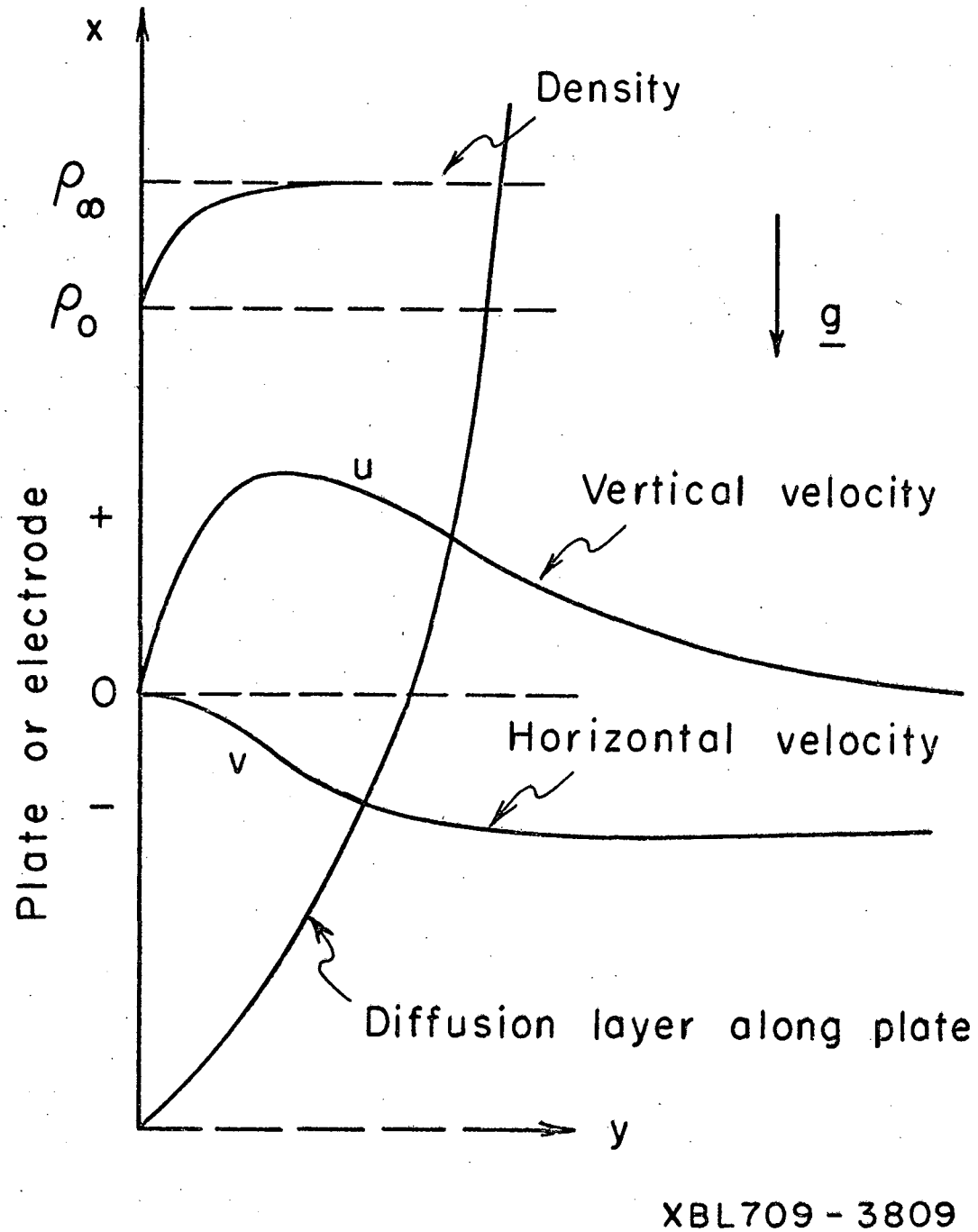

XBL709-3809

Figure 1a. Diffusion boundary layer in free convection at a vertical plate. Shown also are the profiles of density, ρ, vertical velocity, u, and horizontal velocity, v. The gravity force points in the negative x direction.

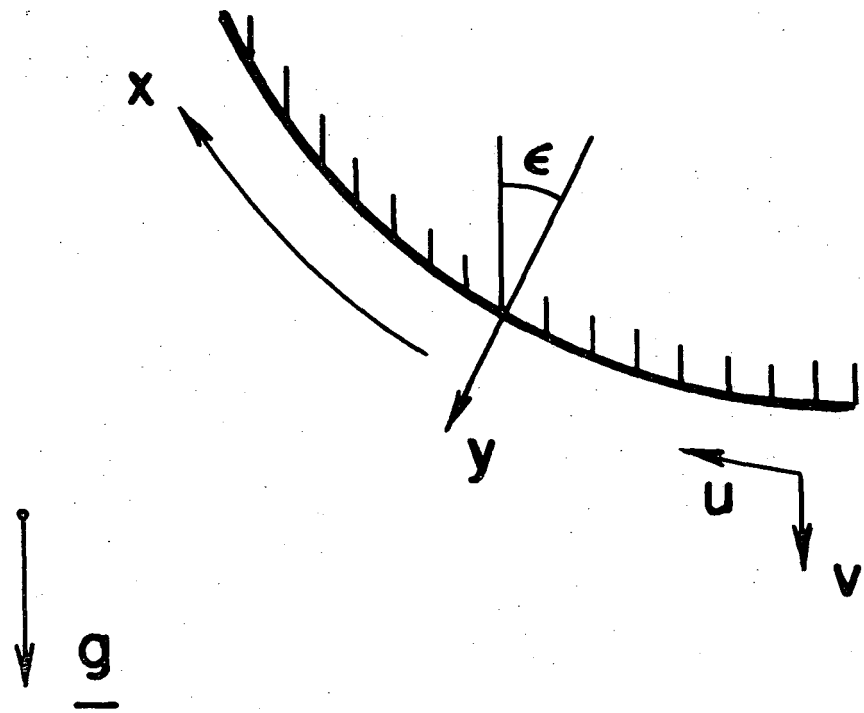

XBL 709 - 3810

Figure 1b. Position directions of the coordinates x and y, the velocity components u and v, and the angle ε, in eq. (3.38).

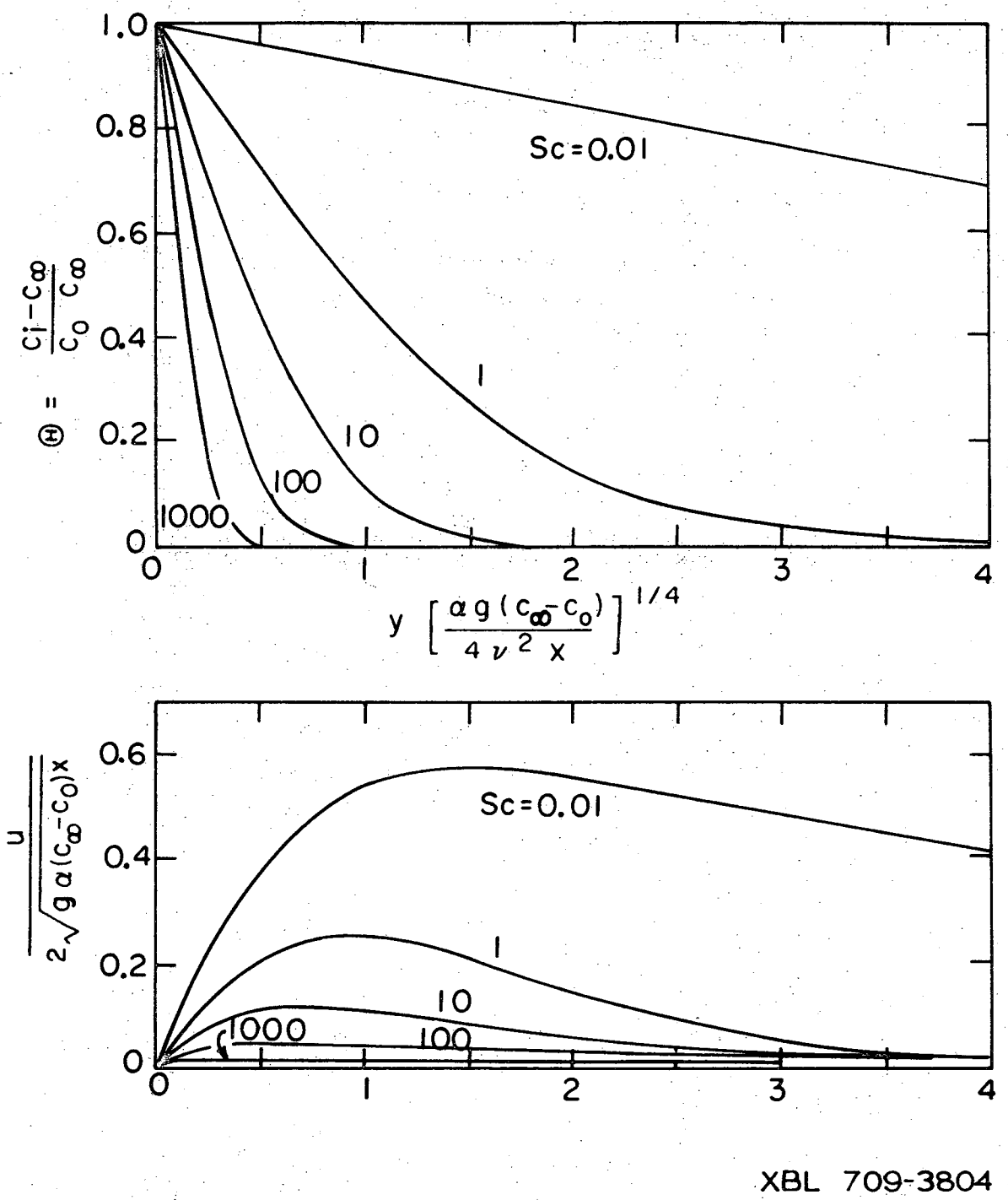

Figure 2. Concentration and velocity profiles for free convection at a vertical plate.

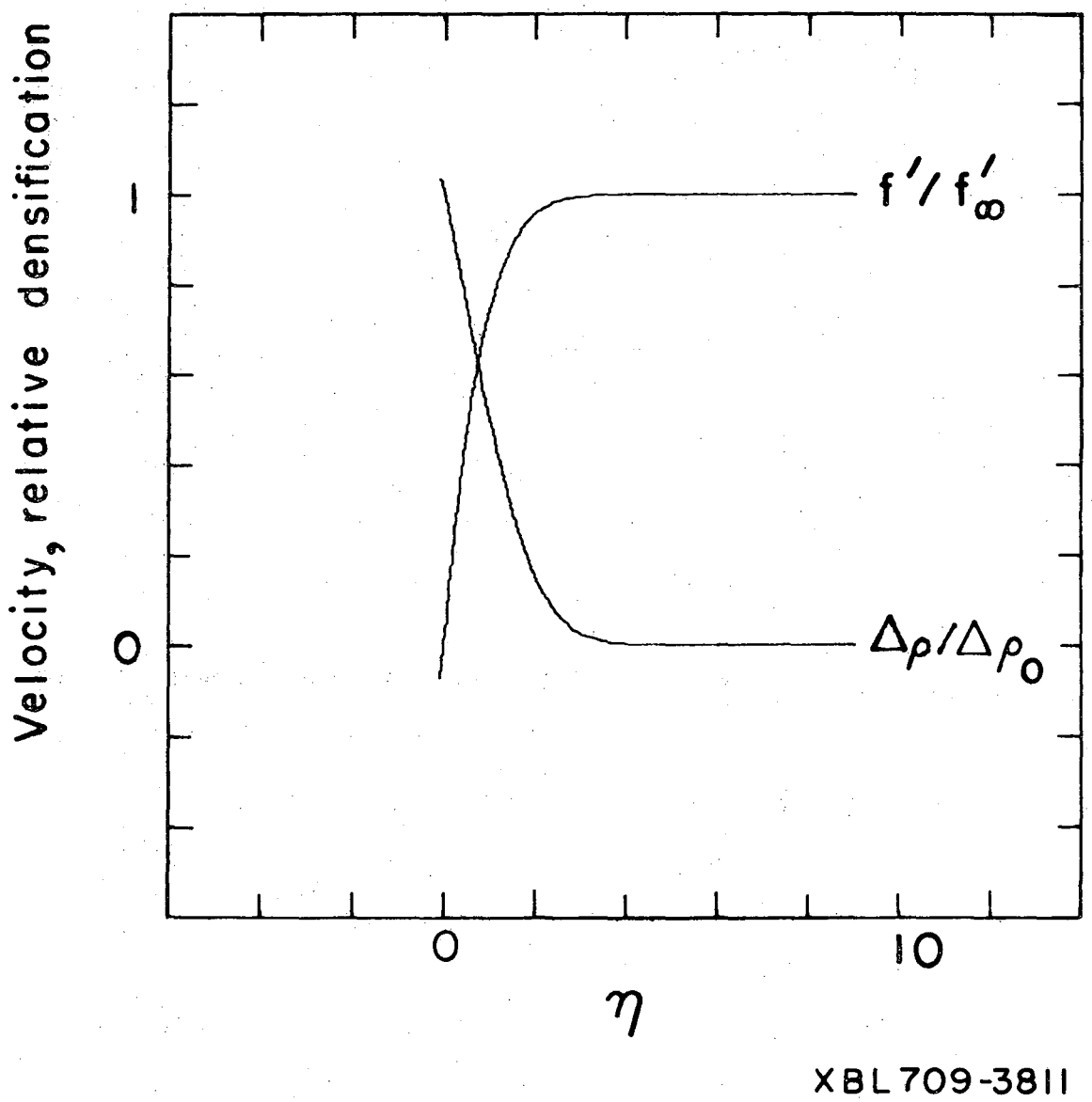

Figure 3. Density and velocity profiles normalized with respect to $(\Delta\rho)_o$ and f'_∞, respectively.

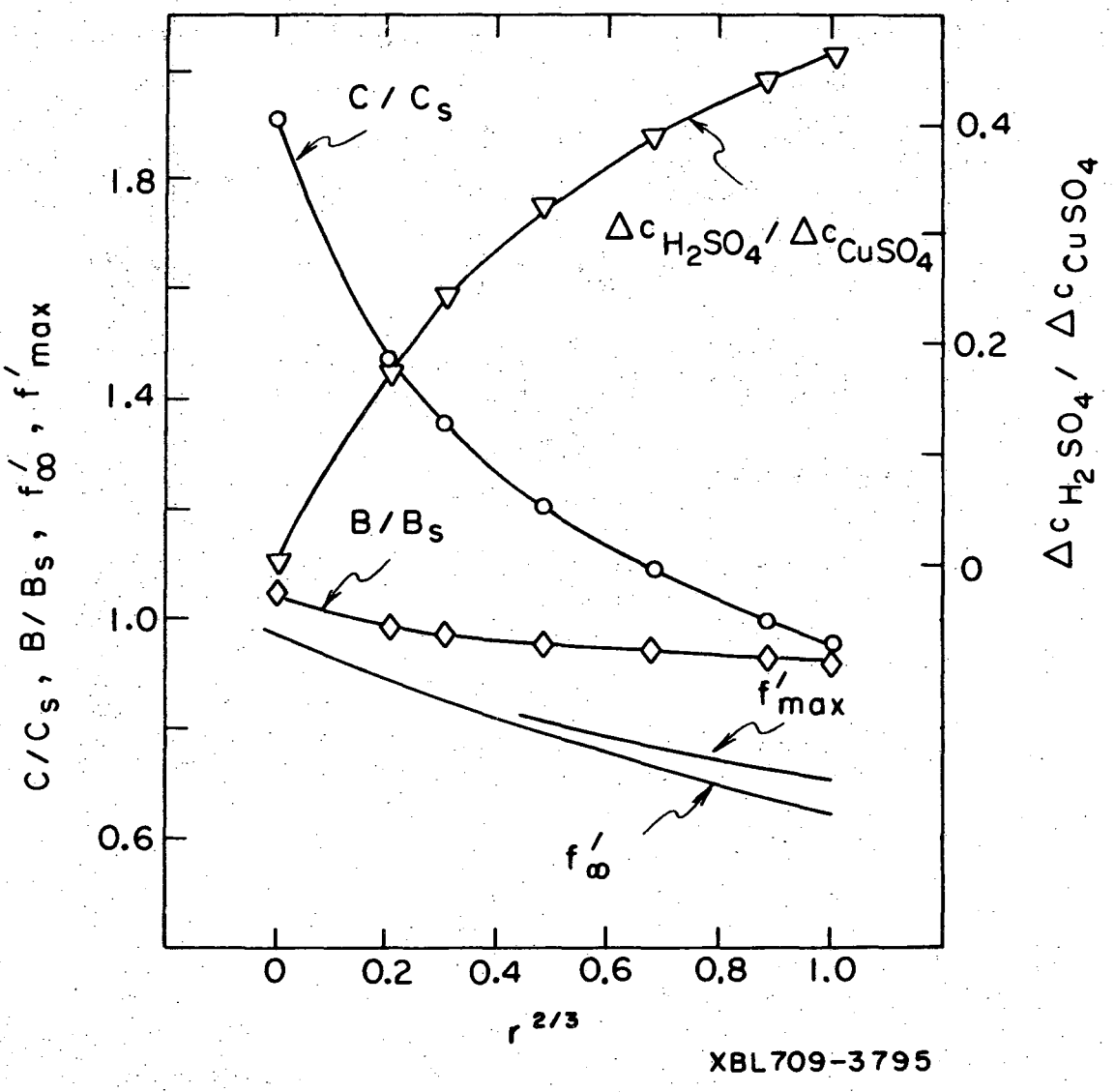

Figure 4. Migration current, shear stress, characteristic velocities, and surface concentrations in the system $CuSO_4$-H_2SO_4-H_2O (complete dissociation assumed).

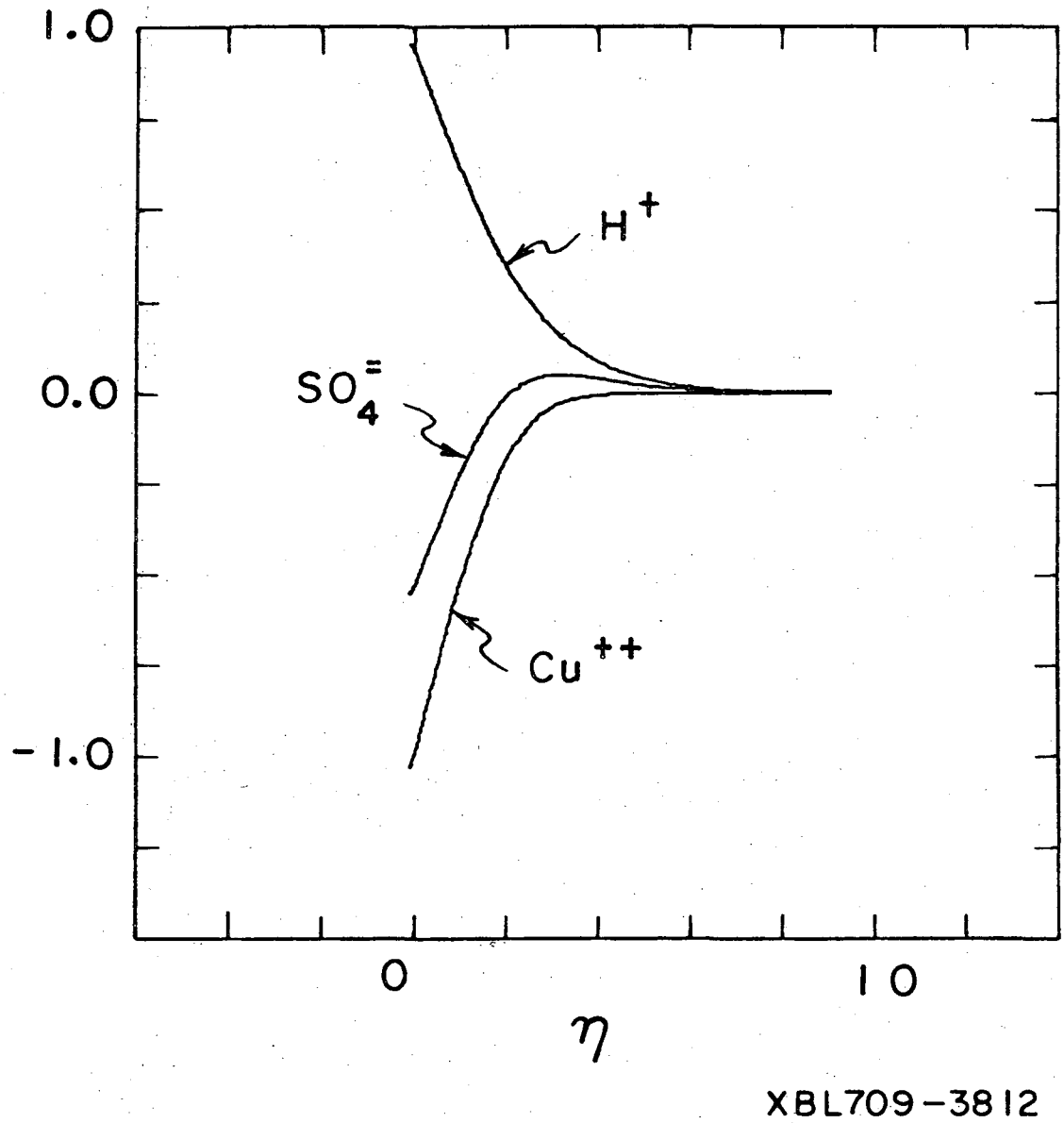

Figure 5. Concentration profiles in $CuSO_4$-H_2SO_4-H_2O, with H_2SO_4 (fully dissociated) in large excess. The concentration excess relative to the bulk is shown normalized with respect to reactant bulk concentration.

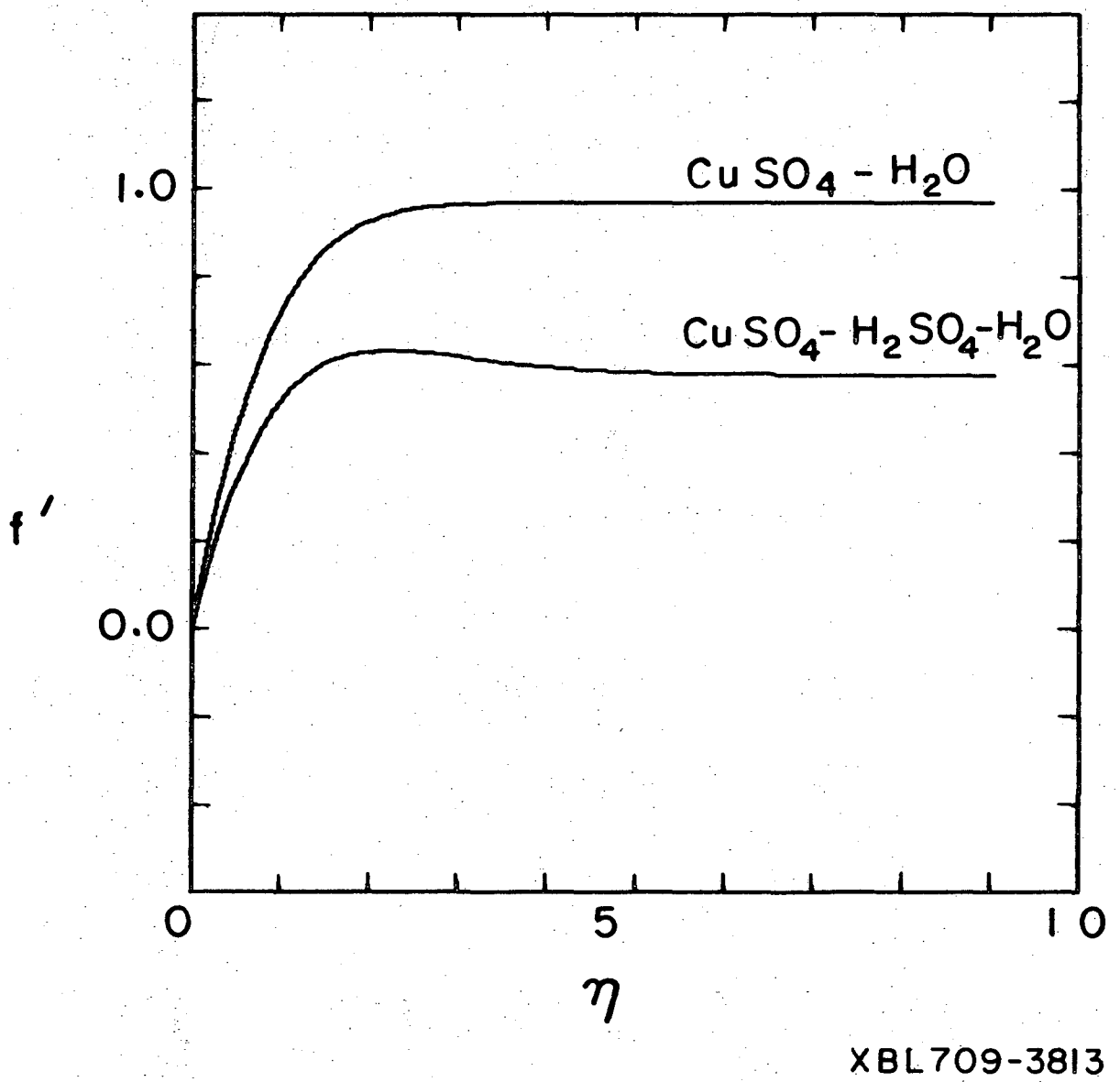

Figure 6. Dimensionless velocity f' in the systems $CuSO_4$-H_2O and $CuSO_4$-H_2SO_4-H_2O (excess H_2SO).

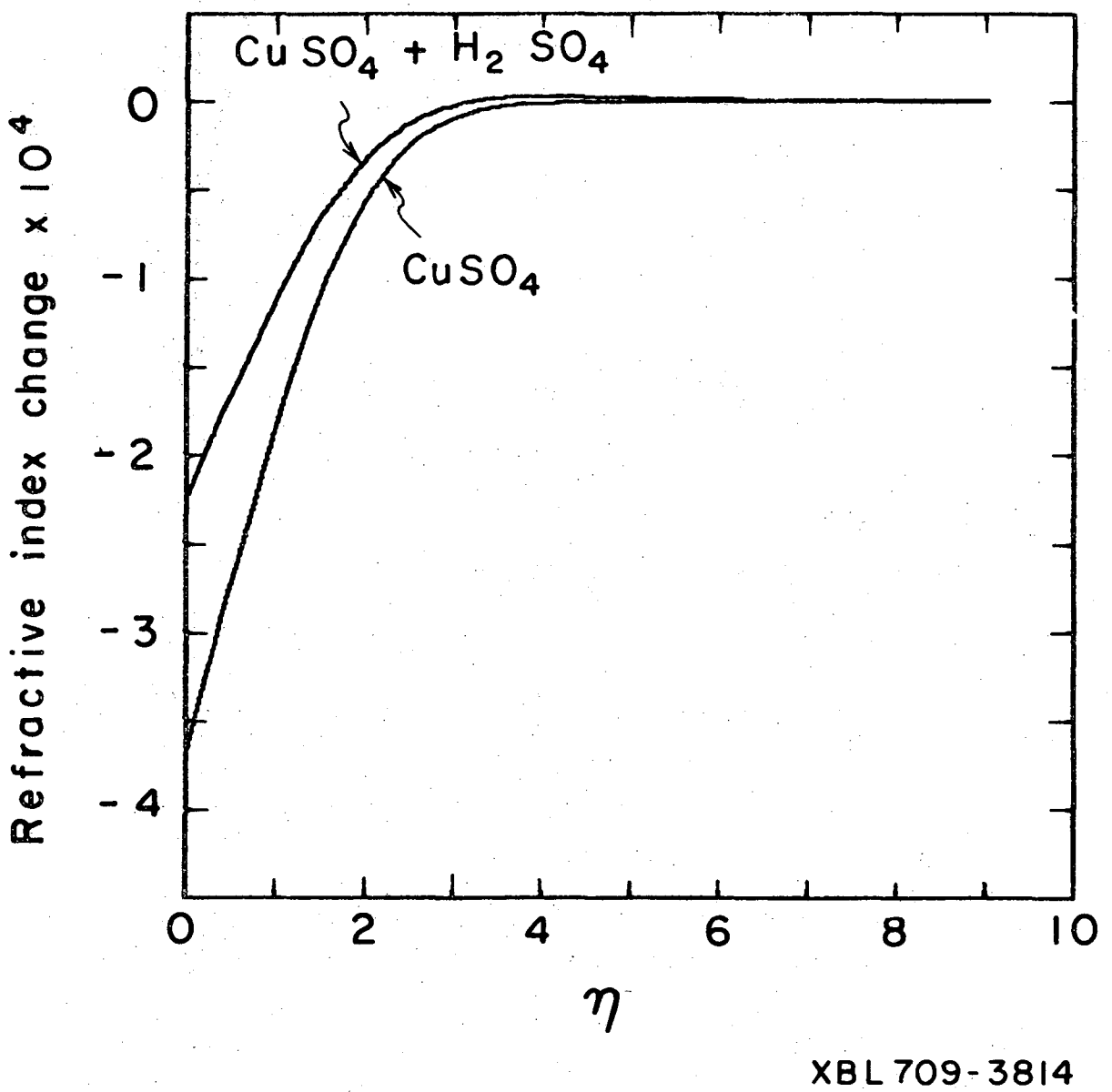

Figure 7. Refractive index (relative to bulk) in $CuSO_4$-H_2O (0.02 M bulk, 0.01 M cathode) and in $CuSO_4$-H_2SO_4-H_2O (excess H_2SO_4, 0.01 M $CuSO_4$ bulk).

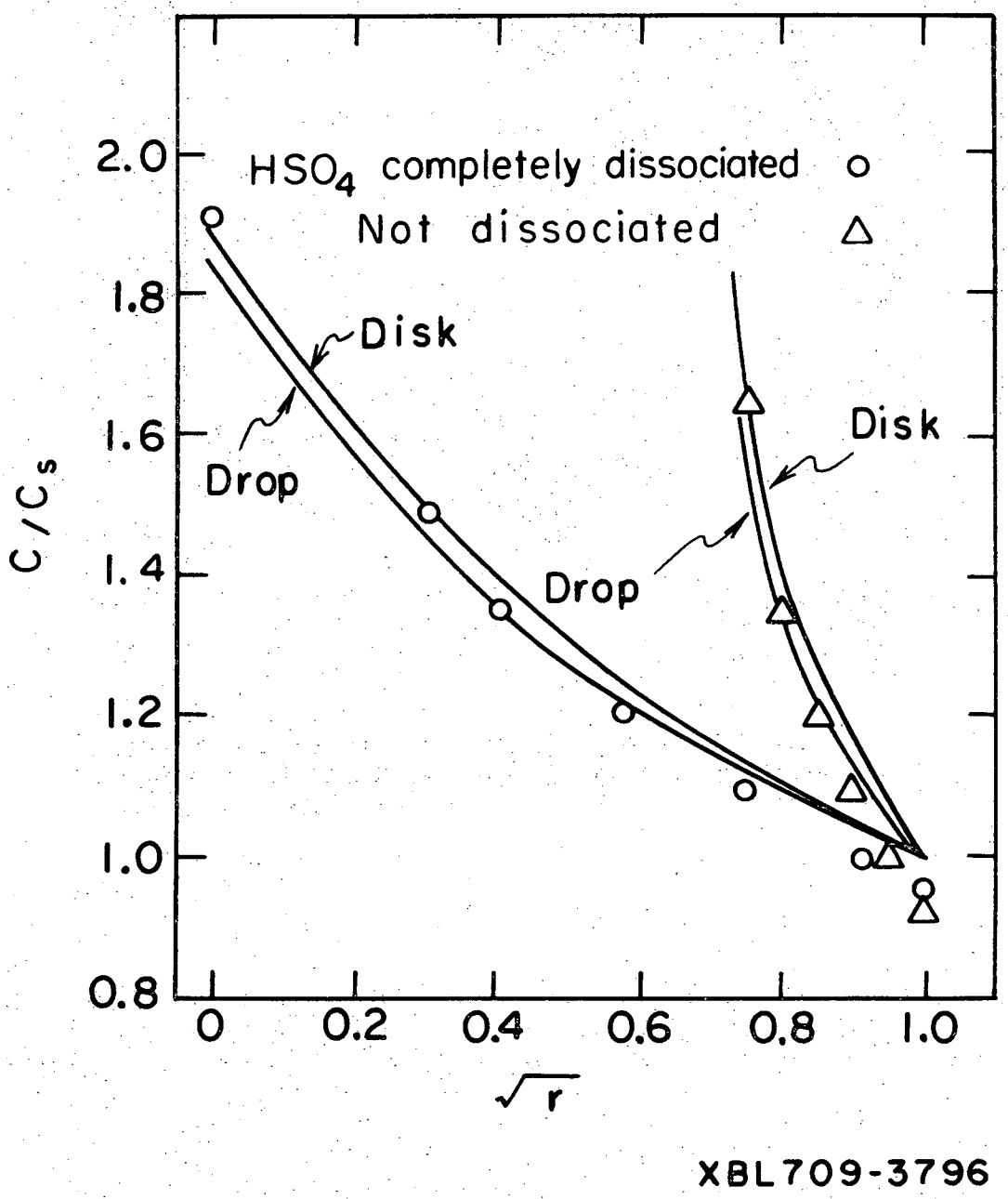

Figure 8. Migration current in $CuSO_4$-H_2SO_4-H_2O.
Solid lines indicate results for rotating disk and growing mercury drop.

$r = c_{H_2SO_4} / (c_{H_2SO_4} + c_{CuSO_4})$

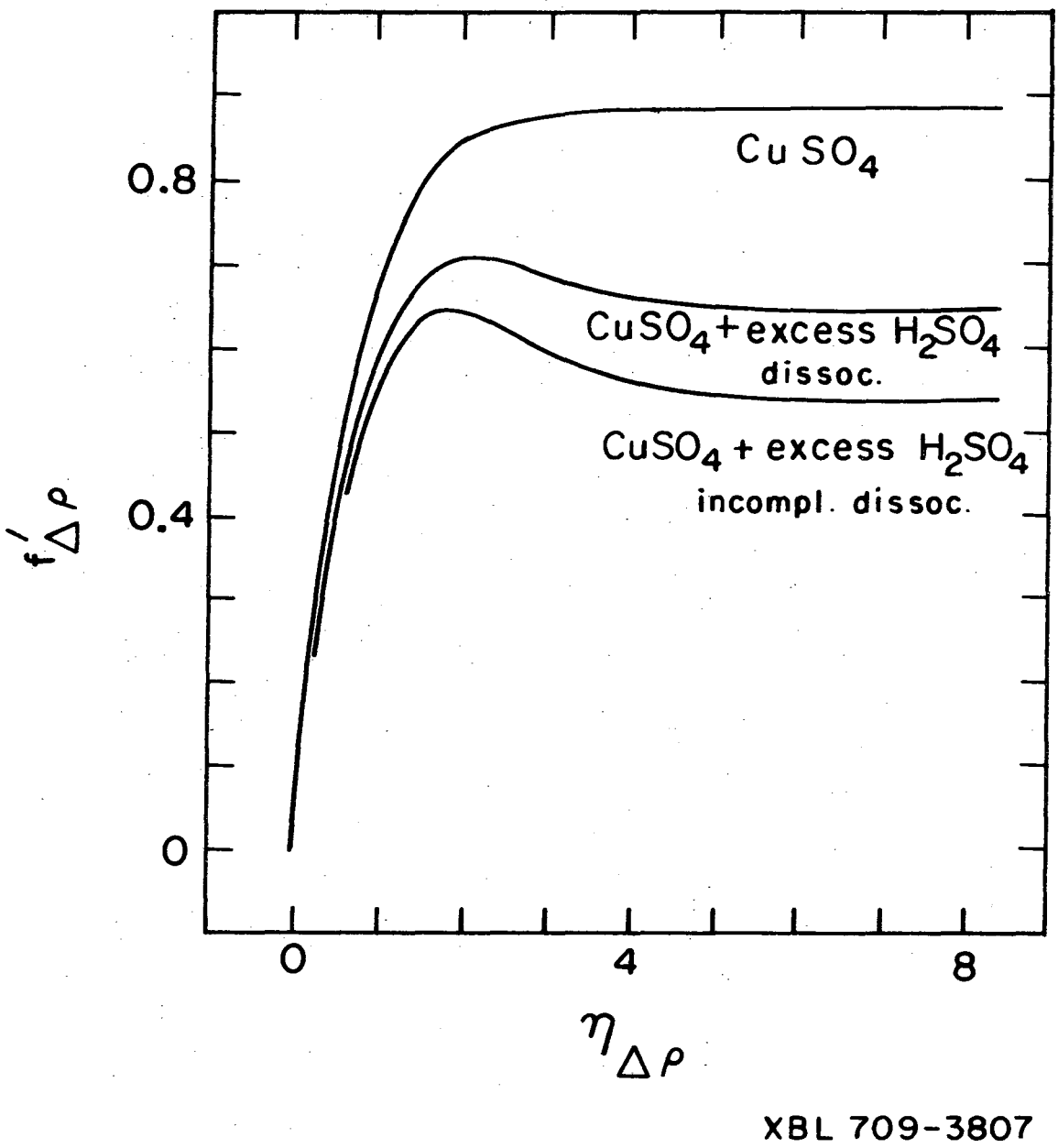

Figure 9. Velocity profiles for binary salt solution ($CuSO_4$) and for $CuSO_4$ with excess H_2SO_4 (r=0.99998) dissociated and partially dissociated.

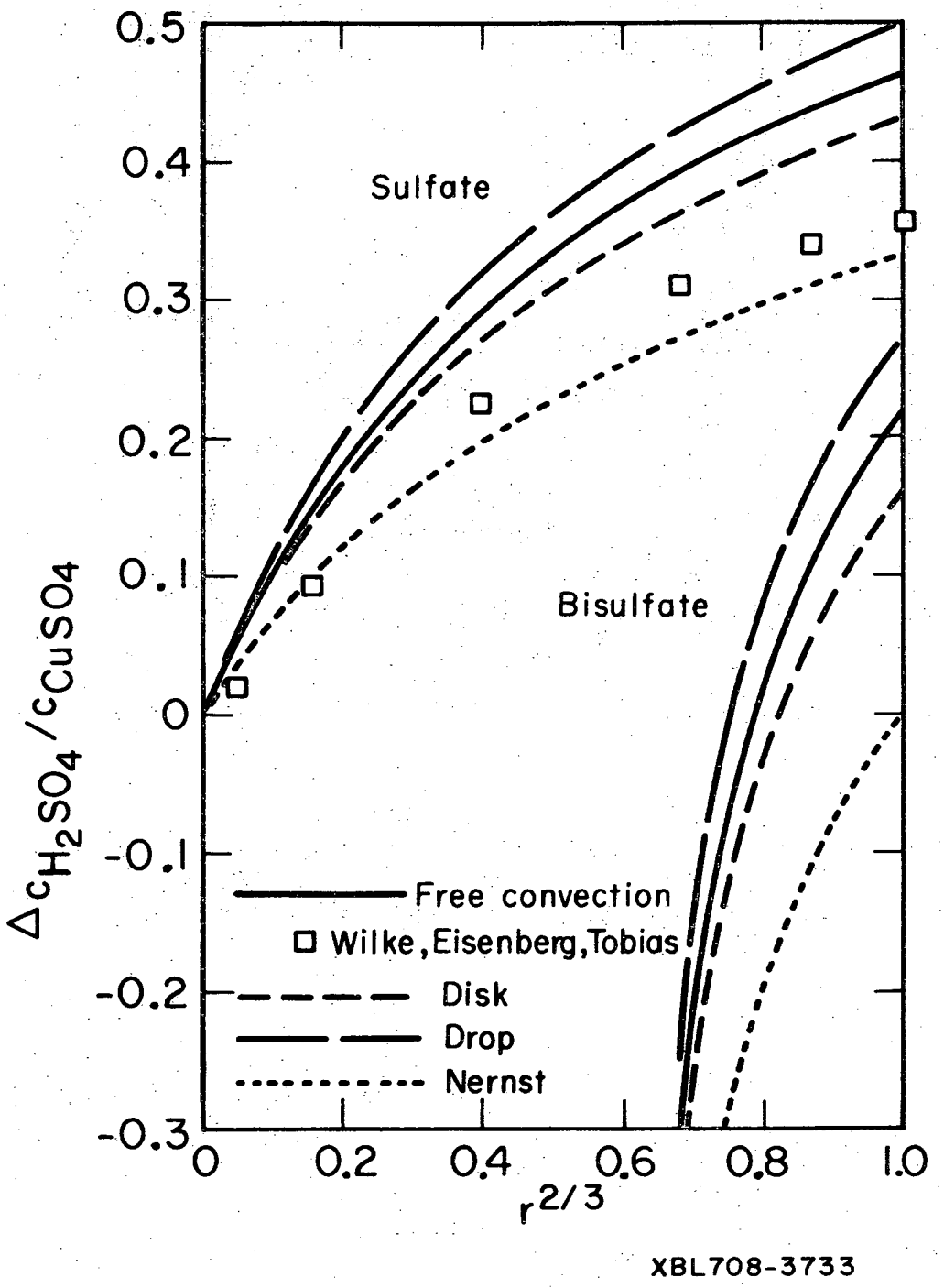

Figure 10a. Excess sulfuric acid at the electrode divided by the bulk copper concentration.
Points indicated "Wike, Eisenberg, Tobias" are values of Table 2.

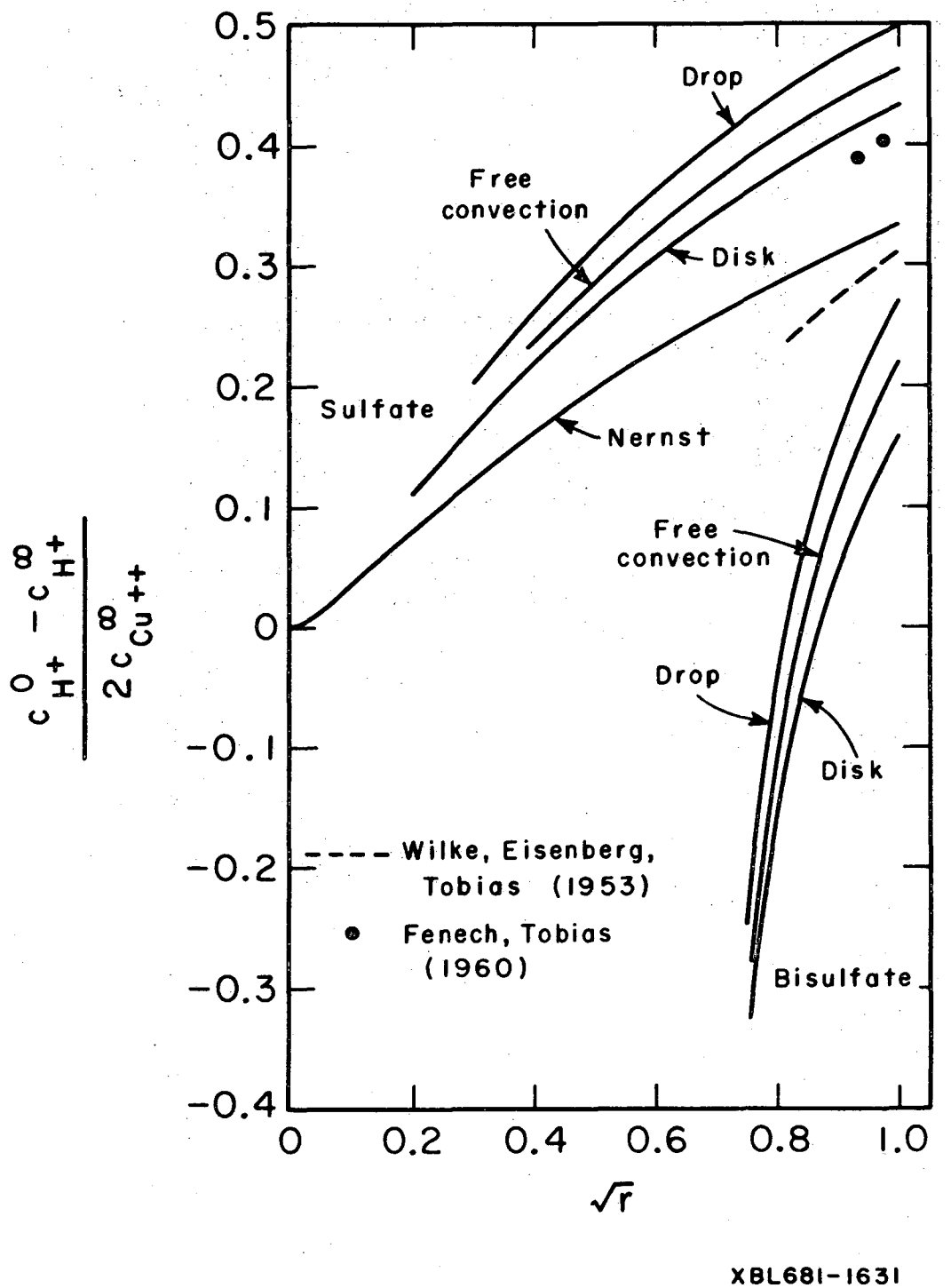

Figure 10b. Excess sulfuric acid at the electrode divided by the bulk copper concentration.
Line indicated "Wilke, Eisenberg, Tobias" are values reported in Ref. 24; points "Fenech, Tobias" in Ref. 50.

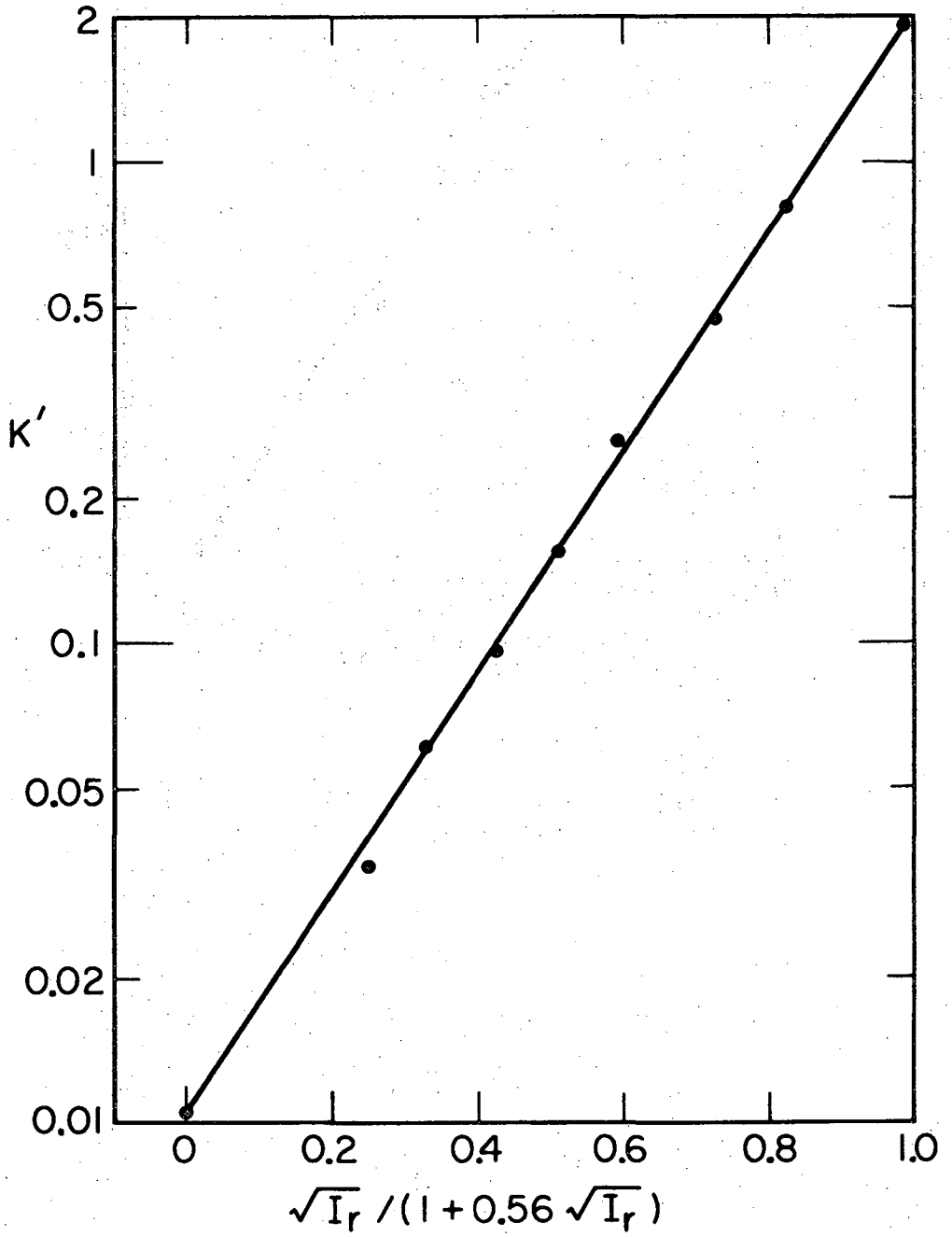

XBL6912-6402

Figure 11. Stoichiometric dissociation constant of HSO_4^- ion in dependence on true ionic strength.

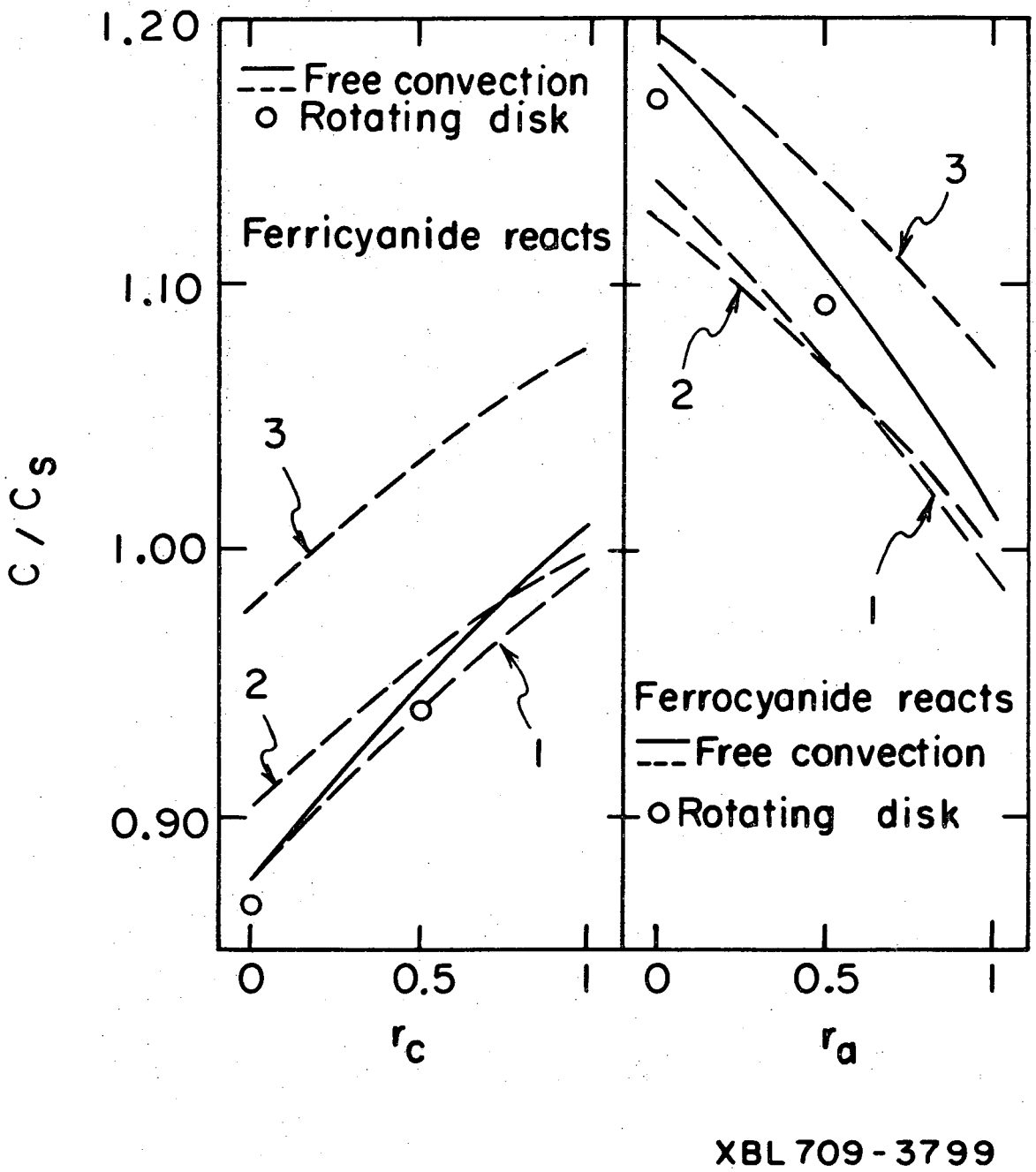

Figure 12. Migration current in the system $K_3Fe(CN)_6$-$K_4Fe(CN)_6$-H O.

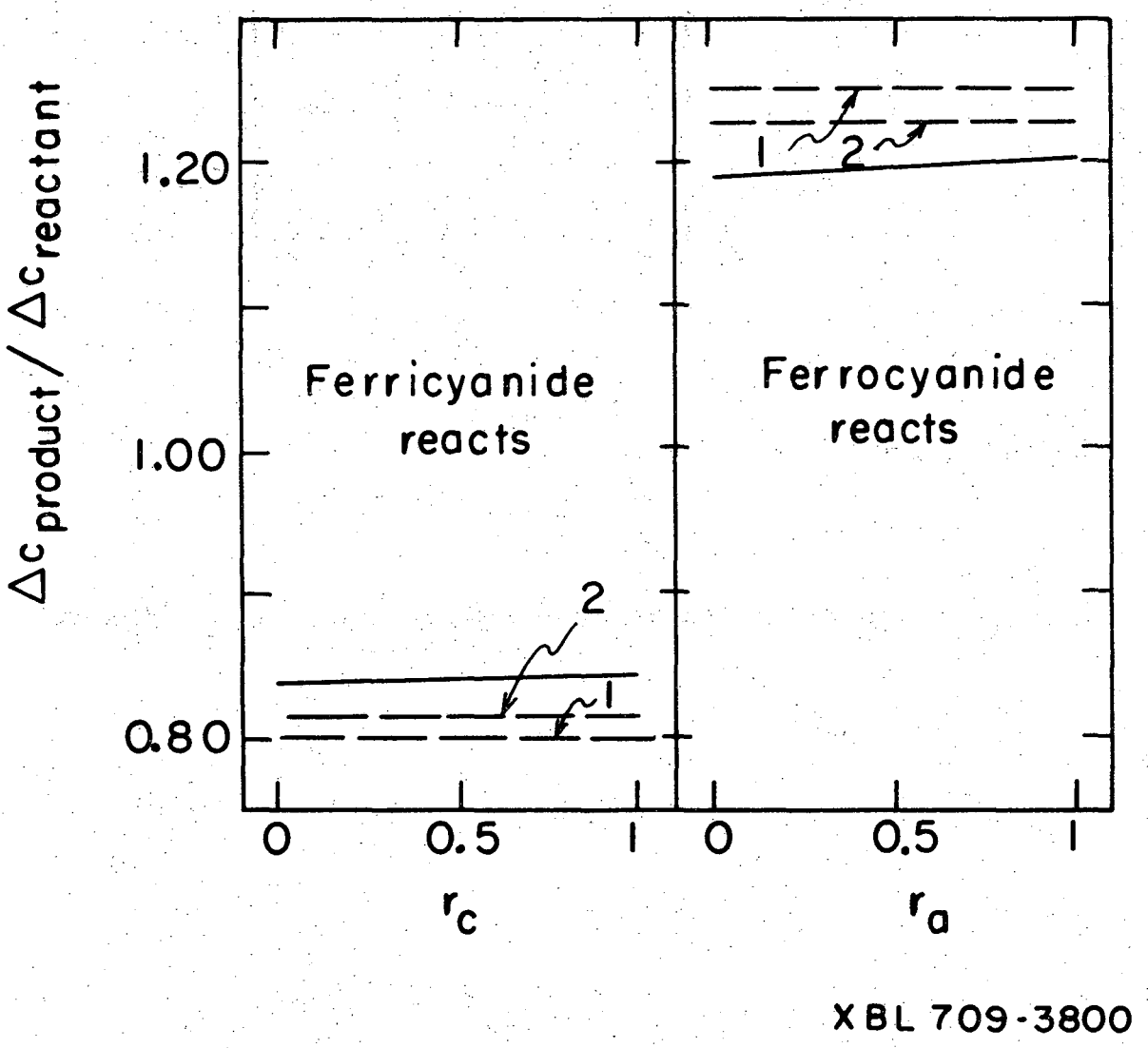

Figure 13. Product ion concentration at the electrode, in the system $K_3Fe(CN)_6$-$K_4Fe(CN)_6$-H_2O.

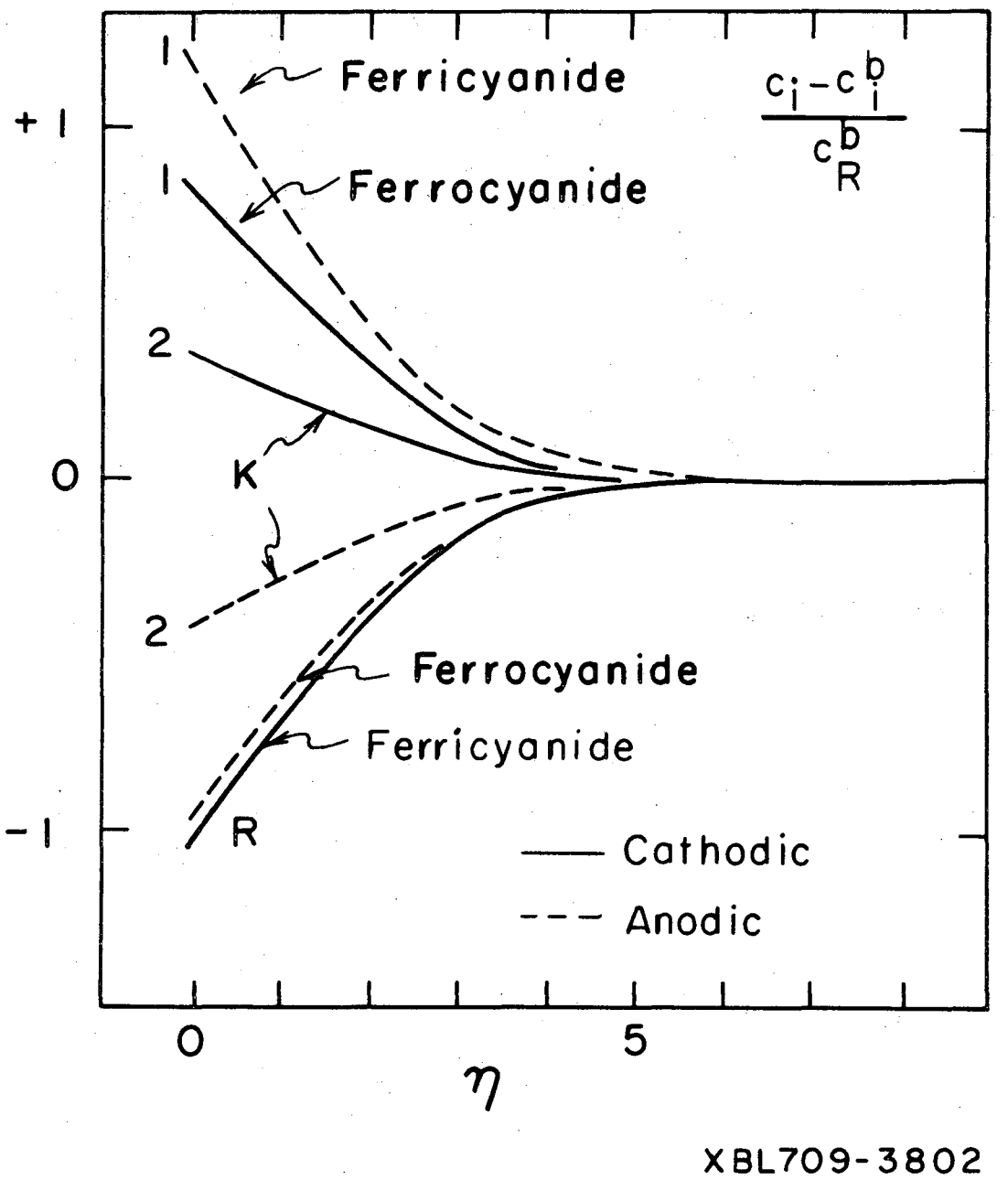

Figure 14. Concentration profiles in $K_3Fe(CN)_6$-$K_4Fe(CN)_6$-H_2O. Concentration excess relative to the bulk is shown normalized with respect to reactant bulk concentration.

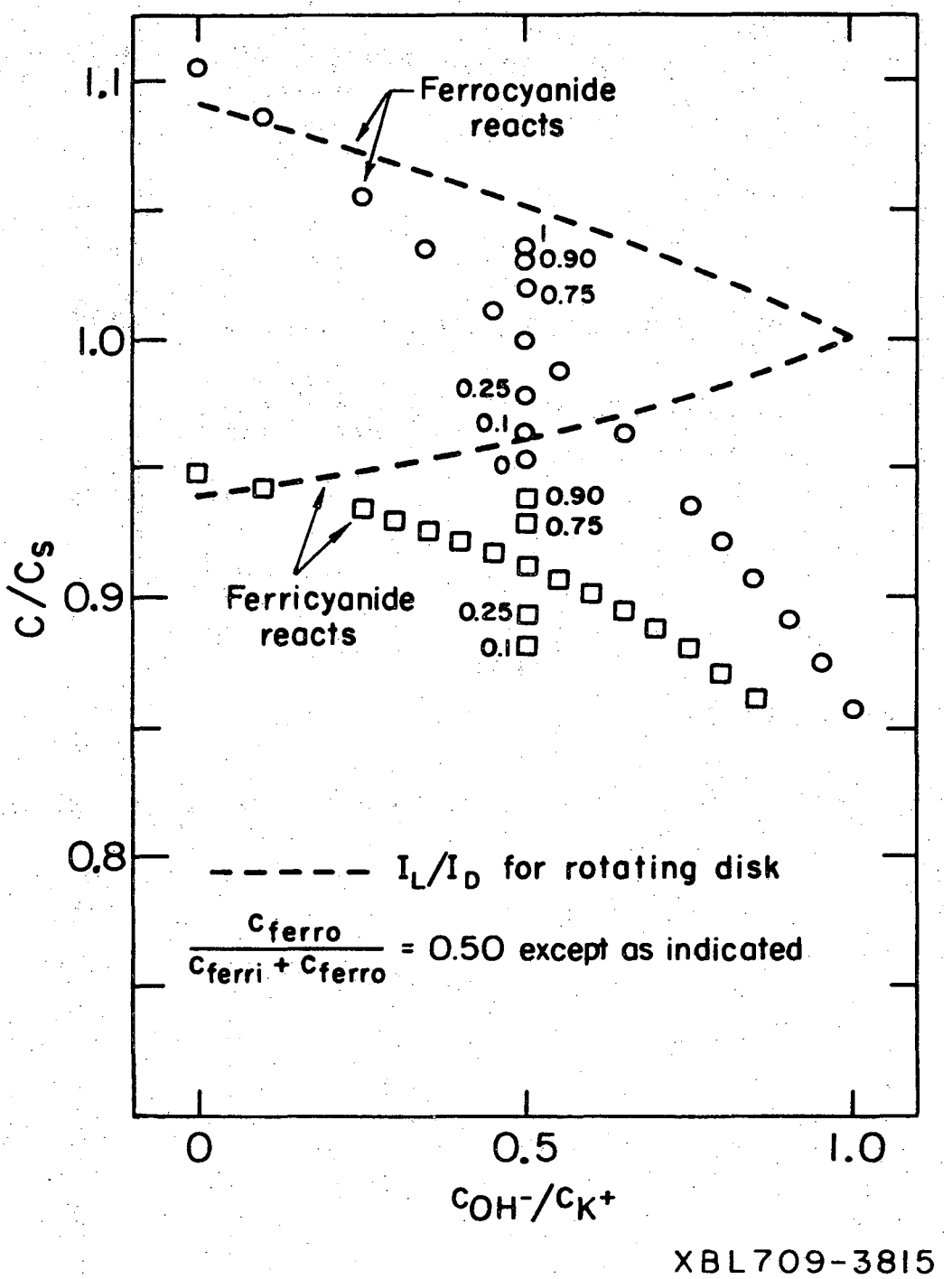

Figure 15. Migration current in the system $K_3Fe(CN)_6$-$K_4Fe(CN)_6$-KOH-H_2O.

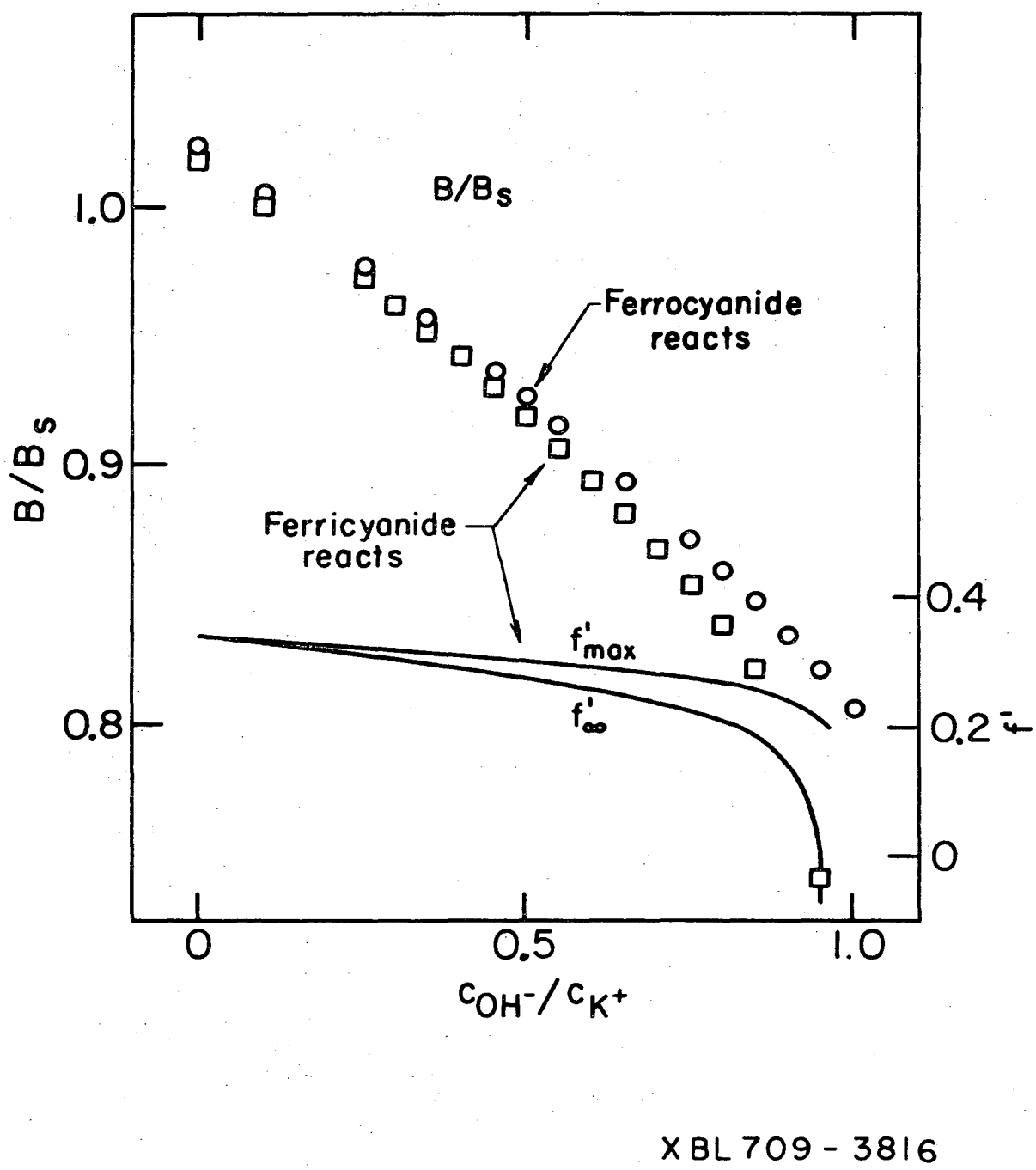

XBL 709 - 3816

Figure 16. Shear stress and characteristic velocities in the system $K_3Fe(CN)_6$-$K_4Fe(CN)_6$-KOH-H_2O.

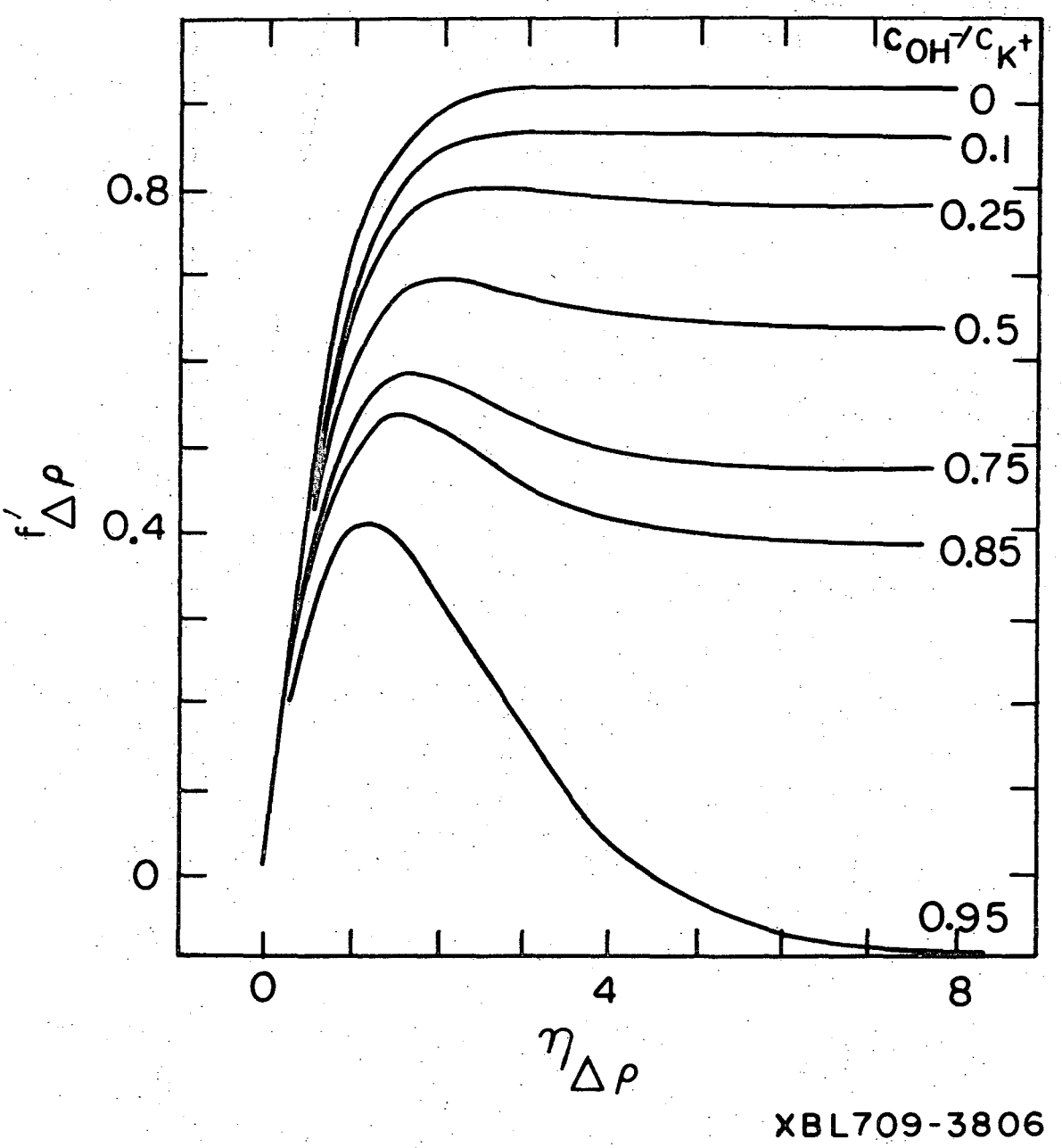

Figure 17. Velocity profiles for various ratios c_{OH^-}/c_{K^+} in the system $K_3Fe(CN)_6$-$K_4Fe(CN)_6$-KOH-H_2O, reacting cathodically.

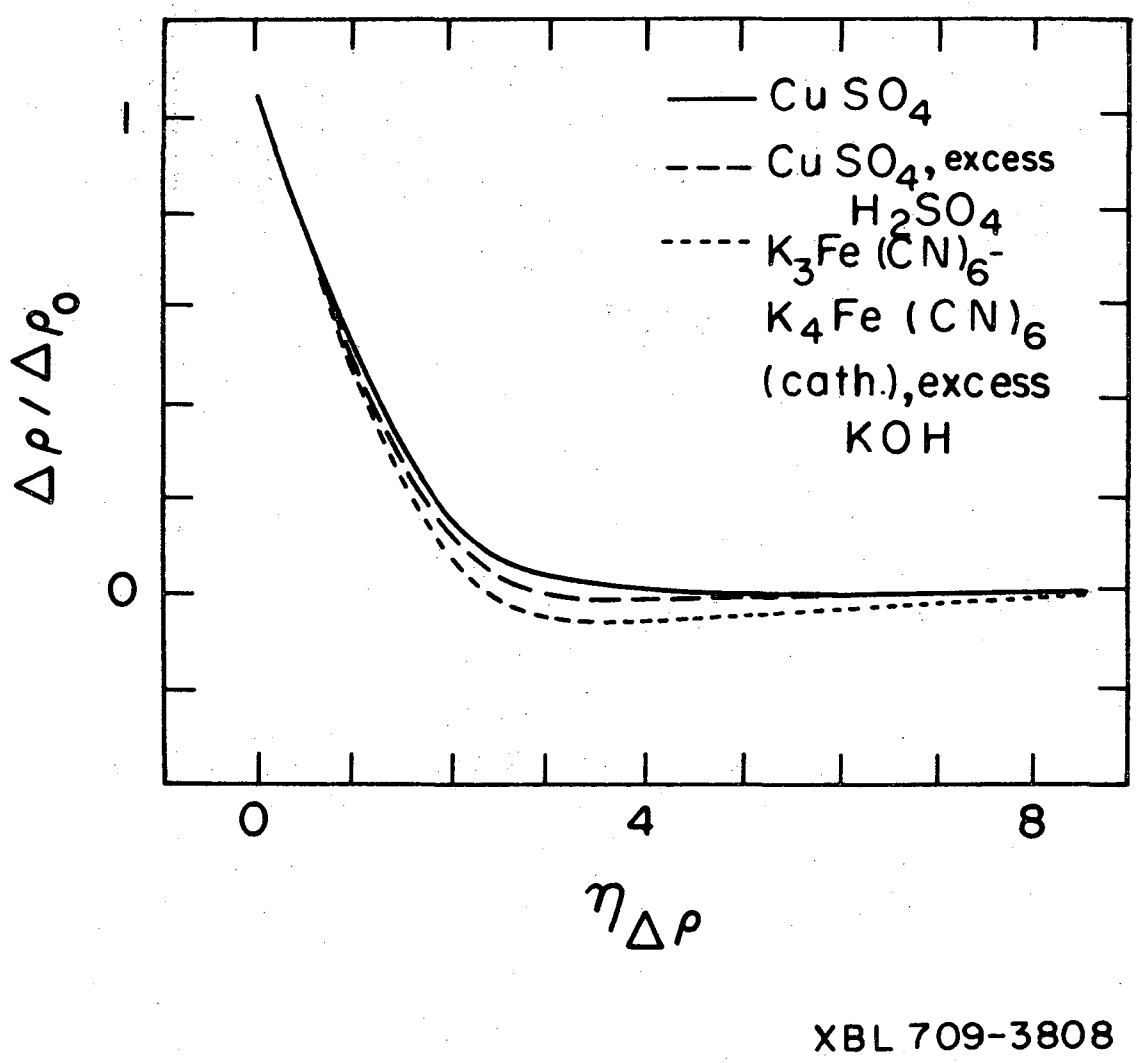

Figure 18. Normalized density profiles for binary salt solution ($CuSO_4$), for $CuSO_4$ with excess H_2SO_4 (r=0.99998) and for equimolar ferri/ferrocyanide with excess KOH (cathodic reaction, c_{OH^-}/c_{K^+}=0.95).

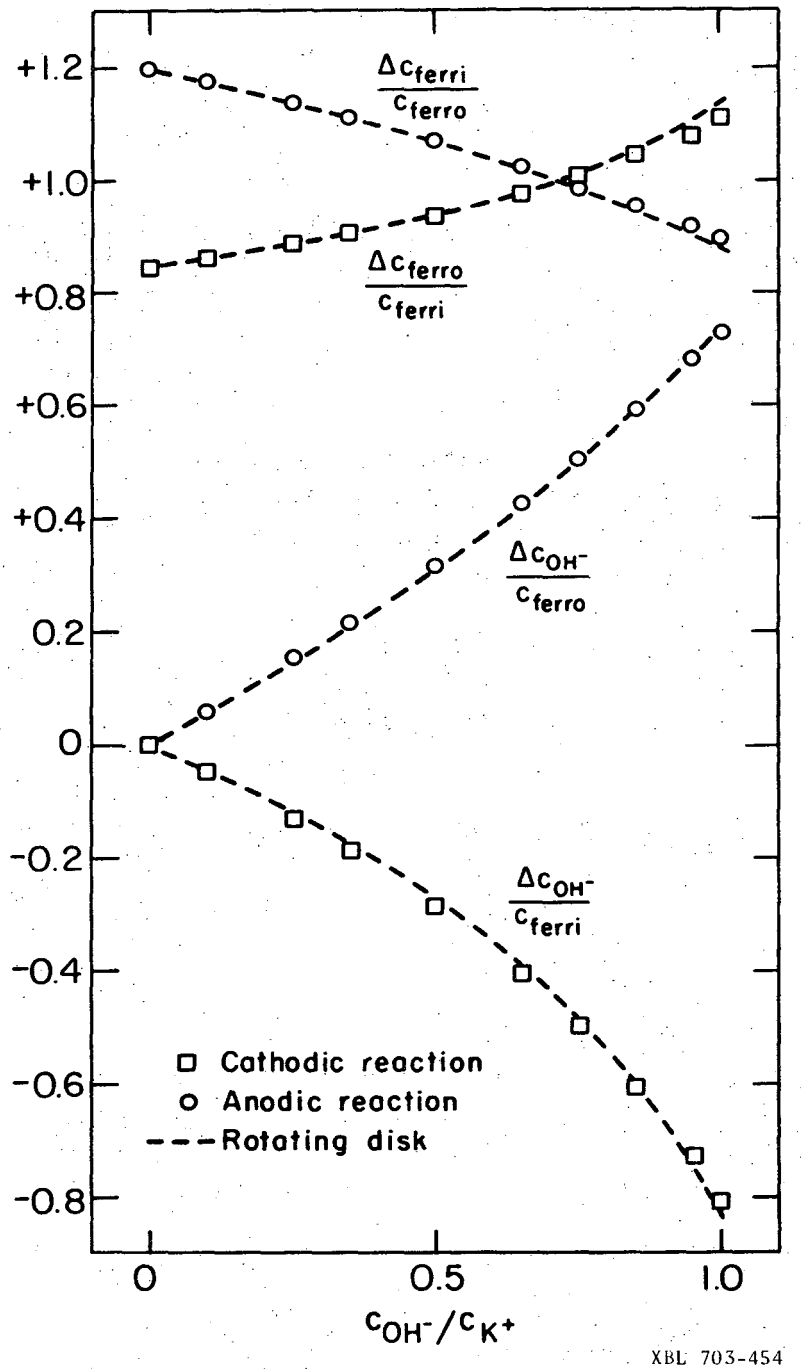

Figure 19. Surface concentrations in the system $K_3Fe(CN)_6$-$K_4Fe(CN)_6$-KOH-H_2O.

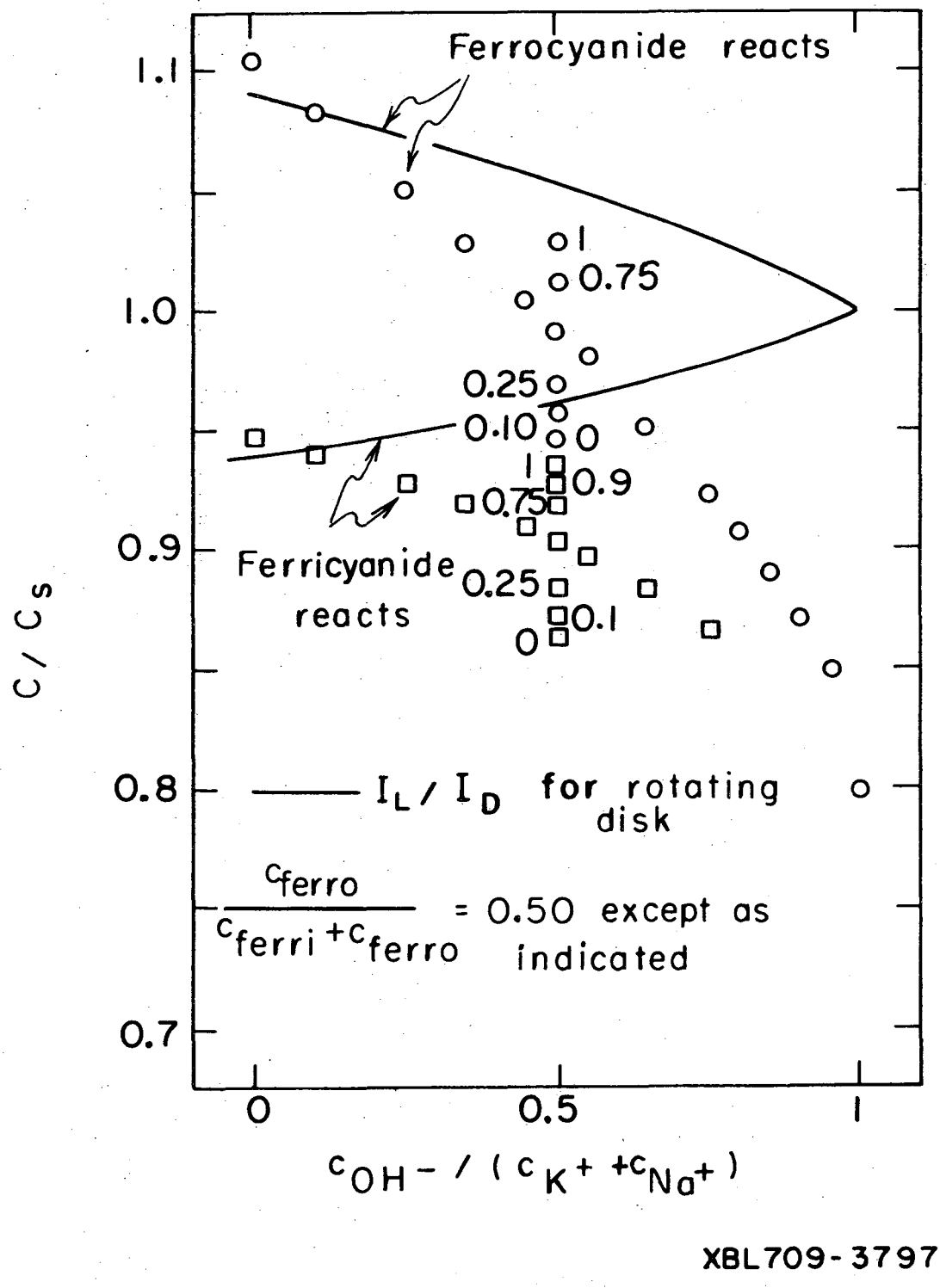

Figure 20. Migration current in the system $K_3Fe(CN)_6$-$K_4Fe(CN)_6$-NaOH-H_2O.

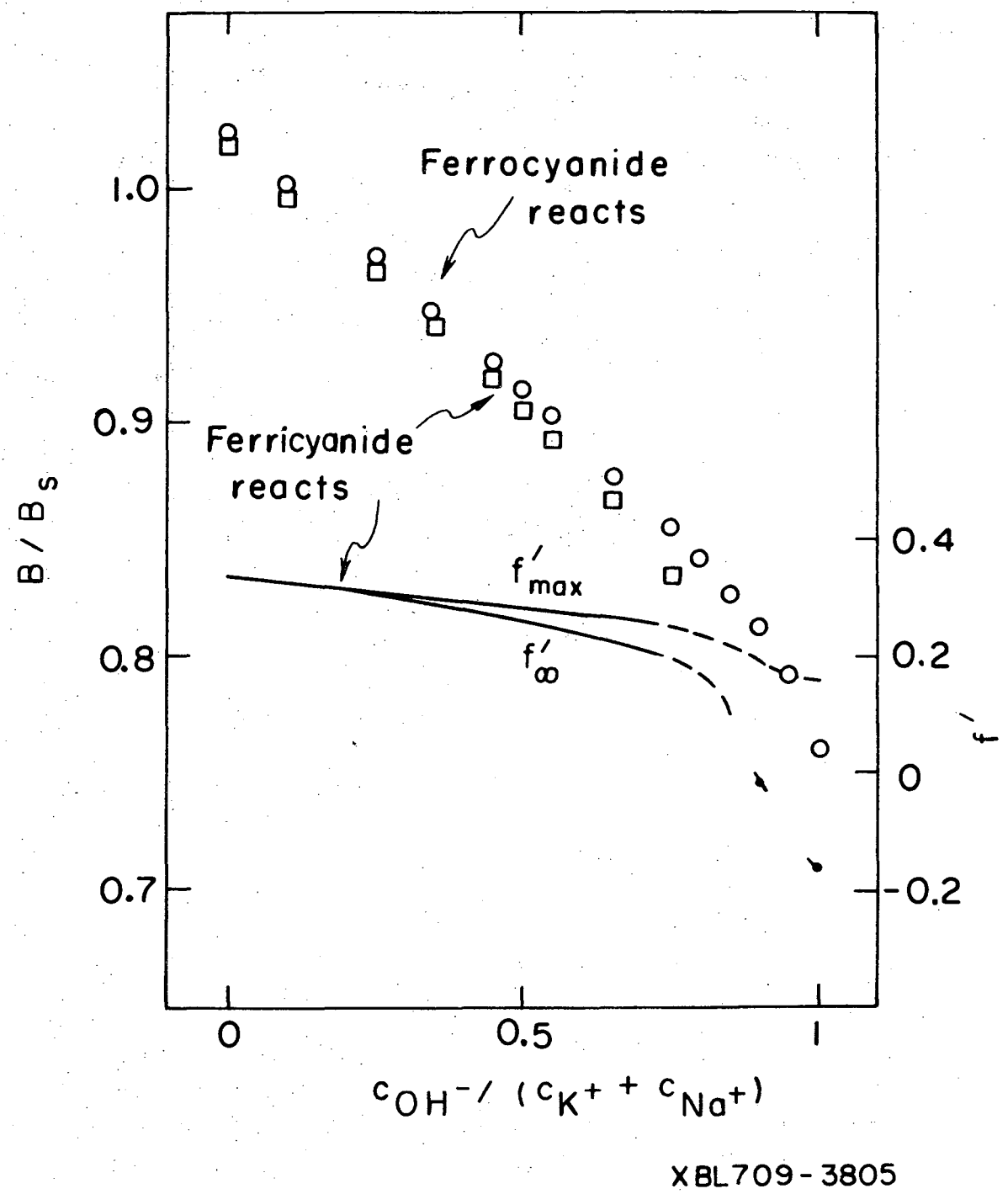

Figure 21. Shear stress and characteristic velocities in the system $K_3Fe(CN)_6$-$K_4Fe(CN)_6$-NaOH-H_2O.

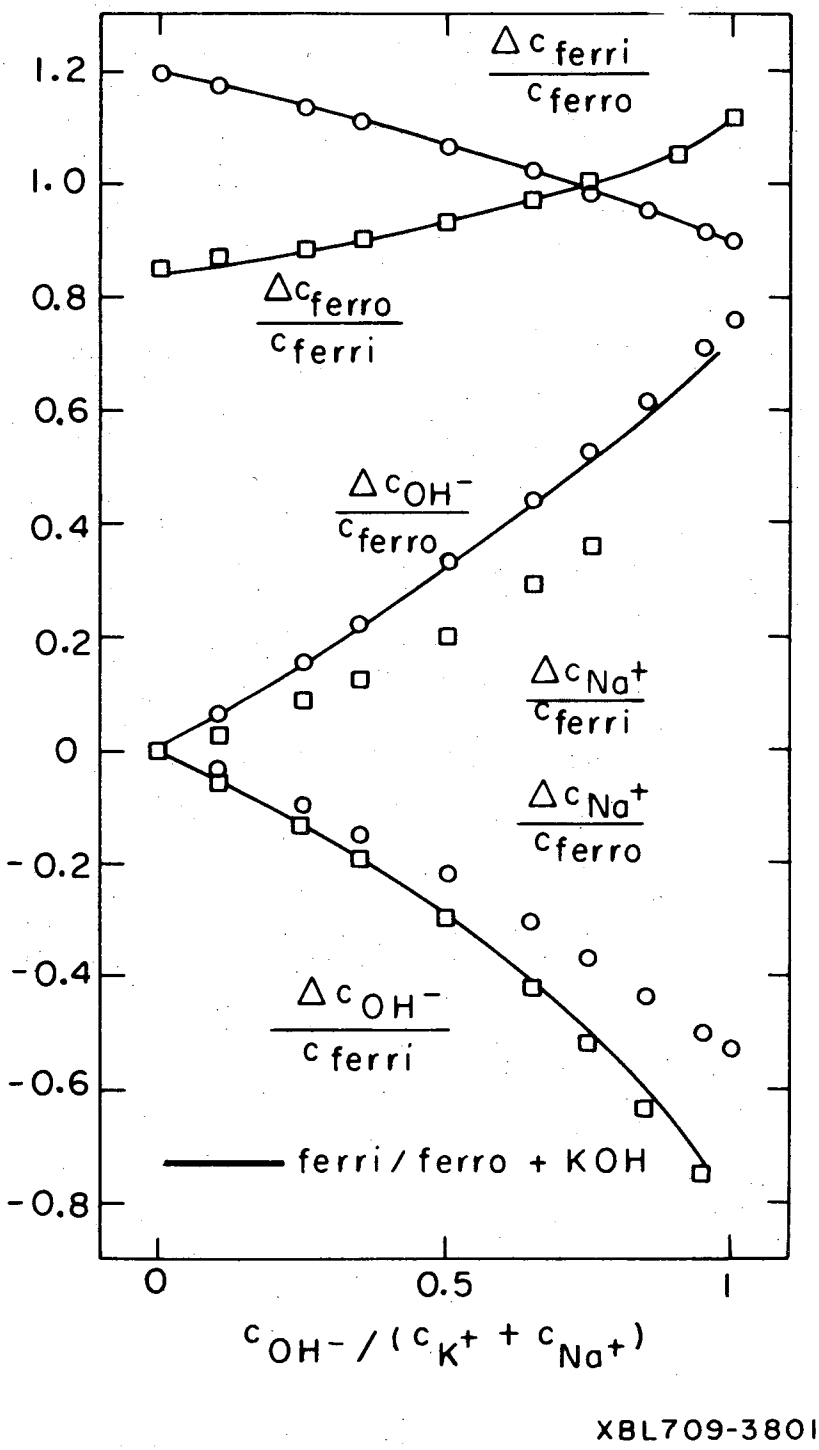

Figure 22. Surface concentrations in the system $K_3Fe(CN)_6$-$K_4Fe(CN)_6$-NaOH-H_2O.

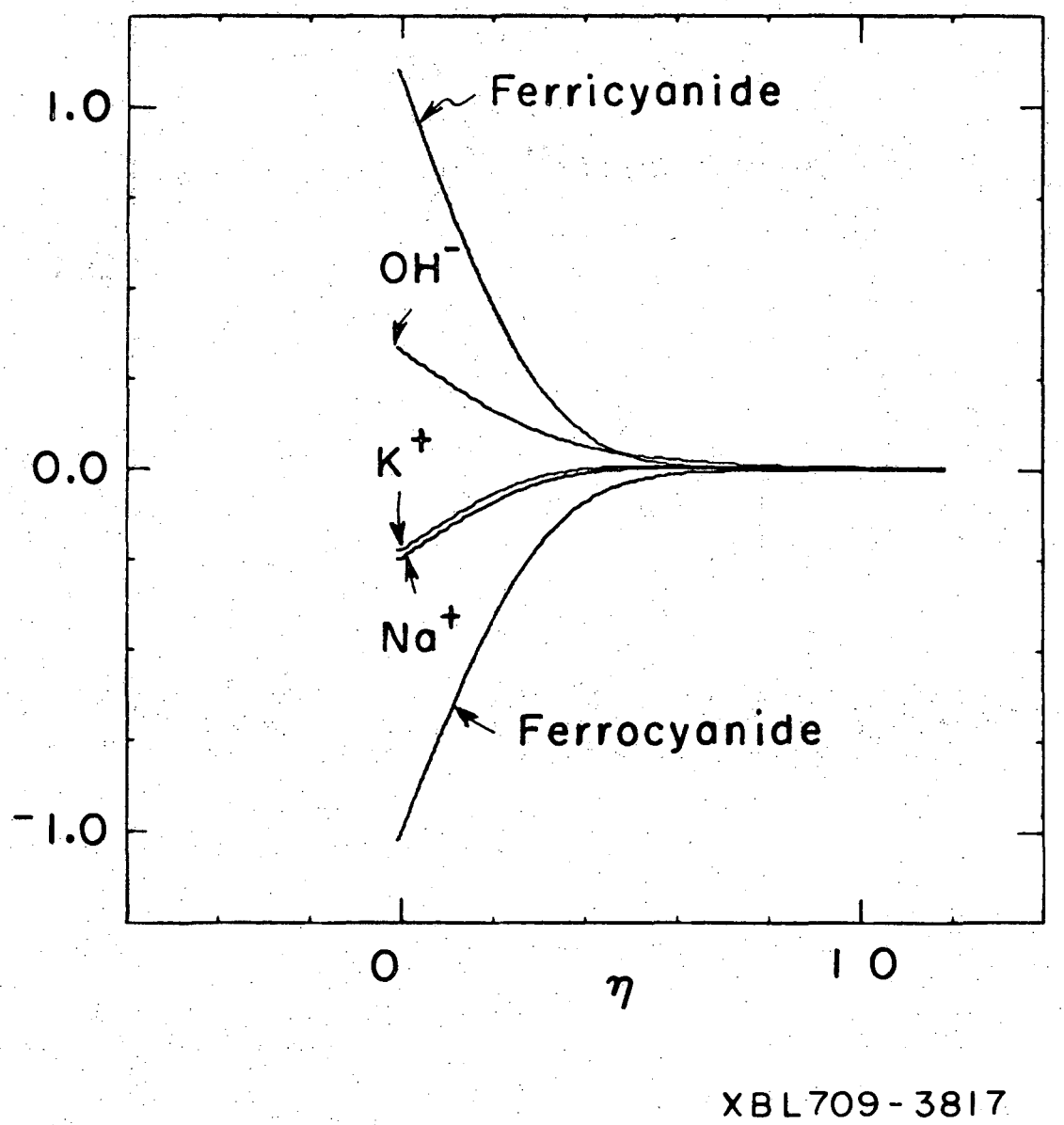

Figure 23. Concentration profiles in the system $K_3Fe(CN)_6$-$K_4Fe(CN)_6$-NaOH-H_2O. Excess relative to the bulk is shown normalized with respect to reactant (ferrocyanide) concentration.

Appendix A. Migration in forced and free convection: correlation of selected present and earlier[13] results.

A1. System $CuSO_4$-H_2SO_4-H_2O (complete dissociation).

The data (shown in figure 8) are correlated by the expressions

$$C/C_s = a_o + a_1 r^{1/3} + a_2 r^{2/3} + a_3 r \qquad (A.1)$$

$$\Delta c_{H_2SO_4}/\Delta c_{CuSO_4} = b_o + b_1 r^{1/3} + b_2 r^{2/3} + b_3 r \qquad (A.2)$$

The coefficients are:

	free convection	rot. disk	growing mercury drop	Nernst layer
a_o	1.91143	1.88574	1.83046	2.00324
a_1	-0.77174	-0.63461	-0.79315	-0.25946
a_2	-0.71969	-0.73990	-0.30667	-1.62904
a_3	+0.53115	0.49257	0.26987	0.88836
SE	0.0043	0.0050	0.0024	0.0064
b_o	-0.00043	-0.000275	-0.00013	-0.001078
b_1	0.22615	0.19193	0.29972	0.08648
b_2	1.71151	0.57679	0.53240	0.54308
b_3	-1.00993	-0.33885	-0.33324	-0.29619
SE	0.0059	0.0025	0.0021	0.0021

S.E. = standard error

$$r = c_{H_2SO_4}/(c_{H_2SO_4} + c_{CuSO_4})$$

System $CuSO_4$ - H_2SO_4 - H_2O (partial dissociation: bisulfate ion undissociated)

$$C/C_s = a_o + a_1(2r-1)^{1/2} + a_2(2r-1) + a_3(2r-1)^{3/2} \quad (A.3)$$

$$\Delta c_{H_2SO_4}/\Delta c_{CuSO_4} = b_o + b_1(2r-1)^{1/2} + b_2(2r-1) + b_3(2r-1)^{3/2} \quad (A.4)$$

	rotating disk	growing mercury drop	Nernst layer
a_o	2.654	2.497	3.000
a_1	-3.9525	-3.8216	-3.7573
a_2	+3.7754	+3.8920	+2.5881
a_3	-1.4818	-1.5726	-0.8323
SE	0.008	0.010	0.003
b_o	-0.9997	-0.9996	-0.9998
b_1	+2.5270	+2.9069	+1.8787
b_2	-2.1062	-2.5427	-1.2942
b_3	+0.7141	+0.9052	+0.4162
SE	0.003	0.004	0.002

A2. System $K_3Fe(CN)_6$-$K_4Fe(CN)_6$-H_2O.

The data for free convection (shown by solid lines in Fig. 12) are correlated by the expressions:

$$C/C_s = a_o + a_1 r + a_2 r^2 \qquad (A.5)$$

$$\Delta c_{\text{product ion}}/\Delta c_R = b_o + b_1 r + b_2 r^2 \quad , \qquad (A.6)$$

where $r = r_a$ if ferrocyanide reacts (anodic)

$r = r_b$ if ferricyanide reacts (cathodic)

Coefficients are:

	anodic	cathodic
a_o	1.013425	0.876152
a_1	0.196820	0.154181
a_2	-0.026707	-0.020666
S.E.	0.00016	0.00012
b_o	1.201934	0.837864
b_1	-0.011434	0.008311
b_2	+0.001656	-0.001198
S.E.	0.00001	0.00001

S.E. = Standard error

A3. System $K_3Fe(CN)_6$-$K_4Fe(CN)_6$-KOH(NaOH)-H_2O.

The data for rotating disk forced convection (shown by solid lines in figures 15, 19, 20 and 22) in equimolar ferri-/ferro-cyanide solutions are correlated by the expressions

$$C/C_s = a_o + a_1R + a_2R^2 + a_3R^3 \tag{A.7}$$

$$\Delta c_{\text{product ion}}/\Delta c_R = b_o + b_1R + b_2R^2 + b_3R^3 \tag{A.8}$$

$$\Delta c_{OH^-}/\Delta c_R = c_o + c_1R + c_2R^2 + c_3R^3 \tag{A.9}$$

where $R = c_{OH^-}/c_{K^+}$ if KOH is supporting

or $R = c_{OH^-}/(c_{K^+} + c_{Na^+})$ if NaOH is supporting.

Coefficients are:

	Anodic KOH	Anodic NaOH	Cathodic KOH	Cathodic NaOH
a_o	1.091071	0.946226	0.938131	0.938138
a_1	-0.070615	0.833289	0.044120	0.041739
a_2	-0.010072	-1.58795	-0.005240	-0.005163
a_3	-0.010580	0.817698	0.022868	0.025128
S.E.	0.0002	0.0176	0.0002	0.0002
b_o	1.197425		0.840521	
b_1	-0.225883		0.185190	
b_2	-0.040879		-0.105595	
b_3	-0.051645		0.215589	
S.E.	0.0002		0.0021	
c_o	0.000035		0.002036	
c_1	0.545220		-0.545496	
c_2	0.083316		0.278367	
c_3	0.104858		-0.564034	
S.E.	0.0004		0.0057	

S.E. = standard error

Appendix B. Fortran program for coupled equations.

Before linearization of the equations (4.14-16) an auxiliary function h is introduced such that

$$h' = f \quad , \tag{B.1}$$

and f' is for convenience represented by g. Moreover the concentrations in the program are all real (dimensioned) concentrations c_i but taken with respect to the bulk concentration $c_{i\infty}$: $\Delta c_i = c_i - c_{i\infty}$.

The set of n equations corresponding to the n variables

$$g,\ h,\ \Delta c_1,\ \Delta c_2,\ \ldots \Delta c_i \ldots,\ \Delta c_R,\ \phi \quad ,$$

is now, after linearization of the equations of convective diffusion:

(1) $$g'' - T_i \Delta c_i = 0 \quad , \tag{B.2}$$

(2) $$g - h'' = 0 \quad , \tag{B.3}$$

(i) $$R_i \Delta c''_i + h'(\Delta c'_i)_o + (h')_o \Delta c'_i + Q_i R_i [\Delta c_i (\phi'')_o + c_{i\infty}\phi'' + (\Delta c_i)_o \phi'' + \Delta c'_i (\phi')_o + (\Delta c'_i)_o \phi'] =$$

$$Q_i R_i [(\Delta c_i)_o (\phi'')_o + (\Delta c'_i)_o (\phi')_o] + (h')_o (\Delta c'_i)_o \tag{B.4}$$

(n) $$\sum_i z_i \Delta c_i = 0 \quad , \tag{B.5}$$

where $Q_i = z_i u_i RT/D_i$.

The boundary conditions are, at the electrode:

(1) $$g = 0 \quad , \tag{B.6}$$

(2) $$h' = 0 \quad , \tag{B.7}$$

(i) $R_i \Delta c_i' + Q_i R_i [\Delta c_i (\phi')_o + c_{i\infty} \phi' + (\Delta c_i)_o \phi']$

$$- \frac{s_i}{s_R} \Delta c_R' - \frac{s_i}{s_R} Q_R (\Delta c_R)_o \phi' = Q_i R_i (\Delta c_i)_o (\phi')_o \quad , \tag{B.8}$$

(n-1) $$\Delta c_R = \Delta c_{Ro} \quad . \tag{B.9}$$

The boundary conditions in the bulk are:

(1) $$g' = 0 \quad , \tag{B.10}$$

(2) $$h = 0 \quad , \tag{B.11}$$

(i) $$\Delta c_i = 0 \quad , \tag{B.12}$$

Moreover ϕ is arbitrarily made zero at the last meshpoint.

After finite differencing the set of equations becomes:

(1) $$g(j-1) + 2g(j) + g(j+1) - \sum_i H^2 T_i \Delta c_i (j) = 0 \quad , \tag{B.13}$$

(2) $$-H^2 g(j) + h(j-1) - 2h(j) + h(j+1) = 0 \quad , \tag{B.14}$$

(i) $-\frac{1}{2} H (\Delta c_i')_o h(j-1) + \frac{1}{2} H (\Delta c_i')_o h(j+1) + \Delta c_i (j-1) \{R_i$

$-\frac{1}{2} H (h')_o - \frac{1}{2} H Q_i R_i (\phi')_o\} + \Delta c_i (j) \{-2R_i + H^2 Q_i R_i (\phi'')_o\}$

$+\Delta c_i (j+1) \{R_i + \frac{1}{2} H (h')_o + \frac{1}{2} H Q_i R_i (\phi')_o\} + \phi(j-1) [Q_i R_i$

$\{(\Delta c_i)_o + c_{i\infty} - \frac{1}{2} H (\Delta c_i')_o\}] + \phi(j) [-2Q_i R_i \{(\Delta c_i)_o +$

$c_{i\infty}\}] + \phi(j+1) [Q_i R_i \{(\Delta c_i)_o + c_{i\infty} + \frac{1}{2} H (\Delta c_i')_o\}]$

$$= H^2 [Q_i R_i \{(\Delta c_i)_o (\phi'')_o + (\Delta c_i')_o (\phi')_o\} + (h')_o (\Delta c_i')_o] \tag{B.15}$$

(n) $$\sum_i z_i \Delta c_i (j) = 0 \tag{B.16}$$

The boundary conditions at the electrode (j=2) are:

$$(1)\quad g(2) = 0 \quad , \tag{B.17}$$

$$(2)\quad h(1) = h(3) \quad , \tag{B.18}$$

$$(i)\quad -\frac{1}{2} R_i \Delta c_i(1) + HQ_i R_i (\phi')_o \Delta c_i(2) + \frac{1}{2} R_i \Delta c_i(3)$$

$$+ \frac{1}{2} \Delta c_R(1)\, s_i/s_R - \frac{1}{2} \Delta c_R(3)\, s_i/s_R + \phi(1)\left[-\frac{H}{2} Q_i R_i \{(\Delta c_i)_o + c_{i\infty}\}\right.$$

$$\left. + \frac{1}{2} Q_R (\Delta c_R)_o s_i/s_R\right] - \phi(3)\left[-\frac{H}{2} Q_i R_i \{(\Delta c_i)_o + c_{i\infty}\} + \right.$$

$$\left. \frac{1}{2} Q_R (\Delta c_R)_o s_i/s_R\right] = HQ_i R_i (\Delta c_i)_o (\phi')_o \quad , \tag{B.19}$$

$$(n\text{-}1)\quad \Delta c_R(2) = \Delta c_{Ro} \quad , \tag{B.20}$$

$$(n)\quad \sum_i z_i \Delta c_i(2) = 0 \quad . \tag{B.21}$$

The boundary conditions at the last meshpoint are:

$$(1)\quad g(NJ) = g(NJ\text{-}1) \quad , \tag{B.22}$$

$$(2)\quad h(NJ) = 0 \quad , \tag{B.23}$$

$$(i)\quad \Delta c_i(NJ) = 0 \quad , \tag{B.24}$$

$$(n)\quad \phi(NJ) = 0 \quad . \tag{B.25}$$

The set of equations (1) through (n) is now solved for one meshpoint after another. At meshpoint j each equation is linear in the following unknown variables:

$C(J,1) = g(j)$,

$C(J,2) = h(j)$,

$C(J,K) = \Delta c_k(j)$ where $k = K\text{-}2$,

$C(J,NM1) = \Delta c_k(j)$,

$C(J,N) = \phi(j)$.

At each point j, except j=1 and j=NJ, there are n equations of the form:

$$\sum_{K=1}^{N} [A(I,K)C(J-1,K) + B(I,K)C(J,K) + D(I,K)C(J+1,K)] = G(I) \quad (B.26)$$

The coefficients A(I,K), B(I,K) and D(I,K) are recomputed at every step. The first meshpoint is treated as an image point, by substituting equations as follows:

$$\sum_{K=1}^{N} [B(I,K)C(1,K) + D(I,K)C(2,K) + X(I,K)C(3,K)] = G(I) \quad (B.27)$$

Details of the numerical solution procedure are given elsewhere.[32]

The first iteration is started with an assumed profile for each variable. Usually it suffices to substitute a linear reactant concentration and a cubic expression for h.

Further nomenclature in the program:

BP = $H(h')_o$

CP = $H(c_i')_o$

PP = $H(\phi')_o$

PPP = $H^2(\phi'')_o$

CIN(I) = $c_{i\infty}$

Q(I) = $Q_i = z_i u_i RT/D_i$

R(I) = $R_i = D_i/D_R$

S(I) = s_i

T(I) = $T_i = \alpha_i/\alpha_R$

Z(I) = z_i

N = number of variables

NJ = number of meshpoints

JCOUNT = iteration

SIGN = sign of density difference

$AK = \Delta\rho_o/\rho_\infty \alpha\ \Delta C_R$

$AMP = C_R$

$AMPRHO = C$

$DINT = \int_o^\infty e^{-\int_o^\eta f d\eta}\, d\eta$

$FPIN = f'_\infty$

$EC(I) = (c_{io}-c_{i\infty})/(c_{R\infty}-c_{Ro})$

$FDPRO = f''_o$

$STRESS = B_R$

$STRRHO = B$

$AMPDIF = C^*/|AK|^{1/4}$

```
      PROGRAM WALL(INPUT,OUTPUT)
C     PROGRAM FOR NATURAL CONVECTION WITH MIGRATION, AT A VERTICAL WALL.
      DIMENSION C(150,7),G(7),A(7,7),B(7,7),D(7,15),X(7,7),CIN(7),Q(7),
     1 R(7),S(7),Z(7),T(7),EC(7),YY(7,7),TT(7),E(150)
      COMMON A,B,C,D,G,X,YY,N,NJ
  101 FORMAT (9E8.4)
  102 FORMAT (8X,5E8.4)
  103 FORMAT(1H1,10X,2HH=,F6.3,6H , NJ=,I4)
  104 FORMAT ( 5X,*Q*, 7X,*R*, 8X,*T*, 6X,*Z*,4X,*S*/(F8.2,2F9.4,2F5.1))
  105 FORMAT (30HOTHE NEXT RUN DID NOT CONVERGE)
  106 FORMAT(/1H0,3X,*AMPRHO*,3X,*STRRHO*,3X,*  AK *,3X,*JCOUNT*/F10.6,
     1F9.6,F8.5,I6)
  107 FORMAT (1H0, 6X,*CINF*,7X,*CZERO*,8X,*EC*/(3F12.6))
  108 FORMAT (1H0,4X,*RAMP*,6X,*RSTR*,5X,*RDAMP*,6X,*FPIN*/4F10.6)
  109 FORMAT(1H0,3X,*ONEMT*,3X,*RSALT*,3X,*TSALT*,3X,*AMPSAL*,3X,*STRSAL
     1*,3X,*FPSAL*,3X,*JCOUNT*/3(X,F7.4),3(3X,F9.6),I3)
      SIGN=-1. $ N=6 $ NJ=150 $ CRO=0. $ H=0.061141 $NM1=N-1 $NM2=N-2
      READ 102, (Q(I),R(I),T(I),Z(I),S(I),I=3,NM1) $ PRINT 103, H,NJ
      PRINT104, (Q(I),R(I),T(I),Z(I),S(I),I=3,NM1) $ NJM1=NJ-1
   99 READ 101, (CIN(I),I=3,NM1)   $ AMP=0.   $ IF (CIN(NM1).EQ.0.) STOP
      DO 14 J=1,NJ $ C(J,1)=0. $ C(J,3)=0. $ C(J,4)=0.
      C(J,2)=(H*(J-2))**3/6. $ C(J,NM1)= CIN(NM1)*(-1.+(J-2)/(NJ-2))
   14 C(J,N)=0.0 $ DO 12 K=3,NM1
   12 TT(K)=H*H*T(K)/(CIN(NM1)-CRO) $ JCOUNT=0
   98 JCOUNT=JCOUNT+1
      DO 11 J=1,NJ $ DO 1 I=1,N $ G(I)=0.0 $ DO 1 K=1,N $ YY(I,K)=0.0
      IF(J.EQ.1) X(I,K)=0.0$ A(I,K)=0.0 $ B(I,K)=0.0
    1  D(I,K)=0.0 $ IF(J.EQ.NJ) GO TO 9 $ DO 2 K=3,NM1
C     COEFFICIENTS OF ELECTRONEUTRALITY EQUATION.
    2 B(N,K)=Z(K) $ JJ=J $ IF(J.EQ.1) JJ=2 $ IF(J.EQ.2) GO TO 7
C     COEFFICIENTS OF DIFFUSION EQUATIONS.
      BP=(C(JJ+1,2)-C(JJ-1,2))/2. $ PP=(C(JJ+1,N)-C(JJ-1,N))/2.
      PPP=C(JJ+1,N)+C(JJ-1,N)-2.*C(JJ,N) $ DO 3 I=3,NM1
      IF(R(I)-BP/2..GT.Q(I)*R(I)*PP/2.) GO TO 5 $ B(I,I)=1.0 $ GO TO 3
    5 CP=(C(JJ+1,I)-C(JJ-1,I))/2. $ A(I,2)=-CP/2. $ D(I,2)=CP/2.
      A(I,I)=R(I)-BP/2.-Q(I)*R(I)*PP/2. $ B(I,I)=-2.*R(I)+Q(I)*R(I)*PPP
      D(I,I)=R(I)+BP/2.+Q(I)*R(I)*PP/2.
      A(I,N)=Q(I)*R(I)*(C(JJ,I)-CP/2.+CIN(I))
      B(I,N)=-2.*Q(I)*R(I)*(C(JJ,I)+CIN(I))
      D(I,N)=Q(I)*R(I)*(C(JJ,I)+CP/2.+CIN(I))
      G(I)=Q(I)*R(I)*(C(JJ,I)*PPP+CP*PP)+BP*CP
    3 CONTINUE
C     COEFFICIENTS OF EQUATION OF MOTION AND COUPLING EQUATION.
      B(2,1)=-H*H $ A(1,1)=1. $ B(1,1)=-2. $ D(1,1)=1. $ DO 4 K=3,NM1
    4 B(1,K)=TT(K)*SIGN $ A(2,2)=1. $ B(2,2)=-2. $ D(2,2)=1.
      IF(J.NE.1) GO TO 11 $ DO 6 I=1,NM1 $ DO 6 K=1,N $ X(I,K)=D(I,K)
      D(I,K)=B(I,K) $ B(I,K)=A(I,K)
    6 A(I,K)=0.0 $ GO TO 11
C     BOUNDARY CONDITIONS AT THE WALL.
    7 B(1,1)=1. $ A(2,2)=-1. $ D(2,2)=1. $ DO 8 I=3,NM2$ A(I,I)=-R(I)/2.
      B(I,I)=Q(I)*R(I)*PP $ D(I,I)=R(I)/2.
      A(I,N)=-Q(I)*R(I)*(C(2,I)+CIN(I))/2. +
     1 S(I)*Q(NM1)*R(NM1)*CRO/S(NM1)/2.
      A(I,NM1)=S(I)/S(NM1)/2. $ D(I,NM1)=-A(I,NM1) $ D(I,N)=-A(I,N)
    8 G(I)=Q(I)*R(I)*C(2,I)*PP $ B(NM1,NM1)=1. $ G(NM1)=CRO-CIN(NM1)
      GO TO 11
C     BOUNDARY CONDITIONS FAR FROM THE WALL.
    9 A(1,1)=1. $ B(1,1)=-1. $ DO 10 I=2,N
   10 B(I,I)=1.
```

```
C      ALGORITHM FOR SOLVING A SET OF SIMULTANEOUS ALGEBRAIC EQUATIONS
   11 CALL BAND(J) $ AMPO=AMP
      AMP = (-3.*C(1,NM1)-10.*C(2,NM1)+18.*C(3,NM1)-6.*C(4,NM1)+C(5,NM1)
     1 +Q(NM1)*CRO*(-3.*C(1,N)-10.*C(2,N)+18.*C(3,N)-6.*C(4,N)+C(5,N)))/
     112. /H /(CIN(NM1)-CRO)*(4./3.)**.75
      IF(ABS(AMP-AMPO).LE.1.0E-5) GO TO 97 $ IF(JCOUNT.LE.12) GO TO 98
      PRINT 105
C      OUTPUT
   97 AK=0. $ DO 15 K=3,NM1 $ TT(K)=C(2,K)+CIN(K)
      EC(K)=C(2,K)/(CIN(NM1)-CRO)
   15 AK= AK +T(K)*C(2,K)/(CRO-CIN(NM1))
      FDPRO=(-3.*C(1,1)-10.*C(2,1)+18.*C(3,1)-6.*C(4,1)+C(5,1))/12./H
      STRESS=FDPRO*(4./3.)**.25*.8
      IF (N.NE.5) GO TO 21
C      CONVERSION FOR BINARY SOLUTION
      ONEMT=     (-Z(NM2)*R(NM2))/(Z(NM1)-(Z(NM2)*R(NM2)))
      RSALT=(Z(NM1)-Z(NM2))/(Z(NM1)/R(NM2)-Z(NM2))
      TSALT= 1.-Z(NM1)*T(NM2)/Z(NM2)
      AMPSAL=AMP*ONEMT/RSALT/((TSALT/RSALT)**.25)
      STRSAL=STRESS/TSALT**.75/RSALT**.25
      FPSAL=FPIN/TSALT**.5/RSALT**.5
      PRINT 109,ONEMT, RSALT,TSALT,AMPSAL,STRSAL,FPSAL,JCOUNT
      GO TO 22
C      CONVERSION TO TOTAL DENSITY BASED QUANTITIES
   21 AMPRHO=AMP/ABS(AK)**.25
      STRRHO=STRESS/ABS(AK)**.75
      PRINT 106, AMPRHO,STRRHO,AK,JCOUNT
      DINT=0. $ DO 16 J=3,NJ
   16 DINT=DINT+EXP(-C(J,2))+EXP(-C(J-1,2)) $ DINT=DINT*EXP(C(2,2))*H*.5
      AMPDIF=(4./3.)**.75/ABS(AK)**.25/DINT $ RAMP=AMPRHO/.67032
      RDAMP=AMPRHO/AMPDIF $ RSTR=STRRHO/.93308
      FPIN=C(NJ,1)/ABS(AK)**.5
      PRINT 108, RAMP,RSTR,RDAMP,FPIN
   22 PRINT 107, (CIN(I),TT(I),EC(I),I=3,NM1)
      GO TO 99 $ END
      SUBROUTINE BAND(J) $ COMMON A,B,C,D,G,X,Y,N,NJ
      DIMENSION C(150,7),G(7),A(7,7),B(7,7),D(7,15),E(7,8,150),X(7,7),
     1 Y(7,7)
  101 FORMAT (15HODETERM=0 AT J=,I4)
      IF(J.GT.1) GO TO 6 $ NP1= N+1 $ DO 2 I=1,N $ D(I,2*N+1)=G(I)
      DO 2 L=1,N $ LPN=L+N
    2 D(I,LPN)=X(I,L) $ CALL MATINV(N,2*N+1,DETERM)
      IF(DETERM.EQ.0.0) PRINT 101, J $ DO 5 K=1,N
      E(K,NP1,1)=D(K,2*N+1) $ DO 5 L=1,N $ E(K,L,1)=-D(K,L) $ LPN=L+N
    5 X(K,L)=-D(K,LPN) $ RETURN
    6 IF(J.GT.2) GO TO 8 $ DO 7 I=1,N $ DO 7 K=1,N $ DO 7 L=1,N
    7 D(I,K)=D(I,K)+A(I,L)*X(L,K)
    8 IF(J.LT.NJ) GO TO 11 $ DO 10 I=1,N $ DO 10 L=1,N
      G(I)=G(I) - Y(I,L)*E(L,NP1,J-2) $ DO 10 M=1,N
   10 A(I,L)=A(I,L) + Y(I,M)*E(M,L,J-2)
   11 DO 12 I=1,N $ D(I,NP1)=-G(I) $ DO 12 L=1,N
      D(I,NP1)=D(I,NP1) + A(I,L)*E(L,NP1,J-1) $ DO 12 K=1,N
   12 B(I,K)=B(I,K) + A(I,L)*E(L,K,J-1) $ CALL MATINV(N,NP1,DETERM)
      IF(DETERM.EQ.0.0) PRINT 101,J $ DO 15 K=1,N $ DO 15 M=1,NP1
   15 E(K,M,J)=-D(K,M) $ IF(J.LT.NJ) RETURN $ DO 17 K=1,N
   17 C(J,K)=E(K,NP1,J) $ DO 18 JJ=2,NJ $ M=NJ-JJ+1 $ DO 18 K=1,N
      C(M,K)=E(K,NP1,M) $ DO 18 L=1,N
   18 C(M,K)=C(M,K) + E(K,L,M)*C(M+1,L) $ DO 19 L=1,N $ DO 19 K=1,N
   19 C(1,K)=C(1,K) + X(K,L)*C(3,L) $ RETURN $ END
      SUBROUTINE MATINV(N,M,DETERM) $ COMMON A,B,C,D
```

```
C     MATRIX INVERSION WITH ACCOMPANYING SOLUTION OF LINEAR EQUATIONS.
      DIMENSION ID(7),B(7,7),D(7,15),A(7,7),C(150,7)
      DETERM=1.0 $ DO 1 I=1,N
    1 ID(I)=0.0 $ DO 18 NN=1,N $ BMAX=0.0 $ DO 6 I=1,N
      IF(ID(I).NE.0) GO TO 6 $ DO 5 J=1,N $ IF(ID(J).NE.0) GO TO 5
      IF(ABS(B(I,J)).LT.BMAX) GO TO 5 $ BMAX=ABS(B(I,J)) $ IROW=I$JCOL=J
    5 CONTINUE
    6 CONTINUE
      IF(BMAX) 7,7,8
    7 DETERM=0.0 $ RETURN
    8 ID(JCOL)=1 $ IF(JCOL.EQ.IROW) GO TO 12 $ DO 10 J=1,N
      SAVE=B(IROW,J) $ B(IROW,J)=B(JCOL,J)
   10 B(JCOL,J)=SAVE $ DO 11 K=1,M $ SAVE=D(IROW,K) $D(IROW,K)=D(JCOL,K)
   11 D(JCOL,K)=SAVE
   12 F=1.0/B(JCOL,JCOL) $ DO 13 J=1,N
   13 B(JCOL,J)=B(JCOL,J)*F $ DO 14 K=1,M
   14 D(JCOL,K)=D(JCOL,K)*F $ DO 18 I=1,N $ IF(I.EQ.JCOL) GO TO 18
      F=B(I,JCOL) $ DO 16 J=1,N
   16 B(I,J)=B(I,J) - F*B(JCOL,J) $ DO 17 K=1,M
   17 D(I,K)=D(I,K) - F*D(JCOL,K)
   18 CONTINUE $ RETURN $ END
-
H+       +38920+1130522+0002139+0+10000-0      0-0
SO4--    -77850+1149250-1000000+0-20000+0      0-0
CU++     +77850+1100000-1100000-1+20000+0+10000+0
010000+3500010+1010000-2
```

Appendix C. Fortran program for uncoupled equations:

The equation of motion (4.14) and the coupling equation

$$h'' = g \tag{B.3}$$

are eliminated in this procedure. The only change in the linearized equations of convective diffusion is the disappearance, in (B.4), of the terms $h' (\Delta c_i')_o$ and $(h')_o(\Delta c_i')_o$, so that (B.15) takes the form:

$$\Delta c_i(j-1)\{R_i - \tfrac{1}{2}H(h')_o - \tfrac{1}{2}HQ_iR_i(\phi')_o\} + \Delta c_i(j)\{-2R_i$$

$$+ H^2Q_iR_i(\phi'')_o\} + \Delta c_i(j+1)\{R_i + \tfrac{1}{2}H(h')_o + \tfrac{1}{2}HQ_iR_i(\phi')_o\}$$

$$+ \phi(j-1)[Q_iR_i\{(\Delta c_i)_o + c_{i\infty} - \tfrac{1}{2}H(\Delta c_i')_o\}] +$$

$$\phi(j)[-2Q_iR_i\{(\Delta c_i)_o + c_{i\infty}\}] + \phi(j+1)[Q_iR_i\{(\Delta c_i)_o$$

$$+ c_{i\infty} + \tfrac{1}{2}H(\Delta c_i')_o\}] = H^2[Q_iR_i\{(\Delta c_i)_o(\phi'')_o$$

$$+ (\Delta c_i')_o(\phi')_o\}] \tag{C.1}$$

If the flux at the electrode (AMP in the nomenclature of Appendix B) converges in the inner loop, the program calculates by Simpson integration:

$$F(J,1) = \Delta\rho/\alpha_R\Delta c_R(\eta) \quad , \tag{C.2}$$

$$F(J,2) = f''(\eta) \quad , \tag{C.3}$$

$$F(J,3) = f'(\eta) = g(\eta) \quad , \tag{C.4}$$

$$F(J,4) = f(\eta) = h'(\eta) \quad , \tag{C.5}$$

and then adjusts $f(\eta)$ to $f_1(\xi) = A_1 f(\eta)$ at every point, after calculating the factor A_1:

$B4 = 1./F(2,2) = 1/f_o'' = \Delta\rho/\alpha_R \Delta c_R = A_1^4$

$BF = A_1$

$BINV = A_2$.

Since at any point $\frac{\Delta\rho}{\alpha_R \Delta c_R}(\eta) = \frac{\Delta\rho}{\alpha_R \Delta c_R}(\xi)$, one has

$$f_1(\xi) = A_1 f(\eta) = A_1 \int_o^\eta \int_o^\eta \int_\infty^\eta \frac{\Delta\rho}{\alpha_R \Delta c_R}(\eta) d\eta d\eta d\eta =$$

$$A_1^4 \int_o^\xi \int_o^\xi \int_\infty^\xi \frac{\Delta\rho}{\alpha_R \Delta c_R}(\xi) \; d\xi d\xi d\xi \quad , \tag{C.6}$$

so $FF(J) \equiv f_1(\xi) = F(J,4) * B4$.

This is then used to compute the factor BP for the next iteration in the outer loop. The iterations in this loop are counted by KCOUNT. Convergence is decided by means of the flux AMP, which first is converted back to an η-based derivative in order to be comparable: AMP = AMP * BINV.

To obtain the shear stress one integrates once:

$$\left(\frac{\partial^2 f_1}{\partial \xi^2}\right)_o = A_1^3 \left(\frac{\partial^2 f}{\partial \eta^2}\right)_o = A_1^3 \int_\infty^o \frac{\Delta\rho}{\alpha_R \Delta c_R}(\eta) \, d\eta = A_1^4 \int_\infty^o \frac{\Delta\rho(\xi)}{\alpha_R \Delta c_R} \, d\xi \quad , \tag{C.7}$$

so:

$$FDPRO = \left(\frac{\partial^2 f}{\partial \eta^2}\right)_o = BF * F(2,2) \quad .$$

Similarly: $FPIN = \left(\frac{\partial f}{\partial \eta}\right)_\infty = A_1^2 \left(\frac{\partial f_1}{\partial \xi}\right)_\infty = BF**2*F(NJ,3)$.

In plotting profiles the dimensionless distance E(J) has to be adjusted, i.e., effectively a new meshwidth equal to H*BF is adopted.

The nomenclature in the program is for the rest essentially the same as in that of Appendix B.

```
      PROGRAM WALL(INPUT,OUTPUT)
C     PROGRAM FOR NATURAL CONVECTION WITH MIGRATION, AT A VERTICAL WALL.
C     EQUATION OF MOTION UNCOUPLED FROM DIFFUSION EQUATIONS
      DIMENSION C(150,7),G(7),A(7,7),B(7,7),D(7,15),X(7,7),CIN(7),Q(7),
     1 R(7),S(7),Z(7),T(7),EC(7),YY(7,7),II(7),E(150)
      DIMENSION F(150,4),FF(150)
      COMMON A,B,C,D,G,X,YY,N,NJ
  101 FORMAT (9E8.4)
  102 FORMAT (8X,5E8.4)
  103 FORMAT(1H1,10X,2HH=,F6.3,6H , NJ=,I4)
  104 FORMAT ( 5X,*Q*, 7X,*R*, 8X,*T*, 6X,*Z*,4X,*S*/(F8.2,2F9.4,2F5.1))
  105 FORMAT(50HOTHE NEXT RUN DID NOT CONVERGE / INNER LOOP           )
  106 FORMAT(/1HO,3X,*AMPRHO*,3X,*STRRHO*,3X,*  AK *,3X,*JCOUNT*/F10.6,
     1F9.6,F8.5,I6)
  107 FORMAT (1HO, 6X,*CINF*,7X,*CZERO*,3X,*EC*/(3F12.6))
  108 FORMAT (1HO,4X,*RAMP*,6X,*RSTR*,5X,*FDPRO*,6X,*FPIN*/4F10.6)
  109 FORMAT(50HOTHE NEXT RUN DID NOT CONVERGE / OUTER LOOP           )
  118 FORMAT(13X,7HICOUNT=,I3)
  119 FORMAT(10X,8H AMP=    ,E15.8,9H,STRRHO= ,E15.8,9H,FPIN=    ,E15.8,
     19H, AK=     ,E15.8)
  120 FORMAT(10X,7H B4=    ,F10.6,9H, B=      ,F10.6,11H,B INVERSE=,F10.6)
  121 FORMAT(106X,   5HIT.= ,I2,1H/,I2)
  122 FORMAT(4E5.2)
      SIGN=-1. $ N=6 $ NJ=150 $ CRO=0. $ H=0.05 $ NM1=N-1    $NM2=N-2
      READ 102, (Q(I),R(I),T(I),Z(I),S(I),I=1,NM1) $ PRINT 103, H,NJ
      PRINT104, (Q(I),R(I),T(I),Z(I),S(I),I=1,NM1) $ NJM1=NJ-1
   97 READ 122,EX,AA,BB,CC
      READ 101, (CIN(I),I=1,NM1)   $ AMP=0.   $ IF (CIN(NM1).EQ.0.) STOP
      DO 15 J=1,NJ
      E(J)=H*(J-2) $FF(J)=0.08*H*(J-2)**2 $ EXT=EXP(-EX*(J-2)*H)
      C(J,NM1)=-EXT*CIN(NM1) $ C(J,1)=AA*EXT*CIN(NM1)
      C(J,2)=BB*EXT*CIN(NM1) $ C(J,3)=CC*EXT*CIN(NM1) $ C(J,4)=C(J,2)
   15 C(J,N)=0.0 $ JCOUNT=0 $ ICOUNT=0 $ MFLAG=0 $ NFLAG=0 $ AMPOO=0.
   98 ICOUNT=ICOUNT+1
   99 JCOUNT=JCOUNT+1
      DO 11 J=1,NJ $ DO 1 I=1,N $ G(I)=0.0 $ DO 1 K=1,N $ YY(I,K)=0.0
      IF(J.EQ.1) X(I,K)=0.05 $ A(I,K)=0.0 $ B(I,K)=0.0
    1  D(I,K)=0.0 $ IF(J.EQ.NJ) GO TO 9 $ DO 2 K=1,NM1
C     COEFFICIENTS OF ELECTRONEUTRALITY EQUATION.
    2 B(N,K)=Z(K) $ JJ=J $ IF(J.EQ.1) JJ=2 $ IF(J.EQ.2) GO TO 7
C     COEFFICIENTS OF DIFFUSION EQUATIONS.
      BP=FF(JJ)*H $ DO 3 I=1,NM1 $ CP=(C(JJ+1,I)-C(JJ-1,I))/2.
      PP=(C(JJ+1,N)-C(JJ-1,N))/2. $ PPP=C(JJ+1,N)+C(JJ-1,N)-2.*C(JJ,N)
      A(I,I)=R(I)-BP/2.-Q(I)*R(I)*PP/2. $ B(I,I)=-2.*R(I)+Q(I)*R(I)*PPP
      D(I,I)=R(I)+BP/2.+Q(I)*R(I)*PP/2.
      A(I,N)=Q(I)*R(I)*(C(JJ,I)-CP/2.+CIN(I))
      B(I,N)=-2.*Q(I)*R(I)*(C(JJ,I)+CIN(I))
      D(I,N)=Q(I)*R(I)*(C(JJ,I)+CP/2.+CIN(I))
    3 G(I)=Q(I)*R(I)*(C(JJ,I)*PPP+CP*PP)
      IF(J.NE.1) GO TO 11 $ DO 6 I=1,NM1 $ DO 6 K=1,N $ X(I,K)=D(I,K)
      D(I,K)=B(I,K) $ B(I,K)=A(I,K)
    6 A(I,K)=0.0 $ GO TO 11
C     BOUNDARY CONDITIONS AT THE WALL.
    7 DO 8 I=1,NM2 $ PP=(C(3,N)-C(1,N))/2. $ A(I,I)=-R(I)/2.
      B(I,I)=Q(I)*R(I)*PP $ A(I,N)=-Q(I)*R(I)*(C(2,I)+CIN(I))/2.
     1+S(I)*Q(NM1)*R(NM1)*CRO/S(NM1)/2.      $ D(I,I)=R(I)/2.
      A(I,NM1)=S(I)/S(NM1)/2. $ D(I,NM1)=-A(I,NM1) $ D(I,N)=-A(I,N)
    8 G(I)=Q(I)*R(I)*C(2,I)*PP $ B(NM1,NM1)=1. $ G(NM1)=CRO-CIN(NM1)
      GO TO 11
```

```
C     BOUNDARY CONDITIONS FAR FROM THE WALL.
    9 DO 10 I=1,N
   10 B(I,1)=1.
C     ALGORITHM FOR SOLVING A SET OF SIMULTANEOUS ALGEBRAIC EQUATIONS
   11 CALL BAND(J) $ AMPO=AMP
      AMP = (-3.*C(1,NM1)-10.*C(2,NM1)+18.*C(3,NM1)-6.*C(4,NM1)+C(5,NM1)
     1 +Q(NM1)*CRO*(-3.*C(1,N)-10.*C(2,N)+18.*C(3,N)-6.*C(4,N)+C(5,N)))/
     112. /H /(CIN(NM1)-CRO)*(4./3.)**.75
C     CHECK CONVERGENCE INNER LOOP
      IF(ABS(AMP-AMPO).LE.1.0E-6) GO TO 12 $ IF(JCOUNT.LE.10) GO TO 99
      MFLAG=1
   12 PRINT 121,ICOUNT,JCOUNT
      IF (MFLAG.EQ.1) PRINT 105
C     COMPUTE LOCAL DENSITY DIFFERENCE AND CONVERSION FACTORS
      DO 13 J=1,NJ $ F(J,1)=0. $ DO 13 K=1,NM1
   13 F(J,1)=F(J,1)+T(K)*C(J,K)/(CIN(NM1)-CRO)
      F(NJ,2)=0. $ DO 14 J=1,NJM1
   14 F(NJ-J,2)=F(NJ-J+1,2)+(F(NJ-J,1)+F(NJ-J+1,1))*H/2.
      F(2,3)=0. $ F(2,4)=0. $ F(1,3)=-(F(2,2)+F(1,2))*H/2.
      F(1,4)=-F(1,3)*H/2. $ DO 16 J=3,NJ
      F(J,3)=F(J-1,3)+(F(J,2)+F(J-1,2))*H/2.
   16 F(J,4)=F(J-1,4) +(F(J,3)+F(J-1,3))*H/2.
      B4=1./ABS(F(2,2)) $ BF=B4**.25 $ BINV=1./BF
      AMP=AMP*BINV $ AK=ABS(F(2,1)) $ AMPRHO=AMP/AK**.25
      FDPRO=BF*F(2,2) $ STRESS=FDPRO*(4./3.)**.25*.8
      STRRHO=STRESS/AK**.75 $ FPIN= F(NJ,3)*BF**2/ABS(AK)**.5
      PRINT 120 ,B4,BF,BINV
      PRINT 119,AMPRHO,STRRHO,FPIN,AK
C     CHECK CONVERGENCE OUTER LOOP
      IF (ABS(AMP-AMPOO).LE.1.0E-6) GO TO 19
      IF (MFLAG.EQ.1) GO TO 19
      IF (ICOUNT.GT.20) GO TO 18  $ DO 17 J=1,NJ
   17 EE(J)=B4*ABS(E(J,4))
      AMPOO=AMP $ AMPO=0. $ JCOUNT=0  $ GO TO 98
   18 PRINT 109 $ NFLAG=1
C     OUTPUT
   19 PRINT  118,ICOUNT
      H=H*BF $ FDPRO=ABS(FDPRO)  $ FPIN =ABS(FPIN) $ STRRHO=ABS(STRRHO)
      PRINT 103 ,H,NJ  $ DO 180 K=1,NM1  $ TT(K)=C(2,K)+CIN(K)
  180 EC(K)= C(2,K)/(CIN(NM1)-CRO)
      PRINT 106, AMPRHO,STRRHO,AK,JCOUNT
      RAMP=AMPRHO/0.67032 $ RSTR=STRRHO/0.93303
      PRINT 108,RAMP,RSTR,FDPRO,FPIN
      PRINT 107, (CIN(I),TT(I),EC(I),I=1,NM1)
      GO TO 97 $ END
      SUBROUTINE BAND(J) $ COMMON A,B,C,D,G,X,Y,N,NJ
      SUBROUTINE MATINV(N,M,DETERM) $ COMMON A,B,C,D
-
OH-     -38920+1712062-1020060-1-10000-0-00000-0
NA+     +38920+1180588-1-29760-2+10000-0      0-0
FERRI-3 -11676+2121321-1074040-1-30000-0-10000-0
K+      +38920+1264925-1000000-0+10000-0000000-0
FERRO-4 -13568+2010001-0010000-1-40000-0+10000-0
+1.00+0.33-0.22+1.07
050000-1050000-1071429-2050000-1071429-2
```

Appendix D: Physical properties used in the numerical solution

1. System $CuSO_4$ - H_2SO_4 - H_2O

1a. Density at 25°C (g/ml)

$$\rho = 0.99994 + 0.13966\, c_{CuSO_4} + 0.059786 c_{H_2SO_4} \qquad (D.1)$$

Standard error: 0.0005

Correlation[35] based on 26 data in the range $0 \leq c_{CuSO_4} \leq 0.10$ M, $0.5 \leq c_{H_2SO_4} \leq 2.5$M

From this $\alpha_{CuSO_4} = 0.13974$ ℓ/mole, $\alpha_{H_2SO_4} = 0.059789$ ℓ/mole.

If HSO_4^- completely dissociated:

Set $\alpha_{SO_4^=}$ equal zero. Then:

$\alpha_{Cu^{++}} = \alpha_{CuSO_4}$; $\alpha_{H^+} = \frac{1}{2}\alpha_{H_2SO_4}$; and

$T_{Cu^{++}} \equiv 1$; $T_{SO_4^=} \equiv 0$; $T_{H^+} = 0.21393$.

If HSO_4^- not dissociated:

Set $\alpha_{HSO_4^-}$ equal zero. Then:

$\alpha_{Cu^{++}} - \alpha_{H^+} = \alpha_{CuSO_4}$; $\alpha_{H^+} = \alpha_{H_2SO_4}$; So:

$T_{Cu^{++}} \equiv 1$; $T_{HSO_4^-} \equiv 0$; $T_{H^+} = 0.29964$

1b. Ionic mobilities at 25°C and at infinite dilution[33,34] (cm^2/Ω eq)

$\lambda_{H^+} = 349.8$, $\lambda_{\frac{1}{2}Cu^{++}} = 53.6$; $\lambda_{\frac{1}{2}SO_4^=} = 80$;

$\lambda_{HSO_4^-} = 50$.

From this follow the R_i values given in Table 4, by way of the relations:

$$\lambda_i = |z_i| u_i F^2 \quad , \text{ and } D_i = RTu_i \quad .$$

1c. Refractive index at 25°C.

$$n_o = 1.33358 + 0.026839\ c_{CuSO_4} + 0.00994 c_{H_2SO_4} \qquad (D.2)$$

Standard error 0.0001

Correlation[35] based on data in the range $0 \leq c_{CuSO_4} \leq 0.1$ M,

$0.5 \leq c_{H_2SO_4} \leq 2.5$ M.

From this, if HSO_4^- completely dissociated:

$$n_D = 1.33358 + 0.026839\ c_{Cu^{++}} + 0.00497\ c_{H^+} \quad ; \qquad (D.3)$$

if HSO_4^- not dissociated:

$$n_D = 1.33358 + 0.036779\ c_{Cu^{++}} + 0.00994\ c_{H^+} \quad . \qquad (D.4)$$

For $CuSO_4$ - H_2O at 25°C:

$$n_D = 1.33360 + 0.036553\ c_{CuSO_4} \quad . \qquad (D.5)$$

2. System $K_3Fe(CN)_6$ - $K_4Fe(CN)_6$ - (KOH/NaOH) - H_2O

2a. Density at 25°C. (g/ml)

$$\rho = 0.99946 + 0.19648\ (c_{K_3Fe(CN)_6} + c_{K_4Fe(CN)_6}) + 0.045266\ c_{KOH} \qquad (D.6)$$

Standard error 0.0011.

Correlation[35] based on 23 data in the range $0.01 \leq c \leq 0.20$ M equimolar ferricyanide and ferrocyanide, $0 \leq c_{KOH} \leq 2$ M by Gordon.[17]

From this $\alpha_{K_3Fe(CN)_6 + K_4Fe(CN)_6} = 0.19659$,

$\alpha_{KOH} = 0.04529$.

An unequal densification for $K_3Fe(CN)_6$ and $K_4Fe(CN)_6$ is assumed, on the basis of a correlation of data measured by Boeffard[37] for non-equimolar ferri/ferrocyanide solutions with NaOH:

$$\rho = 0.996821 + 0.17168\ c_{K_3Fe(CN)_6} + 0.23182\ c_{K_4Fe(CN)_6} + 0.044374\ c_{NaOH}\ (+ \text{quadratic terms}) \qquad (D.7)$$

standard error: 0.0004

Correlation based on 32 data in the range $0.01 < c_{K_3Fe(CN)_6} < 0.2$ M, $0.05 < c_{K_4Fe(CN)_6} < 0.4$ M, $1.0 < c_{NaOH} < 2.0$ M.

From this:

$$\frac{\alpha_{K_3Fe(CN)_6}}{\alpha_{K_4Fe(CN)_6}} = 0.7404$$

Finally therefore, using this ratio:

$$\alpha_{K_3Fe(CN)_6} = 0.16727$$

$$\alpha_{K_4Fe(CN)_6} = 0.22591$$

$$\alpha_{KOH} = 0.04529 \quad .$$

The T_i values in Table 4 follow from this, assuming $\alpha_{K^+} = 0$.

When NaOH is used instead of KOH, or in addition to KOH, there are 5 ionic species in solution. If the α_{K^+} is again set equal to zero, α_{Na^+} and α_{OH^-} follow from the values of α_{NaOH} and α_{KOH}. Density correlations are available only for $K_3Fe(CN)_6$ - $K_4Fe(CN)_6$ - NaOH - H_2O:

$$\rho = 1.000116 + 0.19356\ (c_{K_3Fe(CN)_6} + c_{K_4Fe(CN)_6}) + 0.038535\ c_{NaOH} \qquad (D.8)$$

Standard error = 0.0013

Correlation based on data for equimolar $K_3Fe(CN)_6$ and $K_4Fe(CN)_6$,

range $0.01 < c < 0.2$ M , and

$0 < c_{NaOH} < 2.0$ M , by Gordon.[17]

From this only the coefficient of c_{NaOH} is used to derive α_{NaOH} (with $\rho_o = 0.99946$; see 2a): $\alpha_{NaOH} = 0.03856$.

The densification of the reactants and of KOH in the system $K_3Fe(CN)_6$ - $K_4Fe(CN)_6$ - KOH - NaOH - H_2O is assumed equal to that in the system without NaOH.

The final ionic densifications are:

α	(ℓ/mole)
$Fe(CN)_6^{3-}$	0.16727
$Fe(CN)_6^{4-}$	0.22591
OH^-	0.04529
Na^+	-0.00673
K^+	0

Note: The density of the complete solution, containing 5 ionic species, is considered linear in the concentration of each. No interactions are accounted for. The density of solutions without NaOH or KOH, or both, is found simply by omitting the appropriate terms.

2b. Ionic mobilities at 25°C and at infinite dilution[26] (cm^2/Ω eq):

$\lambda_{\frac{1}{3}Fe(CN)_6^{3-}} = 101$; $\lambda_{\frac{1}{4}Fe(CN)_6^{4-}} = 111$;

$\lambda_{K^+} = 73.5$; $\lambda_{OH^-} = 197.6$; $\lambda_{Na^+} = 50.1$.

The D_i values follow from:

$\lambda_i = |z_i| u_i F^2$

and $D_i = RT\, u_i$.

Appendix E: Migration in stagnant diffusion layers.

1. Irreversible reactions.

The equations to be solved are

$$z_1^2 c_1 \frac{d\phi}{dy} + z_1 \frac{dc_1}{dy} = 0 \quad , \tag{E.1}$$

$$z_2^2 c_2 \frac{d\phi}{dy} + z_2 \frac{dc_2}{dy} = 0 \quad , \tag{E.2}$$

$$z_3^2 c_3 \frac{d\phi}{dy} + z_3 \frac{dc_3}{dy} = - \frac{i}{FD_3} \quad , \tag{E.3}$$

$$z_1 c_1 + z_2 c_2 + z_3 c_3 = 0 \quad , \tag{E.4}$$

where c_1 is the concentration of the supporting ion, c_2 that of the counter ion, c_3 that of the reacting ion, while ϕ is the dimensionless potential $\frac{\phi F}{RT}$. The boundary conditions are:

$$y = 0: \qquad c_3 = c_{30} \tag{E.5}$$

$$y = \delta: \qquad c_1 = c_{1\infty} \; ; \quad c_2 = c_{2\infty} \; ; \quad c_3 = c_{3\infty} \; ; \quad \phi = 0 \tag{E.6}$$

From (1) and (2)

$$c_1 = c_{1\infty} \exp\,(-z_1\phi) \quad , \tag{E.7}$$

$$c_2 = c_{2\infty} \exp\,(-z_2\phi) \quad , \tag{E.8}$$

and by integrating (3) and using (4), (7), (8):

$$- \frac{iy}{FD_3} = z_3 c_{1\infty} \exp\,(-z_1\phi) + z_3 c_{2\infty} \exp\,(-z_2\phi) + z_3 c_3 + K \tag{E.9}$$

The constant K in (9) follows from (6):

$$K = - \frac{i\delta}{FD_3} - (z_3-z_1)c_{1\infty} - (z_3-z_2)\, c_{2\infty} \quad .$$

Therefore:

$$- \frac{i(y-\delta)}{FD_3} = +(z_3-z_1)c_{1\infty}(e^{-z_1\phi} - 1) + (z_3-z_2)c_2\, (e^{-z_2\phi} - 1) \qquad \text{(E.10)}$$

At limiting current $\phi = \phi_o$ at $y = 0$, so ϕ_o can be expressed in terms of

$$\frac{i_{lim}\delta}{FD_3 z_3 c_{2\infty}} = I$$

and $c_{1\infty}/c_{2\infty}$. This is only practical if numerical values for z_1, z_2, z_3 are substituted as in the following cases. The potential ϕ_o can then be substituted in (9), with $c_3 = 0$ at $y = 0$, to obtain I in terms of $c_{1\infty}/c_{2\infty}$.

Case 1A. $z_1 = 1$, $z_2 = -1$, $z_3 = 1$ (e.g., K^+, Cl^-, H^+)

Denote $c_{1\infty}/c_{2\infty}$ by r.

From (10): $I = 2(e^{\phi_o} - 1)$

From (9): $(I + 2)^2 = 4r \rightarrow -I = 2(1 - \sqrt{r})$

Therefore $i_{lim} = - \frac{2FD_3 c_{3\infty}}{\delta} \left(\frac{1}{1 + \sqrt{r}} \right)$.

From this: $\frac{i_{lim,r=0}}{i_{lim,r=1}} = 2$

As $\varepsilon = 1 - r \to 0$:

$$i_{lim} = i_{lim',r=1} \left(1 + \frac{\varepsilon}{4} + O(\varepsilon^2)\right) \quad ;$$

$$\phi_o = \ln\left(1 - \frac{\varepsilon}{2}\right) = -\frac{\varepsilon}{2} + O(\varepsilon^2) \quad ;$$

$$(c_{1o} - c_{1\infty})/c_{3\infty} = \frac{1}{2} - \frac{1}{2}\varepsilon + O(\varepsilon^2) \quad .$$

Case 1B. $z_1 = 1$, $z_2 = -2$ $z_3 = 2$ (e.g., H^+, $SO_4^=$, Cu^{++} , i.e., H_2SO_4 completely dissociated)

Denote $c_{1\infty}/2c_{2\infty}$ by r .

From (10): $I = r(e^{-\phi_o} - 1) + 2(e^{2\phi_o} - 1)$

From (9): $I = r(2e^{-\phi_o} - 1) + e^{2\phi_o} - 2$

Therefore $e^{-\phi_o} = (I + 2 + r)/3r \to$

$$(I + 2 + r)^3 = 27\, r^2 \to$$

$$I = -2 - r + 3r^{2/3} \to$$

$$i_{lim} = \frac{-2FD_3c_{3\infty}}{\delta}\left(\frac{2 + r - 3r^{2/3}}{1-r}\right) =$$

$$\frac{-2FD_3c_{3\infty}}{\delta}\left(\frac{2 + 2x - x^2}{1 + x + x^2}\right)$$

where $x = r^{1/3}$

From this $\dfrac{i_{lim,\, r=0}}{i_{lim,\, r=0}} = 2$

As $\sigma \equiv 1 - x \to 0$:

$$i_{lim} = i_{lim,r=1} \quad \left(1 + \sigma - \frac{\sigma^2}{3} + O(\sigma^3)\right)$$

$$\phi_o = \frac{1}{3}\ln(1 - \varepsilon) = -\frac{\varepsilon}{3} + O(\varepsilon^2)$$

$$(c_{1o} - c_{1\infty})/2c_{3\infty} = \frac{1}{3} - \frac{1}{3}\varepsilon + O(\varepsilon^2)$$

Case 1C. $z_1 = 1$, $z_2 = -1$, $z_3 = 2$ (e.g., H^+, HSO_4^-, Cu^{++}, i.e., H_2SO_4 undissociated)

Denote $(c_{1\infty} + c_{3\infty})/(c_{1\infty} + 2c_{3\infty}) = H_2SO_{4\infty}/(H_2SO_{4\infty} + CuSO_{4\infty})$ by r, so $c_{1\infty}/c_{2\infty} = 2r - 1$

From (10): $2I = (2r - 1)(e^{-\phi_o} - 1) + 3(e^{\phi_o} - 1)$

From (9): $2I = (2r - 1)(2e^{-\phi_o} - 1) + 2e^{\phi_o} - 3$

Therefore $e^{\phi_o} = \frac{I + 1 + r}{2} \rightarrow$

$$I^2 + 2I(r + 1) + r^2 - 6r + 5 = 0 \rightarrow$$

$$I = -(r + 1) + 2\sqrt{2r - 1} \rightarrow$$

$$i_{lim} = -\frac{2FD_3c_{3\infty}}{\delta} = \frac{1 + r}{1 - r} - \frac{2\sqrt{2r - 1}}{1 - r}$$

From this:

$$\frac{i_{lim,r=0.5}}{i_{lim,r=1}} = 3$$

As $\tau \equiv 1 - r^{1/2} \rightarrow 0$:

$$i_{lim} = i_{lim,r=1}\{1 + 4\tau + O(\tau^2)\}$$

$$\phi_o = \ln\sqrt{1 - 2\varepsilon} = -\varepsilon + O(\varepsilon^2)$$

$$(c_{1o} - c_{1\infty} + c_{3o} + c_{3\infty})/(c_{3o} - c_{3\infty}) = -\varepsilon + O(\varepsilon^2)$$

2. Reversible reaction: ternary redox system.

The equations to be solved are in this case

$$z_1c_1\frac{d\phi}{dy} + \frac{dc_1}{dy} = \frac{i}{nFD_1} \qquad (n=z_3-z_1)^* \qquad (E.11)$$

*Since $\frac{i}{nF} = \frac{N_3}{s_3} = \frac{N_1}{s_1}$ (assumed $s_3 = +1$, $s_1 = -1$) and also $i = z_1FN_1 + z_3FN_3$.

$$z_2 c_2 \frac{d\phi}{dy} + \frac{dc_2}{dy} = 0 \tag{E.12}$$

$$z_3 c_3 \frac{d\phi}{dy} + \frac{dc_3}{dy} = \frac{-i}{nFD_3} \tag{E.13}$$

$$z_1 c_1 + z_2 c_2 + z_3 c_3 = 0 \tag{E.14}$$

Summing, we have:

$$\frac{d}{dy}(c_1+c_2+c_3) = \frac{i}{nF}\left(\frac{1}{D_1} - \frac{1}{D_3}\right) \tag{E.15}$$

with the boundary conditions (5) and (6), we can write:

$$c_1 + c_2 + c_3 - c_{1o} - c_{2o} - c_{3o} = \frac{iy}{nF}\left(\frac{1}{D_1} - \frac{1}{D_3}\right) \quad , \tag{E.16}$$

or

$$(c_1 - c_{1o})\left(1 - \frac{z_1}{z_2}\right) + (c_3 - c_{3o})\left(1 - \frac{z_3}{z_2}\right) = \frac{iy}{nF}\left(\frac{1}{D_1} - \frac{1}{D_3}\right) \tag{E.17}$$

At the limiting current:

$$(c_{1\infty} - c_{1o})\left(1 - \frac{z_1}{z_2}\right) + c_{3\infty}\left(1 - \frac{z_3}{z_2}\right) = \frac{i\delta}{nF}\left(\frac{1}{D_1} - \frac{1}{D_3}\right) \tag{E.18}$$

Since

$$c_{3\infty} = \frac{-i\delta}{nFD_3}$$

corresponds to a diffusion current, we have

$$\left(\frac{c_{1\infty} - c_{1o}}{c_{3\infty}}\right)\left(1 - \frac{z_1}{z_2}\right) + \left(1 - \frac{z_3}{z_2}\right) = -\frac{i_L}{i_D}\left(\frac{D_3}{D_1} - 1\right) \tag{E.19}$$

Therefore i_L/i_D and $(c_{1o} - c_{1\infty})/c_{3\infty}$ cannot be determined separately.

If $D_3 = D_1$,

$$\frac{c_{1o} - c_{1\infty}}{c_{3\infty}} = \frac{z_2 - z_3}{z_2 - z_1} \quad , \tag{E.20}$$

independent of r.

If $r \to 1$, $i_L/i_D \to 1$ and

$$\frac{c_{1\infty} - c_{1o}}{c_3} = \frac{\frac{D_3}{D_1} - \frac{z_3}{z_2}}{1 - \frac{z_1}{z_2}} \tag{E.21}$$

In the case of ferricyanide/ferrocyanide:

A. Equal D's.

Cathodic reaction ($z_1 = -4$, $z_2 = +1$, $z_3 = -3$)

$$\frac{c_{1o} - c_{1\infty}}{c_{3\infty}} = 0.80$$

Anodic reaction ($z_1 = -3$, $z_2 = +1$, $z_3 = -4$)

$$\frac{c_{1o} - c_{1\infty}}{c_{3\infty}} = 1.25$$

B. $D_{\text{ferricyanide}}/D_{\text{ferrocyanide}} = 1.2132$, $r \to 1$

Cathodic reaction

$$\frac{c_{1o} - c_{1\infty}}{c_{3\infty}} = 0.8426$$

Anodic reaction

$$\frac{c_{1o} - c_{1\infty}}{c_{3\infty}} = 1.2067 \quad .$$

To solve for i_L/i_D in the case of equal D we start from:

$$c_1 + c_2 + c_3 = \text{constant} = K \quad ; \tag{E.22}$$

$$z_1c_1 + z_2c_2 + z_3c_3 = 0 \quad ; \tag{E.23}$$

$$c_2 = c_{2\infty}e^{-z_2\phi} \quad ; \tag{E.24}$$

$$(z_1^2c_1 + z_2^2c_2 + z_3^2c_3)\frac{d\phi}{dy} = \frac{i}{nF}\,\frac{z_1 - z_3}{D_1} = -\frac{i}{nF} \quad . \tag{E.25}$$

From (E.22) by elimination of c_2 with (E.23):

$$c_3 = -\frac{z_1K}{z_3 - z_1} + \frac{z_1 - z_2}{z_3 - z_1}\,c_2 \quad ; \tag{E.26}$$

$$c_1 = \frac{z_3K}{z_3 - z_1} + \frac{z_2 - z_3}{z_3 - z_1}\,c_2 \quad . \tag{E.27}$$

Then with (E.25):

$$[(z_2^2 - z_2(z_1 + z_3) + z_1z_3)c_2 - z_1z_3K]\frac{d\phi}{dy} = -\frac{i}{FD_1} \quad , \tag{E.28}$$

or:

$$[(z_2 - z_1)(z_2 - z_3)c_{2\infty}e^{-z_2\phi} - z_1z_3K]\frac{d\phi}{dy} = -\frac{i}{FD_1} \quad . \tag{E.29}$$

By integration:

$$\frac{(z_2 - z_1)(z_2 - z_3)c_{2\infty}(e^{-z_2\phi} - 1)}{-z_2} - \phi z_1z_3K = -\frac{i}{FD_1}(y - \delta) \quad , \tag{E.30}$$

and at y = 0:

$$\frac{(z_2 - z_1)(z_2 - z_3)(c_{2o} - c_{2\infty})}{-z_2} - \phi_o z_1 z_3 K = \frac{i\delta}{FD_1} \quad . \tag{E.31}$$

Also, from (E.23):

$$\frac{c_{3\infty}}{c_{2\infty}} \left(\frac{z_3 - z_1}{z_2 - z_1}\right) + 1 = e^{-z_2\phi_o} \quad , \tag{E.32}$$

so that $-z_2\phi_o = \ln\left(\frac{z_1 K}{(z_1 - z_2)c_2}\right)$. (E.33)

Consequently (E.31) gives:

$$\frac{i\delta}{nFD_1 C_{3\infty}} = -\frac{z_2 - z_3}{z_2} + \frac{z_1 z_3 K}{z_2(z_3 - z_1)c_{3\infty}} \ln\left(\frac{z_1 K}{(z_1 - z_2)c_{2\infty}}\right) \quad , \tag{E.34}$$

or:

$$\frac{i_L}{i_D} = \frac{z_2 - z_3}{z_2} - \frac{z_1 z_3 K}{z_2(z_3 - z_1)c_{3\infty}} \ln\left(\frac{z_1 K}{(z_1 - z_2)c_{2\infty}}\right) \tag{E.35}$$

In the limit $c_{1\infty} >> c_{3\infty}$ this yields $i_L/i_D = 1$.

If $c_{1\infty} = 0$,

$$\frac{i_L}{i_D} = \frac{z_2 - z_3}{z_2} + \frac{z_1 z_3}{z_2^2}\left(\frac{z_3 - z_2}{z_3 - z_1}\right) \ln\left(\frac{z_1}{z_3}\left(\frac{z_3 - z_2}{z_1 - z_2}\right)\right) \tag{E.36}$$

In the case of ferricyanide/ferrocyanide:

Cathodic reaction ($z_1 = -4$, $z_2 = 1$, $z_3 = -3$) :

$$\frac{i_L}{i_D} = 4 - 48 \ln\frac{16}{15} = 0.902151 \ ;$$

Anodic reaction ($z_1 = -3$, $z_2 = 1$, $z_3 = -4$):

$$\frac{i_L}{i_D} = 5 - 60 \ln \frac{16}{15} = 1.127689 \quad .$$

Appendix F: Electrolyte composition according to the method of Wilke, Eisenberg, and Tobias.[24]

1. $CuSO_4 + H_2SO_4$ (completely dissociated) $+ H_2O$

$$N_{Cu^{++}} = \frac{i(1 - t_{Cu^{++}})}{2F} = k_{Cu^{++}}(c_{Cu^{++},\infty} - c_{Cu^{++},0}) \quad ; \tag{F.1}$$

$$N_{H^+} = \frac{it_{H^+}}{F} = k_{H^+}(c_{H^+,0} - c_{H^+,\infty}) \quad , \tag{F.2}$$

At limiting current:

$$\frac{c_{H^+,0} - c_{H^+,\infty}}{2c_{Cu^{++},\infty}} = \frac{t_{H^+}}{1 - t_{Cu^{++}}}\left(\frac{D_{CuSO_4}}{D_{H_2SO_4}}\right)^{3/4} \quad . \tag{F.3}$$

Define: $D_i/D_{Cu^{++}} = u_i/u_{Cu^{++}} = R_i$,

$$\frac{c_{H^+}}{2c_{SO_4^=}} = r \quad .$$

With the help of (2.10), (2.20):

$$\frac{c_{H^+,o} - c_{H^+,\infty}}{2c_{Cu^{++},\infty}} = \left(\frac{R_{H^+}r}{2R_{SO_4^=} + R_{H^+}r}\right)\left[\frac{2}{3}\left(\frac{R_{H^+} + 2R_{SO_4^=}}{(1 + R_{SO_4^=})R_{H^+}}\right)\right]^{3/4} \quad . \tag{F.4}$$

2. $K_3Fe(CN)_6 + K_4Fe(CN)_6 + H_2O$.

a. cathodic reaction!

$$N_{ferri} = \frac{i(1 - t_{ferri})}{F} = k_{ferri}(c_{ferri,\infty} - c_{ferri,0}) \quad ; \tag{F.5}$$

$$N_{ferro} = -\frac{i(1 - t_{ferro})}{F} = k_{ferro}\,(c_{ferro,0} - c_{ferro,\infty}) \quad ; \qquad (F.6)$$

$$\frac{\Delta c_{ferro}}{\Delta c_{ferri}} = \frac{1 - t_{ferro}}{1 - t_{ferri}} \left[\frac{D_{K_3Fe(CN)_6}}{D_{K_4Fe(CN)_6}}\right]^{3/4} \quad . \qquad (F.7)$$

Define: $D_i/D_{ferri} = u_i/u_{ferri} = R_i$;

$$\frac{c_{ferro}}{c_{ferro} + c_{ferri}} = r \quad .$$

Then:

$$\frac{\Delta c_{ferro}}{\Delta c_{ferri}} = \left[\frac{R_{K^+}(3 + r) + 9(1 - r)}{R_{K^+}(3 + r) + 16rR_{ferro}}\right]\left[\frac{4}{5}\left\{\frac{4 + \frac{R_{K^+}}{R_{ferro}}}{3 + R_{K^+}}\right\}\right]^{3/4} \qquad (F.8)$$

b. anodic reaction

Define: $D_i/D_{ferro} = u_i/u_{ferro} = R_i$;

$$\frac{c_{ferri}}{c_{ferri} + c_{ferro}} = r \quad .$$

Finally:

$$\frac{\Delta c_{ferri}}{\Delta c_{ferro}} = \left[\frac{R_{K^+}(4 - r) + 16(1 - r)}{R_{K^+}(4 - r) + 9rR_{ferri}}\right]\left[\frac{5}{4}\left\{\frac{3 + \frac{R_{K^+}}{R_{ferri}}}{4 + R_{K^+}}\right\}\right]^{3/4} \quad . \qquad (F.9)$$

3. $K_3Fe(CN)_6 + K_4Fe(CN)_6 + KOH + H_2O$

a. cathodic reaction

$$\frac{it}{F}_{OH^-} = k_{KOH}(c_{KOH,\infty} - c_{KOH,0}) \quad ; \qquad (F.10)$$

$$\frac{i(i-t_{ferri})}{F} = k_{ferri}(c_{ferri,\infty} - c_{ferri,0}) \; ; \tag{F.11}$$

$$\frac{c_{KOH,\infty} - c_{KOH,0}}{c_{ferri,\infty} - c_{ferri,0}} = \frac{t_{OH^-}}{1 - t_{ferri}} \frac{k_{ferri}}{k_{KOH}} = \tag{F.12}$$

$$\left(\frac{t_{OH^-}}{1 - t_{ferri}}\right)\left(\frac{D_{K_3Fe(CN)_6}}{D_{KOH}}\right)^{3/4} \tag{F.13}$$

Equimolar ferricyanide/ferrocyanide:

Define $r_{OH} = c_{OH^-}/c_{K^+}$; $D_i/D_{ferri} = u_i/u_{ferri} = R_i$.

Finally:

$$\frac{\Delta c_{KOH}}{\Delta c_{ferri}} = \frac{R_{OH}\left(\frac{D_{K_3Fe(CN)_6}}{D_{KOH}}\right)^{3/4}}{R_K + R_{OH} + \frac{1 - r_{OH}}{r_{OH}}\left(R_K + \frac{16}{7} R_{ferro}\right)} \; . \tag{F.14}$$

b. anodic reaction.

Define $r_{OH} = c_{OH^-}/c_{K^+}$; $D_i/D_{ferri} = u_i/u_{ferri} = R_i$.

Finally:

$$\frac{\Delta c_{KOH}}{\Delta c_{ferro}} = \frac{R_{OH}\left(\frac{D_{K_4Fe(CN)_6}}{D_{KOH}}\right)^{3/4}}{R_K + R_{OH} + \frac{1 - r_{OH}}{r_{OH}}\left(\frac{9}{7} + R_k\right)} \tag{F.15}$$

The numerical values used for R_i are those given in Appendix D.

Appendix G. Notation used in various references on free convection.

The similarity transformations used by most authors differ from (3.17), (4.10) and (4.11) by a constant. Table G1 lists some variants of both the classical and the stretched variables, as well as the resultant forms of the equation of motion and the convective diffusion equation. Table G2 gives the relation between the invariant coefficients C_1(3.14), B_1(3.15), C(3.24), B(3.25) and the dimensionless variables defined by various authors.

Table G1. Notations for similarity variables used by various authors.

Reference	Classical variables	Stretched variables
1. This work	$\zeta = \frac{y}{G}(\frac{3}{4x})^{1/4}$; $f = \frac{\psi G}{\nu}(\frac{3}{4x})^{3/4}$;$\theta$	$\eta = \zeta\sigma^{1/4}$; $\bar{f} = f\sigma^{3/4}$;$\bar{\theta}$
2. Roy[7]	$\eta = \frac{y}{G(4x)^{1/4}}$; $f_o = \frac{\psi G}{\nu(4x)^{3/4}}$;$\phi$	$\zeta_1 = \eta(3\sigma)^{1/4}$; $F_o = f_o(3\sigma)^{3/4}$;Φ_o
3. Le Fevre[4]	$\eta = \frac{y}{G(4x)^{1/4}}$; $f = \frac{\psi G}{\nu(4x)^{3/4}}$;$g$	$\zeta = \eta(3\sigma)^{1/4}$; $\phi = f(3\sigma)^{3/4}$;θ
4. Kuiken[6]	$\mu = \frac{y}{G(4x)^{1/4}}$; $g = \frac{\psi G}{\nu(4x)^{3/4}}$;$h$	$\eta = \mu\sigma^{1/4}$; $f = g\sigma^{3/4}$;θ
5. Ostrach[1]	$\eta = \frac{y}{G(4x)^{1/4}}$; $F = \frac{\psi G}{\nu(4x)^{3/4}}$;$H$	
6. Schlichting[2]	$\eta = \frac{y}{G(4x)^{1/4}}$; $\zeta = \frac{\psi G}{\nu(4x)^{3/4}}$;$\theta$	
7. Morgan & Warner[5]	$\zeta = \frac{y}{Gx^{1/4}}$; $f = \frac{\psi G}{4\nu x^{3/4}}$;$h$	$\eta = \zeta\sigma^{1/4}$; $F = f\sigma^{3/4}$;H

Note: 1. $G = \left[\frac{\nu^2\rho_o}{g\Delta\rho}\right]^{1/4} = \left(\frac{\nu^2}{g\alpha\Delta c}\right)^{1/4}$ or $\left(\frac{\nu^2}{g\beta\Delta T}\right)^{1/4}$,

and $\sigma = \frac{\nu}{D}$ or $\frac{\nu}{a} = \left(\frac{\mu c_p}{k}\right)$

2. In the present work the equation of motion is:

$$f''' + ff'' - \frac{2}{3}(f')^2 + \theta = 0 \quad ,$$

and the equation of convective diffusion:

$$\sigma f\theta' + \theta'' = 0$$

The classical transformation in all other references leads to:

$$f''' + 3ff'' - 2(f')^2 + \theta = 0;$$

$$3\sigma f\theta' + \theta'' = 0 \quad .$$

The stretched variables of the present work, and of Roy,[7] and Le Fevre,[4] lead to:

$$\bar{f}''' + \bar{\theta} = 0 \quad ;$$

$$\bar{f}\,\bar{\theta}' + \bar{\theta}'' = 0 \quad .$$

In Kuiken's,[6] and Morgan and Warner's[5] work the equation of convective diffusion is:

$$3\sigma \bar{f}\,\bar{\theta}' + \bar{\theta}'' = 0 \quad .$$

Table G2. Conversion factors for dimensionless quantities used by various authors.

Reference	Classical variables	Stretched variables
1. This work		$C = (\frac{4}{3})^{3/4}\bar{\theta}'(0)$; $B = \frac{4}{5}(\frac{4}{3})^{1/4}\bar{f}''(0)$
2. Roy[7]		$C = (\frac{4}{3})^{3/4}\Phi'(0)$; $B = \frac{4}{5}(\frac{4}{3})1/4_{F''_o}(0)$
3. Le Fevre[4]		$C = (\frac{4}{3})^{3/4}\theta'(0)$; $B = \frac{4}{5}(\frac{4}{3})^{1/4}\phi''(0)$
4. Kuiken[6]		$C = \frac{4^{3/4}}{3}\theta'(0)$; $B = \frac{4^{5/4}}{5}f''(0)$
5. Morgan & Warner[5]		$C = \frac{4}{3}H'(0)$; $B = \frac{16}{5}F''(0)$
6. Ostrach[1]	$C_1 = \frac{4^{3/4}}{3}H'(0)$; $B_1 = \frac{4^{5/4}}{5}F''(0)$	
7. Schlichting[2]	$C_1 = \frac{4^{3/4}}{3}\theta'(0)$; $B_1 = \frac{4^{5/4}}{5}\zeta''(0)$	

NOMENCLATURE

a	thermal diffusivity [cm^2/sec]
a_i	activity of species i
A_1	proportionality factor streamfunction (10.5)
A_2	proportionality factor distance variable (10.5)
b	constant in streamfunction expression (7.8)
B	constant in $_o/ Lg\ (c_o - c\ ) = B(GrSc)^{-1/4}$ (3.25)
B_1	constant in $_o/ Lg\ (c_o - c\ ) = B_1 Gr^{-1/4}$ (3.15)
c	concentration [$mole/cm^3$]
C	constant in $Nu = C(GrSc)^{1/4}$ (3.24)
C_1	constant in $Nu = C_1 Gr^{1/4}$ (3.14)
C_2	constant in $Nu = C_2(GrSc^2)^{1/4}$ (3.20)
C^*	constant C corresponding to diffusive mass transfer only (7.16)
D	diffusivity [cm^2/sec]
E	parameter in similarity variables (3.7)[$cm^{3/4}$]
f	dimensionless streamfunction (3.7), (4.11)
f_1	adjustable streamfunction (10.5)
F	Faraday's constant [96,494 coul/equiv]
g	auxiliary function in numerical computation (Appendix B,C)
g	acceleration of gravity [cm/sec^2]
h	auxiliary function in numerical computation (Appendix B)
H	mesh width in numerical computation
i	current density [a/cm^2]
I_r	true ionic strength [mole/l]
k	mass transfer coefficient [cm/sec]

K	thermodynamic dissociation constant
K'	stoichiometric dissociation constant
L	length electrode [cm]
M	chemical species in charge-transfer reaction (2.1)
n	number of electrons transferred (2.1)
N	flux [mole/cm^{2}sec]
p	pressure [dn/cm^2]
Q_i	ratio $z_i u_i F/D_R$
r	dilution ratio $c_{H_2SO_4}/(c_{H_2SO_4} + c_{CuSO_4})$
r_a	dilution ratio $c_{\text{ferricyanide}}/(c_{\text{ferricyanide}} + c_{\text{ferrocyanide}})$
r_c	dilution ratio $c_{\text{ferrocyanide}}/(c_{\text{ferricyanide}} + c_{\text{ferrocyanide}})$
R_i	ratio D_i/D_R
R	gas constant [erg/mole - °C]
s_i	number of ions or molecules of species i participating in charge-transfer reaction (2.1)
t	time [sec]
t_i	transference number of ionic species i
T	absolute temperature [°K]
T_i	ratio α_i/α_R
u	velocity in x direction [cm/sec]
u_i	mobility of ionic species i [cm^2-mole/joule-sec]
v	velocity in y direction [cm/sec]
x	distance parallel to electrode [cm]
y	distance perpendicular to electrode [cm]
z_i	valence of ionic species i

α_i	densification coefficient of species i [1/mole]
$\Gamma(\frac{4}{3})$	gamma function of 4/3 (=0.8934)
δ	diffusion layer thickness [cm]
δ_c	diffusion layer thickness [cm]
δ_i	diffusion layer thickness of species i [cm]
δ_v	velocity boundary layer thickness [cm]
ε	angle of inclination with respect to vertical
ζ	dimensionless distance (3.7)
η	dimensionless distance (3.28), (4.10)
ξ	adjustable dimensionless distance (10.5)
θ	dimensionless concentration (3.7)
μ	dynamic viscostiy [g/cm-sec]
ν	kinematic viscosity [cm^2/sec]
ν_i	stoichiometric dissociation number of species i in binary compound
ρ	density [g/cm^3]
τ	shear stress [dn/cm^2]
ϕ	dimensionless potential (4.12)
Φ	potential [volt]
ψ	streamfunction [cm^2/sec]

Dimensionless numbers

Gr	Grashof number for uniform concentration $= \left(\frac{g\Delta\rho L^3}{\rho\nu^2}\right)$
Gr^*	Grashof number for uniform flux $= \left(\frac{g\alpha N L^4}{\nu D^2}\right)$
Nu	Nusselt number for mass transfer $= (\frac{kL}{D}) = \frac{S_R i_{avg} L}{nFD_R(c_{R\infty}-c_{RO})}$
Pr	Prandtl number $(\frac{\nu}{a})$
Sc	Schmidt number $(\frac{\nu}{D})$

Subscripts

o	at the electrode
∞	in the bulk; far from the electrode
i	pertaining to species i
s	pertaining to a binary salt
R	pertaining to reacting species
+	pertaining to positive ion of binary salt
-	pertaining to negative ion of binary salt
loc	local value
avg	averaged value
$\Delta\rho$	value based on actual $\Delta\rho$

Superscripts

'	derivative
-	inner variable
~	outer variable

Prescript

Δ	difference between value in bulk and at electrode

References

1. Simon Ostrach. "An Analysis of Laminar Free-Convection Flow and Heat Transfer about a Flat Plate parallel to the Direction of the Generating Body Force." Report 1111. Thirty-Ninth Annual Report of the National Advisory Committee for Aeronautics, 1953, Including Technical Reports Nos. 1111 to 1157. Washington: United States Government Printing Office, 1955.

2. Hermann Schlichting. Boundary-Layer Theory, 6th edition, pp. 300-305. New York: McGraw-Hill Book Company, 1968.

3. E. M. Sparrow and J. L. Gregg. Details of exact low Prandtl number boundary layer solutions for forced and for free convection. NASA Memo 2-27-59E (1959). (Via reference 2.)

4. E. J. Le Fevre. "Laminar Free Convection from a Vertical Plane Surface." Actes, IX Congrès International de Mécanique Appliquée, 4, 168-174 (Brussels, 1957).

5. George W. Morgan and W. H. Warner. "On Heat Transfer in Laminar Boundary Layers at High Prandtl Number." Journal of the Aeronautical Sciences, 23, 937-948 (1956).

6. H. K. Kuiken. "An Asymptotic Solution for Large Prandtl Number Free Convection." Journal of Engineering Mathematics, 2, 355-371 (1968).

7. Sreedhan Roy. "A Note on Natural Convection at High Prandtl Numbers." International Journal of Heat and Mass Transfer, 12, 239-241 (1969).

8. Andreas Acrivos. "A Theoretical Analysis of Laminar Natural Convection Heat Transfer to Non-Newtonian Fluids." A.I.Ch.E. Journal, 6, 584-590 (1960).

9. H. K. Kuiken. Perturbation Techniques in Free Convection. Dissertation, Delft, 1967.

10. John Newman. "Transport Processes in Electrolytic Solutions." Advances in Electrochemistry and Electrochemical Engineering, 5, 87-135 (1967).

11. Arnold Eucken. "Über den stationären Zustand zwischen polarisierten Wasserstoffelektroden." Zeitschrift für physikalische Chemie, 59, 72-117 (1907).

12. D. Ilkovič. "Polarographic Studies with the Dropping Mercury Kathode. - Part XLIV. - The Dependence of Limiting Currents on the Diffusion Constant, on the Rate of Dropping and on the Size of Drops." Collection of Czechoslovak Chemical Communications, 6, 498-513 (1934).

13. John Newman. "Effect of Ionic Migration on Limiting Currents." Industrial and Engineering Chemistry Fundamentals, 5, 525-529 (1966).

14. Shinzo Okada, Shiro Yoshizawa, Fumio Hine, and Kameo Asada. "Effect of Migration on Polarographic Limiting Current." Journal of the Electrochemical Society of Japan (Overseas Edition), 27, E51-E52 (1959).

15. John Newman. "The Effect of Migration in Laminar Diffusion Layers." International Journal of Heat and Mass Transfer, 10, 983-997 (1967).

16. John Newman and Limin Hsueh. "Currents Limited by Gas Solubilities." Industrial and Engineering Chemistry Fundamentals, to be published. (UCRL-19098. October, 1969.)

17. Stanley L. Gordon, John S. Newman, and Charles W. Tobias. "The Role of Ionic Migration in Electrolytic Mass Transport; Diffusivities of $[Fe(CN)_6]^{3-}$ and $[Fe(CN)_6]^{4-}$ in KOH and NaOH Solutions." Berichte der Bunsengesellschaft für physikalische Chemie, 70, 414-420 (1966).

18. V. V. Malev and Ya. V. Durdin. "The Dependence of the Limiting Current on a Rotating Disc Electrode on the Concentration of a Foreign Electrolyte." Elektrokhimya, 2, 1354-1358 (1966). (Soviet Electrochemistry, 2, 1240-1243 (1966).)

19. V. V. Malev and R. V. Balukov. "Effect of Mobility of Nondischarging Particles on Limiting Currents during Anion Reduction." Elektrokhimiya, 4, 348-353 (1968). (Soviet Electrochemistry, 4, 312-316 (1968).)

20. V. V. Malev. "The Construction of an Approximate Solution for the Ternary-Electrolyte Problem." Elektrokhimiya, 4, 1094-1096 (1968). (Soviet Electrochemistry, 4, 986-988 (1968).)

21. Limin Hsueh and John Newman. "The Role of Bisulfate Ions in Ionic Migration Effects." UCRL-19102, July, 1970.

22. N. Ibl. "The Use of Dimensionless Groups in Electrochemistry." Electrochimica Acta, 1, 117-129 (1959).

23. John Newman. "Engineering Design of Electrochemical Systems." Industrial and Engineering Chemistry, 60, no. 4, 12-27 (1968).

24. C. R. Wilke, M. Eisenberg, and C. W. Tobias. "Correlation of Limiting Currents under Free Convection Conditions." Journal of the Electrochemical Society, 100, 513-523 (1953).

25. Carl Wagner. "The Role of Natural Convection in Electrolytic Processes." Transactions of the Electrochemical Society, 95, 161-173 (1949).

26. N. Ibl and U. Braun. "Evaluation of the Concentration Changes near the Electrodes in Electrolysis with Natural Convection." Chimia, 21, 395-404 (1967).

27. Kameo Asada, Fumio Hine, Shiro Yoshizawa, and Shinzo Okada. "Mass Transfer and Current Distribution under Free Convection Conditions." Journal of the Electrochemical Society, 107, 242-246 (1960).

28. E. Ravoo. "Density Differences and Concentration Gradients in Electrochemical Systems with Free Convection." Extended Abstracts, pp. 54-58. 20th meeting, Comité International de Thermodynamique et de Cinétique Electrochimique, Strasbourg, France, September, 1969.

29. A. Brenner. "A Method for Studying Cathode Films by Freezing." Proc. Amer. Electroplaters' Soc., pp. 95-98 (1940).

30. N. Ibl and R. H. Müller. "Studies of Natural Convection at Vertical Electrodes." Journal of the Electrochemical Society, 105, 346-353 (1958).

31. G. Schütz. "Natural Convection Mass-transfer Measurements on Spheres and Horizontal Cylinders by an Electrochemical Method. "International Journal of Heat and Mass Transfer, 6, 873-879 (1963).

32. John Newman. "Numerical Solution of Coupled, Ordinary Differential Equations." Industrial and Engineering Chemistry Fundamentals, 7, 514-517 (1968).

33. B. E. Conway. Electrochemical Data. Amsterdam: Elsevier Publishing Company, 1952.

34. Benton Brooks Owen and Robert W. Gurry. "The Electrolytic Conductivity of Zinc Sulfate and Copper Sulfate in Water at 25°." Journal of the American Chemical Society, 60, 3074-3078 (1938).

35. Jan Robert Selman a.o., "Transport Properties of Supported Electrolytic Solutions," UCRL forthcoming.

36. Limin Hsueh. Diffusion and Migration in Electrochemical Systems. Dissertation, University of California, Berkeley, December, 1968. (UCRL-18597)

37. Alain Jean-Louis Pierre Marie Boeffard. Ionic Mass Transport by Free Convection in a Redox System. M.S. thesis, University of California, Berkeley, January, 1966. (UCRL-16624)

38. M. G. Fouad and N. Ibl. "Natural Convection Mass Transfer at Vertical Electrodes under Turbulent Flow Conditions." Electrochimica Acta, 3, 233-243 (1960).

39. L. D. Landau and E. M. Lifschitz. Fluid Mechanics, Ch. IV, Boundary Layers. London: Pergamon Press, 1959.

40. Reference 2, pp. 438-446.

41. R. Cheesewright. "Turbulent Natural Convection From a Vertical Plane Surface." Journal of Heat Transfer, 90, 1-8 (1968).

42. Albin A. Szewczyk. "Stability and Transition of the Free-convection Layer along a Vertical Flat Plate." International Journal of Heat and Mass Transfer, 5, 903-914 (1962).

43. Carl Wagner. "The Dissolution Rate of Sodium Chloride with Diffusion and Natural Convection as Rate-determining Factors." Journal of Physical and Colloid Chemistry, 53, 1030-1033 (1949).

44. M. G. Fouad and T. Gouda. "Natural Convection Mass Transfer at Vertical Electrodes." Electrochimica Acta, 9, 1071-1076 (1964).

45. Y. S. Touloukian, G. A. Hawkins, and M. Jakob. "Heat Transfer by Free Convection from Heated Vertical Surfaces to Liquids." Transactions of the American Society of Mechanical Engineers, 70, 13-18 (1948).

46. C. R. Wilke, C. W. Tobias, and Morris Eisenberg. "Free Convection Mass Transfer at Vertical Plates." Chemical Engineering Progress, 49, 663-674 (1953).

47. B. Gebhart. "Natural Convection Flow, Instability, and Transition." Journal of Heat Transfer, 91, 1-17 (1969).

48. E. M. Sparrow and J. L. Gregg, "Laminar Free Convection from a Vertical Plate with Uniform Surface Heat Flux," Transactions of the American Society of Mechanical Engineers", 78, 435-440 (1956).

49. Carl Wagner, "Current Distribution in Galvanic Cells Involving Natural Convection," Journal of the Electrochemical Society 104, 129-131 and 753 (1957).

50. E. J. Fenech, C. W. Tobias, "Mass Transfer by Free Convection at Horizontal Electrodes," Electrochimica Acta 2, 311-325 (1960).

51. N. Ibl, "Studies of Mass Transfer During Electrolysis with Natural Convection," Proceedings, pp. 174-189, 8th Reunion, Comité International de Thermodynamique et de Cinétique Electrochimique, Madrid, Spain, September 1956.

52. E. Ravoo and B. Roffel, "Free Convection Mass Transfer during Electrode Reactions in a Centrifugal Field," Extended Abstracts, pp. 59-62, 20th Meeting, Comité International de Thermodynamique et de Cinétique Electrochimique, Strasbourg, France, September 1969.

TECHNICAL INFORMATION DIVISION
LAWRENCE RADIATION LABORATORY
UNIVERSITY OF CALIFORNIA
BERKELEY, CALIFORNIA 94720